hexagon:2611.01288v1

SMALL REAL PROJECTIVE CODES

HENRY COHN, JAVIER GÓMEZ-SERRANO, LIUDMYLA KRYVONOS,
LUKAS LIEHR, AND MITCHELL A. TAYLOR

Abstract. We classify the arrangements of up to twelve lines through the origin in $\mathbb{R}^3$ that maximize the smallest angle between them, as well as eleven or twelve lines in $\mathbb{R}^4$, and we formalize the proofs using Lean. The cases that had not previously been classified are ten through twelve lines in $\mathbb{R}^3$ and eleven lines in $\mathbb{R}^4$.

Contents

1. Introduction 2
2. Results, conventions, and the organization of the proof 8
3. Matrix bounds and their equality cases 10
4. Exact constructions for the remaining three-dimensional cases 14
5. One isolation-and-selection principle 20
6. Preliminary bounds and contact geometry 29
7. One exhaustive census of signed contact maps 40
8. Area and angle certificates 48
9. Metric and orientation identities 55
10. Variational certificates and sparse stress supports 58
11. Exact interval certificates and missing points 70
12. Terminal map arguments 74
13. The finite calculations and the assembled classification 79
References 81

This document is a progress report from our joint project on Lean verification of computer-assisted proofs, with code available at `https://github.com/henrycohn/line-packings`. We plan to describe our methodology and what we have learned from these experiments in a future paper.

All of the proofs developed for this project were found by artificial intelligence, specifically the GPT-6 Astra, GPT-6.1 Sol, GPT-6.2 Sol, and GPT-6.2 Astra models from OpenAI. The authors provided guidance and suggestions, but we did not carry out any of the detailed work ourselves. We have verified that the Lean theorems are correctly stated, and we understand the overall proof techniques, but we rely on Lean verification for our confidence in the enumeration and analysis of contact graphs.

Section 1 was written by the authors and reflects what we believe most human readers would want to learn from this document. Sections 2 through 13 were written entirely by artificial intelligence and are the AI models' account of their work. We have not made any substantive edits to the AI-written sections and cannot ensure that they precisely correspond with the Lean proofs.

1. Introduction

How far apart can we make N lines through the origin in $\mathbb{R}^d$? Specifically, how large can we make the smallest angle between two of them? This problem is equivalent to separating N points in $\mathbb{RP}^{d-1}$ as much as possible under the Fubini–Study metric.

Suppose the lines are $\mathbb{R}x_1, \dots, \mathbb{R}x_N$, where $x_1, \dots, x_N$ are unit vectors in $\mathbb{R}^d$. We define the *coherence* of the line configuration to be

$$\max_{i<j} |\langle x_i, x_j \rangle|,$$

or 0 by convention if $N = 1$, and our goal is to minimize the coherence. The minimal coherence is of course 0 for $N \le d$, attained by orthogonal lines, and so we assume $N \ge d + 1$.

In this document, we determine the optimal coherence for up to 12 lines in $\mathbb{R}^3$ and for 11 or 12 in $\mathbb{R}^4$, and we classify all the optimal line configurations (see below for which cases were previously known). The proofs are formalized end to end in Lean at `https://github.com/henrycohn/line-packings`. The optimal configurations are unique up to isometry, except in three cases: there are two optimal configurations of 9 lines in $\mathbb{R}^3$, a two-parameter family for 10 lines in $\mathbb{R}^3$ since one line is a rattler (i.e., it is not in contact with any other, except on the boundary of its allowed region), and two for 11 lines in $\mathbb{R}^4$.

Table 1.1 lists the coherence and the optimal line configurations, and Figures 1.1 through 1.5 (drawn by GPT-6.2 Astra) show the optimal three-dimensional configurations via a stereographic view of one hemisphere. In the figures, each dot represents one line, with arcs joining the closest pairs and continuing across the boundary with opposite points identified. The decimal expansions in Table 1.1 are roots of the polynomials $1537x^9 + 677x^8 - 584x^7 - 80x^6 + 146x^5 - 78x^4 - 80x^3 - 8x^2 + 5x + 1$ for 8 lines in $\mathbb{R}^3$, $13x^3 + x^2 - 5x - 1$ for 9 lines in $\mathbb{R}^3$, and $5x^6 + 200x^5 - 115x^4 - 40x^3 + 15x^2 - 1$ for 11 lines in $\mathbb{R}^3$.

For $\mathbb{R}^3$, the answers were previously known for $N \le 9$: Fejes Tóth [17] dealt with $N \le 6$, Conway, Hardin, and Sloane [11] proved optimality for $N = 7$ while Cohn and Woo [9] proved uniqueness, Mixon and Parshall [26] dealt with $N = 8$, and van den Berg [5] dealt with $N = 9$. For $\mathbb{R}^4$, Levenšteĭn [22] proved optimality for $N = 12$, Conway, Hardin, and Sloane [11] proved optimality for $N = 11$, and Anstreicher [1] proved uniqueness for $N = 12$. The optimal configurations for $N = 8$ through 12 in $\mathbb{R}^3$ were constructed by Conway, Hardin, and Sloane [11], and Cohn and Woo [9] found the 11-line configuration in $\mathbb{R}^4$ that does not consist of 24-cell diagonals.

Our proofs take two different approaches. The three-dimensional proofs work by exhaustive enumeration of contact graphs (except for 4 and 6 lines, for which more direct proofs were already known, and 7 lines, for which we give a simple proof), and the four-dimensional proofs are based on analyzing the orthoplex bound of Conway, Hardin, and Sloane [11].

In three dimensions, enumeration of contact graphs was previously employed by Mixon and Parshall [26] to solve the 8-line problem, inspired by work of Musin and Tarasov [29, 30, 31, 32] on spherical codes. In our initial investigation, our AI agents used the program `surftri` developed by Sulanke [38] to generate candidate contact maps and wrote Python code to rule out infeasible cases. For the final proof, the agents formalized the geometric reduction in Lean, implemented a direct

TABLE 1.1. The optimal line configurations. Here a diagonal always connects opposite vertices, and the configurations without explicit descriptions are defined in the text or figures.

N	d	Coherence	Optimal configurations
4	3	$1/3$	Cube diagonals
5	3	$1/\sqrt{5}$	Five icosahedron diagonals
6	3	$1/\sqrt{5}$	All six icosahedron diagonals
7	3	$1/\sqrt{3}$	Cube diagonals and facet normals
8	3	$0.647588\ldots$	
9	3	$0.669362\ldots$	two configurations
10	3	$6/(3+\sqrt{33})$	two-parameter family of configurations
11	3	$0.714434\ldots$	
12	3	$1/(7-4\sqrt{2})$	Rhombicuboctahedron diagonals
11	4	$1/2$	Eleven 24-cell diagonals or Cohn–Woo configuration [9]
12	4	$1/2$	All twelve 24-cell diagonals

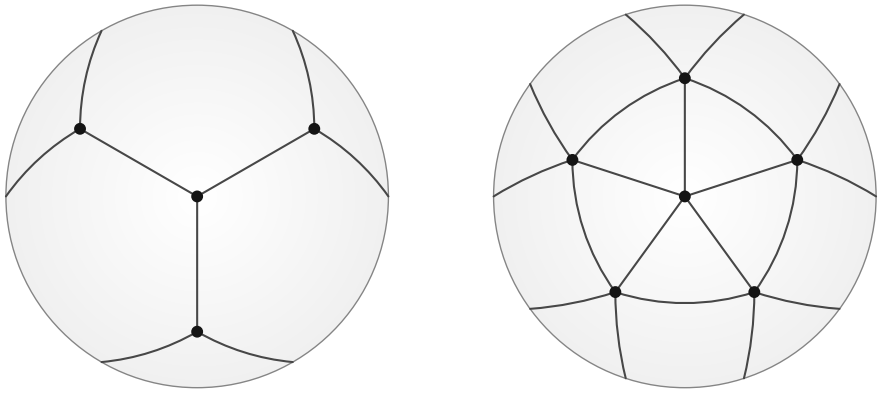

FIGURE 1.1. Optimal configurations of four lines (left) and six lines (right). The optimal configuration of five lines can be obtained by deleting any one of the six lines.

enumeration of signed contact maps, and verified the case analysis. Our only substantial contribution to the formalization was to suggest storing adjacency data as integer bit masks, which made the enumeration practical in Lean (see Subsection 7.4).

By contrast, the four-dimensional arguments and the seven-line argument in $\mathbb{R}^3$ can be checked by hand, and the Lean verification in these cases is just for the sake of completeness. In the remainder of this introduction, we will explain these proofs.

The orthoplex bound used in these proofs is based on an embedding of $\mathbb{RP}^{d-1}$ into the space of $d \times d$ symmetric matrices under the trace inner product $\langle A, B\rangle = \operatorname{tr}(AB)$, which takes a unit vector x_i spanning a line to the matrix $M_i = x_i x_i^{\mathsf{T}} - I_d/d$. Then

$$\langle M_i, M_j\rangle = \langle x_i, x_j\rangle^2 - \frac{1}{d},$$

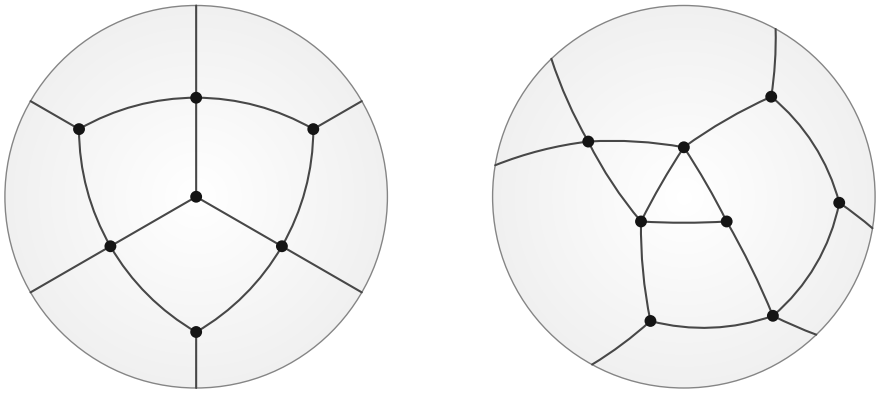

FIGURE 1.2. Optimal configurations of seven lines (left) and eight lines (right).

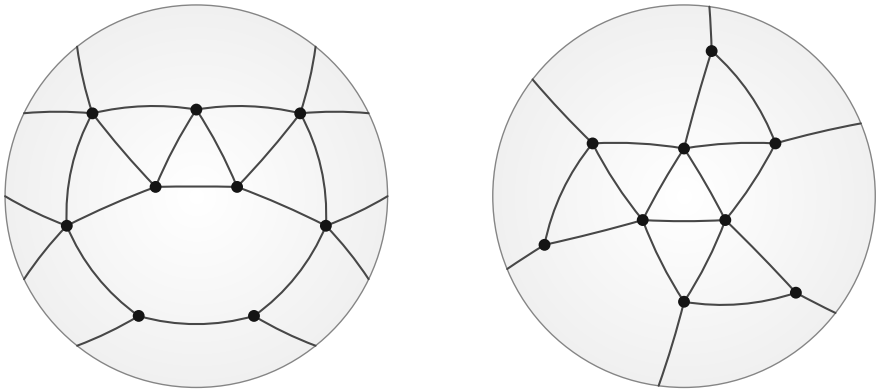

FIGURE 1.3. The two inequivalent optimal configurations of nine lines.

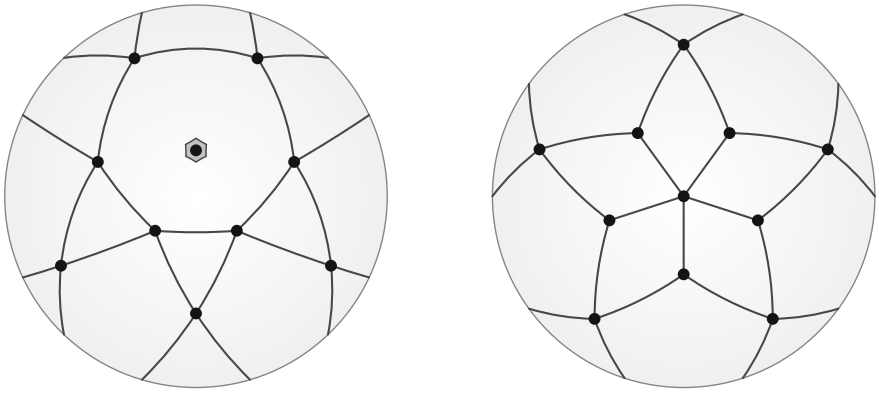

FIGURE 1.4. Optimal configurations of ten lines (left) and eleven lines (right). The shaded region shows where the ten-line rattler can move with the other nine lines fixed.

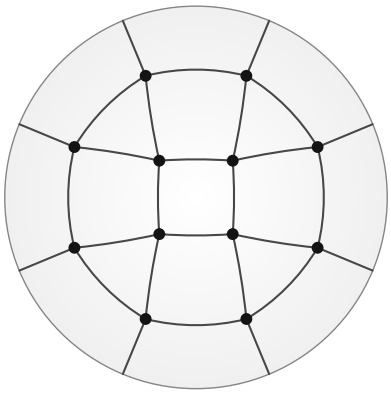

FIGURE 1.5. The optimal configuration of twelve lines.

and the matrices $M_1, \ldots, M_N$ are contained in the subspace of matrices with trace zero, which has dimension

$$D = \frac{d(d+1)}{2} - 1.$$

Now suppose the line configuration has coherence at most $1/\sqrt{d}$, as is the case for the optimal configurations of 7 lines in $\mathbb{R}^3$ and 11 or 12 lines in $\mathbb{R}^4$. We turn the lines into vertices of a graph by placing an edge between each pair with $|\langle x_i, x_j\rangle| < 1/\sqrt{d}$ (i.e., for $i \neq j$, there is an edge when $\langle M_i, M_j\rangle < 0$ and no edge when $\langle M_i, M_j\rangle = 0$). When we refer to the Gram matrix of a set of lines in this section, we will mean the Gram matrix of the corresponding matrices M_i (later sections use a different convention).

Lemma 1.1. *Let G be the Gram matrix of a connected component of the graph formed by the lines, and suppose G is singular. Then $\dim\ker G = 1$, the kernel is spanned by a vector with positive entries, and there exist positive weights α_i such that*

$$\sum_i \alpha_i x_i x_i^\mathsf{T} = I_d,$$

where the sum is over i for which $\mathbb{R}x_i$ is in the connected component. The connected component must have size at least d, and if it has size d, then it consists of d orthogonal lines.

Proof. Suppose $v \in \ker G \setminus \{0\}$, and let w have entries $w_i = |v_i|$ for i in the index set of v (i.e., the indices of lines contained in the connected component). Then $w^\mathsf{T} G w \leq v^\mathsf{T} G v = 0$, because G has nonpositive entries outside the diagonal, and so $Gw = 0$ since G is symmetric and positive semidefinite. If $w_i = 0$ for some i, then

$$\sum_{j\neq i} G_{i,j} w_j = (Gw)_i = 0,$$

and all the terms in the sum are nonpositive. Thus, $w_j = 0$ whenever $w_i = 0$ and $G_{i,j} < 0$, and connectedness implies that $w = 0$ if any entry w_i vanishes. We conclude that $\ker G$ must be one-dimensional, since otherwise it would contain a nonzero vector that vanishes in some coordinate, and it is generated by a positive vector w.

Setting $\alpha_i = dw_i / \sum_j w_j$ turns $Gw = 0$ into

$$\sum_i \alpha_i x_i x_i^\mathsf{T} = I_d. \tag{1.1}$$

The rank of $\sum_i \alpha_i x_i x_i^\mathsf{T}$ is therefore d, and so the connected component must have size at least d. If it has size d, then the lines in the connected component must be orthogonal: if we let the matrix A have columns $\sqrt{\alpha_i} x_i$, then $AA^\mathsf{T} = I_d$ by (1.1), and therefore $A^\mathsf{T} A = I_d$, which implies that the columns of A are orthonormal. □

The Gram matrix of the entire line configuration is an $N \times N$ matrix with rank at most D, and it has a block decomposition into blocks corresponding to the connected components. Thus, there must be at least $N - D$ connected components that have singular Gram matrices, which we will call singular connected components.

We can now prove the orthoplex bound for the special case of projective space. If the coherence were strictly less than $1/\sqrt{d}$ with $N > D + 1$, then the graph would be complete, which would contradict having at least $N - D$ singular connected components. The inequality $N > D + 1$ holds for $(N, d) \in \{(7, 3), (11, 4), (12, 4)\}$ so the optimal coherence in each of these cases is $1/\sqrt{d}$, and all that remains is to classify the configurations that achieve coherence $1/\sqrt{d}$.

1.1. **Seven lines in $\mathbb{R}^3$.** Lemma 1.1 is already enough to give a simple proof of optimality and uniqueness for the optimal configurations of seven lines in $\mathbb{R}^3$. There must be at least $N - D = 2$ singular connected components, each containing at least three lines, and therefore there must be a singular connected component of size three. The corresponding vectors form an orthonormal basis, and all the other vectors have coordinates $\pm 1/\sqrt{3}$ with respect to this basis, because the corresponding Gram matrix entries must be 0. The eight choices of signs yield a unique set of four lines, and the configuration is unique up to isometry.

1.2. **Twelve lines in $\mathbb{R}^4$.** The proof is equally simple for twelve lines in $\mathbb{R}^4$. There must be at least $N - D = 3$ singular connected components, each of size at least four and therefore equal to four. If we choose one component to form an orthonormal basis, then all the remaining vectors must have coordinates $\pm 1/2$ with respect to this basis, and the sixteen choices of signs yield a unique set of eight lines. The resulting line configuration is the diagonals of a regular 24-cell.

1.3. **Eleven lines in $\mathbb{R}^4$.** The same argument works for eleven lines in $\mathbb{R}^4$, provided that there is a singular connected component of size four, and it yields eleven of the twelve 24-cell diagonals (all deletions are equivalent by symmetry). However, it is also possible that every singular connected component might have size five or greater. They cannot all have size six or greater, since there must be at least two of them and there are only eleven lines.

The remaining case of size five will give the Cohn–Woo configuration. We will number the lines so that $x_1, \ldots, x_5$ correspond to a singular connected component, and we will call the other six lines *external lines*. By Lemma 1.1, there are positive weights α_i with

$$\sum_{i=1}^{5} \alpha_i x_i x_i^\mathsf{T} = I_4, \tag{1.2}$$

and so $x_1, \dots, x_5$ must span $\mathbb{R}^4$. They have a unique linear dependence $\sum_i c_i x_i = 0$, up to scaling, and we can ensure that $c_i \geq 0$ by replacing x_i with $-x_i$ whenever $c_i < 0$.

For each unit vector representative y of an external line, let $s_i(y) = 2\langle x_i, y\rangle \in \{\pm 1\}$ for $1 \leq i \leq 5$. These signs satisfy $\sum_i c_i s_i(y) = 0$, and they completely determine y because $x_1, \dots, x_5$ span $\mathbb{R}^4$.

First, we will show that all positive coefficients c_i must be equal. The vectors $x_1, \dots, x_5$ are nonzero, and thus there are at least two nonzero coefficients c_i and c_j in the linear dependence. Given such an i and j, there must be two distinct external lines $\mathbb{R}y$ and $\mathbb{R}z$ with $(s_k(y))_{k \notin \{i,j\}} = \pm(s_k(z))_{k \notin \{i,j\}}$, because there are six external lines and only four sign patterns up to a factor of ± 1. By replacing z with $-z$ if necessary, we can assume that $s_k(y) = s_k(z)$ for all $k \notin \{i, j\}$. It then follows that $(s_i(y), s_j(y))$ and $(s_i(z), s_j(z))$ must differ, and they cannot differ in just one sign, because $\sum_\ell c_\ell s_\ell(y) = \sum_\ell c_\ell s_\ell(z) = 0$. We must therefore have $(s_i(y), s_j(y)) = -(s_i(z), s_j(z))$, which implies that $c_i s_i(y) + c_j s_j(y) = 0$. Because c_i and c_j are nonnegative, we conclude that $c_i = c_j$, as desired.

There must be an even number of positive coefficients, so that the signs can sum to zero, and there cannot be just two, since $x_i + x_j = 0$ would imply that $\mathbb{R}x_i = \mathbb{R}x_j$. Thus, we can relabel the lines so that the linear dependence is

$$x_1 + x_2 + x_3 + x_4 = 0,$$

with $x_1, \dots, x_4$ spanning a three-dimensional space V. If we apply (1.2) to a nonzero vector y orthogonal to V, then we obtain $\alpha_5 x_5 \langle x_5, y\rangle = y$, and thus x_5 must be orthogonal to V. Furthermore, $\alpha_1 + \cdots + \alpha_4 = 3$ follows from taking the trace on V.

Next we will show that $x_1, \dots, x_4$ form a regular tetrahedron. For $i \neq j$, let $m_{i,j} = (x_i + x_j)/2$ be the midpoint of the edge between x_i and x_j. If $\{1, 2, 3, 4\} = \{i, j, k, \ell\}$, then $m_{i,j} = -m_{k,\ell}$ since $x_1 + x_2 + x_3 + x_4 = 0$. Furthermore,

$$\langle x_i - x_j, m_{i,j}\rangle = \frac{\|x_i\|^2 - \|x_j\|^2}{2} = 0,$$

so x_i and x_j have the same projection onto the line $\mathbb{R}m_{i,j}$. Since their average is $m_{i,j}$, both must project to $m_{i,j}$, and similarly x_k and x_ℓ both project to $-m_{i,j}$. In particular,

$$\langle x_i, m_{i,j}\rangle = \langle x_j, m_{i,j}\rangle = \|m_{i,j}\|^2 \quad \text{and} \quad \langle x_k, m_{i,j}\rangle = \langle x_\ell, m_{i,j}\rangle = -\|m_{i,j}\|^2.$$

We can now determine $\|m_{i,j}\|$ by applying (1.2) to $m_{i,j}$ and taking the inner product with $m_{i,j}$ to obtain

$$\begin{aligned}\|m_{i,j}\|^2 &= \alpha_1\langle x_1, m_{i,j}\rangle^2 + \alpha_2\langle x_2, m_{i,j}\rangle^2 + \alpha_3\langle x_3, m_{i,j}\rangle^2 + \alpha_4\langle x_4, m_{i,j}\rangle^2 \\ &= (\alpha_1 + \alpha_2 + \alpha_3 + \alpha_4)\|m_{i,j}\|^4 \\ &= 3\|m_{i,j}\|^4.\end{aligned}$$

We cannot have $m_{i,j} = 0$, since that would mean $\mathbb{R}x_i = \mathbb{R}x_j$, so $\|m_{i,j}\|^2 = 1/3$ and therefore $\langle x_i, x_j\rangle = 2\|m_{i,j}\|^2 - 1 = -1/3$. The four points $x_1, \dots, x_4$ therefore form a regular tetrahedron, as desired.

Each of the six external lines is of the form $\mathbb{R}y$ for a unit vector y with $\langle x_i, y\rangle = \pm 1/2$ for $1 \leq i \leq 5$, with the signs being $s_i(y)$ from above, and without loss of generality we can choose y so that $\langle x_5, y\rangle = 1/2$. Because $x_1 + \cdots + x_4 = 0$, we must have $s_1(y) + \cdots + s_4(y) = 0$, so two of $s_1(y), \dots, s_4(y)$ are positive and two

are negative. This constraint pins down the only six possible external lines: if $s_i(y) = s_j(y) = 1$ with $i < j$, then

$$y = \frac{3}{2}m_{i,j} + \frac{1}{2}x_5,$$

and the resulting line configuration is isometric to the Cohn–Woo configuration from Appendix A of [9]. It is not isometric to eleven of the 24-cell's diagonals, because $|\langle x_1, x_2\rangle| = 1/3$, while only 0 and $1/2$ can occur for distinct diagonals of the 24-cell.

This completes the proofs for 7 lines in $\mathbb{R}^3$ and 11 or 12 in $\mathbb{R}^4$. The rest of this document consists of an AI-written account of the Lean proofs of the classification theorems.

2. Results, conventions, and the organization of the proof

Represent N distinct lines in $\mathbb{R}^d$ by unit vectors $X = (x_1, \dots, x_N)$. Their *coherence* is

$$\mu(X) = \max_{i<j} |\langle x_i, x_j\rangle|.$$

For $N = 1$, set $\mu(X) = 0$. For $N \geq 2$, the least unoriented angle is $\arccos \mu(X)$. Equivalence means an orthogonal transformation, a permutation, and independent changes of representative signs. Equal Gram matrices give orthogonally equivalent configurations, even when the vectors do not span the ambient space. Indeed, the map $\sum_i a_i x_i \mapsto \sum_i a_i y_i$ between their spans is well defined: the squared norm of either sum is the same quadratic form in the coefficients. The same Gram identity shows that this map preserves inner products. Completing orthonormal bases of the two spans extends it to an orthogonal transformation of $\mathbb{R}^d$. For unoriented lines in odd dimension, restricting to proper rotations does not change equivalence, since Q and $-Q$ act identically on lines.

Theorem 2.1. *The optimal coherences in $\mathbb{R}^3$, and all their equality cases, are listed in Table 2.1. Every size except nine and ten has a unique optimum. Nine lines have exactly the two displayed classes. The ten-line entry denotes the entire closed family specified in Section 4.4, including its boundary.*

Fejes Tóth solved the four- and five-line cases, obtained the six-line case from the regular icosahedron, and credited A. Heppes with the seven-line conjecture [17, pp. 437–439]. Conway, Hardin, and Sloane proved optimality for seven lines [11], and Cohn and Woo proved uniqueness [9]. Mixon and Parshall proved the eight-line classification [26]. For nine through twelve lines, Theorem 2.1 proves optimality of the configurations reported in [11, Table 1] and determines all equality cases.

Throughout the proof, c_N denotes the proposed value in Table 2.1. In particular c_8, c_9, c_{11} are the unique roots in the indicated rational intervals of the following polynomials:

$$P_8(c) = 1537c^9 + 677c^8 - 584c^7 - 80c^6 + 146c^5 - 78c^4 - 80c^3 - 8c^2 + 5c + 1, \tag{2.1}$$

$$P_9(c) = 13c^3 + c^2 - 5c - 1, \tag{2.2}$$

$$P_{11}(c) = 5c^6 + 200c^5 - 115c^4 - 40c^3 + 15c^2 - 1. \tag{2.3}$$

The respective intervals are

$$(0.647588, 0.647589), \qquad (0.669362, 0.669363), \qquad (0.714434, 0.714435).$$

TABLE 2.1. Optimal line packings in three dimensions. For $N = 1$ there is no pairwise angle to optimize; the convention only fills the table.

N	Optimal coherence	Equality cases
1	0, by convention	Any single line
2	0	Two perpendicular lines
3	0	An orthonormal basis
4	$1/3$	Four cube diagonals
5	$1/\sqrt{5}$	Five of the six icosahedral lines
6	$1/\sqrt{5}$	Six icosahedral lines
7	$1/\sqrt{3}$	Three axes and four cube diagonals
8	$c_8 = 0.647588978734\ldots$	The Gram matrix (4.3)
9	$c_9 = 0.669362319\ldots$	The two matrices (4.4), (4.5)
10	$c_{10} = (\sqrt{33} - 3)/4$	A fixed nine-line core and one admissible line
11	$c_{11} = 0.714434\ldots$	A pole and two staggered pentagons
12	$c_{12} = (7 + 4\sqrt{2})/17$	The rhombicuboctahedral lines

Each decimal endpoint here is an exact rational number. Direct rational evaluation gives a negative value at the left endpoint and a positive value at the right endpoint. For a short monotonicity certificate, expand $P_N(a_N + t)$, with

$$a_8 = 16/25, \qquad a_9 = 33/50, \qquad a_{11} = 71/100.$$

Every nonconstant coefficient in each expansion is strictly positive. The coefficient of t is, respectively,

$$\frac{35436775921093}{152587890625}, \qquad \frac{33271}{2500}, \qquad \frac{55698438053}{1000000000}.$$

All coefficients are reconstructed from the displayed polynomials by the formula $\sum_{j \geq i} p_j \binom{j}{i} a_N^{j-i}$ for the coefficient of t^i. Thus P_N is strictly increasing on $[a_N, \infty)$, which contains the prescribed interval. The intermediate value theorem and strict monotonicity give existence and uniqueness. Irreducibility is unnecessary. These exact calculations are formalized in `LinePackings/Arithmetic/AlgebraicParameters.lean`.

Theorem 2.2. *The optimal coherence of eleven lines in $\mathbb{R}^4$ is $1/2$. Exactly two congruence classes attain it: the twelve-line 24-cell code with one line deleted, and the Cohn–Woo code described in Section 3.3. The optimal coherence for twelve lines in $\mathbb{R}^4$ is also $1/2$, attained only by the 24-cell up to congruence.*

Cohn and Woo exhibited both eleven-line configurations and observed that the orthoplex bound proves their optimality [9, Appendix A]. The new assertion for eleven lines is that these two exhaust the equality cases. For twelve lines, Anstreicher proved that the 24-cell is the unique antipodal kissing configuration of size 24 in $\mathbb{R}^4$ [1]. For arbitrary kissing configurations in $\mathbb{R}^4$, Musin proved that the maximum size is 24 [28], and de Laat, Leijenhorst, and de Muinck Keizer proved that the 24-cell is the unique maximizer up to congruence [13].

The numerical orthoplex bound by itself does not classify equality cases. Section 3.2 supplies the additional rank-one projector argument, resolving both seven lines in $\mathbb{R}^3$ and eleven lines in $\mathbb{R}^4$.

For five lines and for eight through twelve lines we use a common selection argument. First construct the proposed equality families and prove their uniform local isolation. If any other competitive configuration exists, minimize its sorted absolute inner products lexicographically outside these families. For five lines, the strict contact stars already suffice for a short signed-graph proof. In the larger cases we use the connected antipodal contact core and its convex disk faces to enumerate the full signed map. The census includes smaller cores, and the case analysis accounts for all lines absent from the core. Every case either contradicts the selection conditions or forces membership in a proposed family. Since each family member attains the proposed coherence, this proves the lower bound and exhausts the equality cases.

Sections 7–11 give the mathematical rules used in the finite checks. Section 13.2 shows how the census and certificate theorems apply to the selected packing. Section 13.3 combines that argument with the explicit constructions to prove the classifications.

All file paths are relative to the root of the accompanying `LinePackings/` package. The definitions of packings, coherence, and congruence are in `LinePackings/Basic.lean`. The root module `LinePackings.lean` imports the three- and four-dimensional classification modules. The proofs share geometry, arithmetic, and optimality lemmas, with the finite enumeration in `LinePackings/Census/` and the certificate checks in `LinePackings/Certificates/`.

3. Matrix bounds and their equality cases

3.1. **The trace bound.** For $d \geq 1$, let $G = (\langle x_i, x_j \rangle)$ and $A = \sum_i x_i x_i^T$. Expanding the finite sums gives

$$\sum_a A_{aa} = N, \qquad \operatorname{tr}(G^2) = \sum_{i,j} \langle x_i, x_j \rangle^2 = \sum_{a,b} A_{ab}^2.$$

Cauchy–Schwarz applied to the diagonal entries gives $N^2 \leq d \sum_a A_{aa}^2 \leq d \sum_{a,b} A_{ab}^2$. Bounding each off-diagonal Gram entry by the coherence therefore yields

$$\frac{N^2}{d} \leq \operatorname{tr}(G^2) \leq N + N(N-1)\mu(X)^2. \tag{3.1}$$

For $N > 1$, rearranging gives the Welch bound [43], $\mu(X)^2 \geq (N-d)/(d(N-1))$. Equality in the lower bound holds exactly when $A = (N/d)I$: the off-diagonal squares must vanish and the diagonal entries must all agree. Equivalently, expanding squares gives

$$\sum_{a,b} \bigl(A_{ab} - (N/d)\delta_{ab}\bigr)^2 = \operatorname{tr}(G^2) - N^2/d.$$

Equality in the upper bound holds exactly when every off-diagonal absolute Gram entry equals $\mu(X)$. Moreover $A = (N/d)I$ implies $G^2 = (N/d)G$, directly by matrix multiplication. These finite-sum arguments give all the equality information needed below without invoking spectral theory. For $N = 1, 2, 3$ in $\mathbb{R}^3$, the first N coordinate vectors represent distinct lines of coherence zero. Coherence is nonnegative, so these attain the minimum. If another unit family has coherence zero, its Gram matrix is the identity: this is immediate for a singleton, and every off-diagonal entry vanishes for $N = 2, 3$. Equality of Gram matrices therefore makes it congruent to the coordinate family. Conversely, orthogonal transformations, permutations, and

sign changes preserve absolute inner products and hence coherence. This proves both directions of the classification for these three sizes.

For $N = 4$, (3.1) gives $c \geq 1/3$. At equality every off-diagonal Gram entry has absolute value $1/3$ and $G^2 = (4/3)G$. Switch representative signs to obtain a Gram matrix H with $H_{01} = H_{02} = H_{03} = -1/3$. Sign changes preserve the quadratic identity. Write $a = H_{12}$, $b = H_{13}$, and $c' = H_{23}$. The $(0,1), (0,2), (0,3)$ entries of $H^2 = (4/3)H$ give

$$a + b = a + c' = b + c' = -2/3.$$

Thus $a = b = c' = -1/3$, which determines the signed Gram matrix. The four unit vectors $(1, \pm 1, \pm 1)/\sqrt{3}$, ordered as $(1,1,1), (1,1,-1), (1,-1,1), (1,-1,-1)$, have precisely this Gram matrix after sign changes $(1,-1,-1,1)$. They are distinct lines with coherence $1/3$. Gram equivalence and invariance of coherence prove optimality and the full four-line classification.

For $N = 6$, the bound is $c \geq 1/\sqrt{5}$. At equality switch representative signs so that the resulting Gram matrix H has $H_{0i} = c$ for $i \neq 0$, and write $H = I + cS$. Then S has zero diagonal and off-diagonal entries ± 1. The $(0,i)$ equation in $H^2 = 2H$ gives $c^2 \sum_{j=1}^{5} S_{ij} = 0$ for $i = 1, \ldots, 5$. Thus exactly two of the other four entries in each such row are positive, and the positive-entry graph on the other five indices is 2-regular. It is a five-cycle, since a simple cycle has length at least three. Indeed, following the unused edge at each visited vertex eventually closes a cycle. No further vertex can join that cycle, since its vertices already have degree two. Thus every component is a cycle, and two components would require at least six vertices. This determines S up to switching and permutation, proving uniqueness.

The Lean proof verifies this last finite assertion directly. Encode the ten entries S_{ij}, $1 \leq i < j \leq 5$, in lexicographic order by ten bits, assigning $+1$ to true and -1 to false. Complete the symmetric matrix with zero diagonal and $S_{0i} = 1$. For each of the 2^{10} bit strings, test the five integer row sums $\sum_{j=1}^{5} S_{ij} = 0$. If they vanish, test the twelve orders $(1, q_2, q_3, q_4, q_5)$, where (q_2, q_3, q_4, q_5) ranges over permutations of $(2,3,4,5)$ with $q_2 < q_5$. In at least one order the positive entries are exactly the five cycle edges. These exact finite tests are evaluated by the Lean kernel; the full identity $S^2 = 5I$ is not needed.

The six representatives

$$(0, 1, \pm\varphi), \quad (1, \pm\varphi, 0), \quad (\varphi, 0, \pm 1), \qquad \varphi = \frac{1+\sqrt{5}}{2}, \tag{3.2}$$

normalized by $\sqrt{1+\varphi^2}$, realize it. Five of these lines give the five-line construction; its optimality and uniqueness require the separate six-case argument of Section 12.1. For the arithmetic checks below, one convenient signed ordering of that five-line construction has Gram matrix

$$G_5 = \begin{pmatrix} 1 & c & -c & c & -c \\ c & 1 & c & c & -c \\ -c & c & 1 & c & c \\ c & c & c & 1 & c \\ -c & -c & c & c & 1 \end{pmatrix}, \qquad c = 1/\sqrt{5}. \tag{3.3}$$

3.2. **A positive-kernel lemma.** Conway, Hardin, and Sloane obtained the projective orthoplex bound by applying Rankin's spherical bound [35] to centered projection matrices [11, § 5]. We use the Gram matrix of these projectors to recover additional information at equality.

Lemma 3.1. *Let M be symmetric positive semidefinite, with nonpositive off-diagonal entries. If the graph joining i, j whenever $M_{ij} < 0$ is connected, then* $\dim\ker M \le 1$. *If M is singular, its kernel has a strictly positive generator.*

Proof. If $Mv = 0$, set $w_i = |v_i|$. Then $0 \le w^T M w \le v^T M v = 0$, so $Mw = 0$. If $w_i = 0$, row i forces $w_j = 0$ at every neighbor, and connectedness propagates this to every coordinate. Thus every nonzero kernel vector has no zero coordinate. Two independent kernel vectors would have a nonzero linear combination with a zero coordinate. Finally $|v|$ is a strictly positive kernel vector. □

Proposition 3.2 (Projector blocks)**.** *Suppose N distinct lines in $\mathbb{R}^d$ have coherence at most $1/\sqrt{d}$, and put $D = d(d+1)/2-1$. Their centered projectors $Q_i = x_i x_i^T - I/d$ have a Gram matrix*

$$H_{ij} = \operatorname{tr}(Q_i Q_j) = (\langle x_i, x_j\rangle)^2 - \frac{1}{d}, \qquad \operatorname{rank} H \le D.$$

Split the indices into connected components of $H_{ij} < 0$. If r blocks are singular, then

$$\operatorname{rank} H = N - r, \qquad r \ge N - D.$$

Every singular block contains at least d lines and admits positive weights satisfying

$$\sum_{i\in B} a_i x_i x_i^T = I, \qquad \sum_{i\in B} a_i = d. \tag{3.4}$$

A singular block of size d is an orthonormal basis. Lines in different blocks are mutually unbiased: $|\langle x_i, x_j\rangle| = 1/\sqrt{d}$.

Proof. Each Q_i is symmetric and traceless. Symmetric d-by-d matrices have $d(d+1)/2$ independent upper-triangular entries; the trace equation determines one diagonal entry from the others. Thus their traceless subspace has dimension D. The map from coefficients to $\sum_i t_i Q_i$, followed by its adjoint, gives the Gram matrix H, so $\operatorname{rank} H \le D$. Expanding $\operatorname{tr}(Q_i Q_j)$ gives the displayed entry formula. Entries between components vanish. Apply Lemma 3.1 to each block. A positive kernel vector gives $\sum a_i Q_i = 0$, because the squared norm of this sum is its zero Gram quadratic form. Rescale to obtain (3.4). Its right side has rank d, so $|B| \ge d$. If equality holds, put $V = [x_i]$ and let row i of T be $a_i x_i^T$. Then $VT = I$, hence $TV = I$; its entries are $a_i\langle x_i, x_j\rangle$. The diagonal entries give $a_i = 1$, and the other entries give orthogonality. □

If $N > D+1$, coherence strictly below $1/\sqrt{d}$ would make the whole negative-entry graph connected. Its nullity would be at most one, contradicting $\operatorname{rank} H \le D$. This proves the orthoplex bound in precisely the range used here.

For seven lines in $\mathbb{R}^3$, at least two singular blocks occur, each of size at least three. One has size three and is an orthonormal basis. The four remaining lines are unbiased to it, so their coordinates have absolute value $1/\sqrt{3}$. There are exactly four such unoriented lines: all four cube diagonals. They are compatible with one another. This proves both optimality and uniqueness for seven lines, using the projector structure in addition to the numerical bound.

3.3. **Eleven lines in four dimensions.** For eleven lines in $\mathbb{R}^4$, $D = 9$, so at least two singular blocks occur and every singular block has size at least four. If there is a four-line block, rotate it to the coordinate basis. Every other line is represented

by $(\pm1, \pm1, \pm1, \pm1)/2$. There are eight such lines; any seven are equivalent by coordinate sign changes. This is the 24-cell with one line deleted.

Otherwise a singular block has exactly five lines: two blocks of size at least six cannot fit. Its other six lines are unbiased to it. Let A have columns $\sqrt{a_i}x_i$ for the five-line block. Then $AA^T = I$, and for a unit $z \in \mathbb{R}^5$,

$$A^T A = I - zz^T, \qquad a_i = 1 - z_i^2 > 0. \tag{3.5}$$

Switch representatives to make $z_i \geq 0$. At least three z_i's are nonzero: one nonzero coordinate would give $a_i = 0$; exactly two would make the corresponding lines coincide.

A unit vector unbiased to the block has $\langle x_i, v\rangle = \sigma_i/2$, $\sigma_i \in \{\pm1\}$. Since A^T is an isometry onto $z^\perp$, such a vector exists uniquely precisely when

$$\sum_{i=1}^{5} w_i\sigma_i = 0, \qquad w_i = z_i\sqrt{1 - z_i^2}. \tag{3.6}$$

Indeed the prescribed image has squared norm $\sum_i a_i/4 = 1$. Opposite sign patterns give the same line.

Lemma 3.3 (Balanced subsets)**.** *For $r \geq 1$ positive weights, the subsets with half the total weight form an antichain. If m_j of them have cardinality j, then*

$$\sum_{j=0}^{r} \frac{m_j}{\binom{r}{j}} \leq 1.$$

Their total number is even and is at most $\max_j \binom{r}{j}$.

Proof. Proper inclusion strictly increases weight. A j-set is the initial segment of $j!(r-j)!$ permutations, and a permutation has at most one initial segment in an antichain. Count permutations and divide by $r!$. Complementation pairs the balanced subsets without fixed points. □

Let k be the number of zero weights in (3.6). If $k = 0$, at most ten sign patterns give at most five lines. If $k = 2$, the three positive weights have at most two balanced subsets; the free zero signs give at most $2 \cdot 4/2 = 4$ lines. Thus $k = 1$. The four positive weights have at most six balanced subsets, and six lines require equality. The antichain inequality then forces all six subsets to have size two. All pair sums agree, so these four weights are equal.

Put $u_i = z_i^2$. Equal nonzero weights give $(u_i - u_j)(1 - u_i - u_j) = 0$ for the four positive coordinates. If two differed, their sum would be one, contradicting the other positive coordinates and $\sum_i u_i = 1$. Thus all four are equal, and each is $1/4$; the fifth is zero. Equation (3.5) now gives four tetrahedral vectors with mutual inner product $-1/3$, and one perpendicular axis.

By Gram equivalence and representative sign changes, take the tetrahedral lines to be the cube diagonals $(1, \pm1, \pm1, 0)/\sqrt{3}$, and the axis to be the last coordinate. Orient each unbiased vector $v = (x, y, z, t)$ so that $t = 1/2$. Put $r = \sqrt{3}/2$. The four remaining unbiasedness equations are

$$\begin{aligned} x + y + z &= r\sigma_0, & x + y - z &= r\sigma_1, \\ x - y + z &= r\sigma_2, & x - y - z &= r\sigma_3, \end{aligned}$$

where $\sigma_i \in \{\pm 1\}$. They force $\sigma_0 + \sigma_3 = \sigma_1 + \sigma_2$. Exactly six sign patterns satisfy this, giving $(x, y, z) = (\pm r, 0, 0), (0, \pm r, 0), (0, 0, \pm r)$. Thus all six remaining lines are exactly

$$(\pm\sqrt{3}/2, 0, 0, 1/2), \quad (0, \pm\sqrt{3}/2, 0, 1/2), \quad (0, 0, \pm\sqrt{3}/2, 1/2).$$

Together with the four cube diagonals in $\mathbb{R}^3 \times \{0\}$ and the last coordinate axis, this is the Cohn–Woo construction from Appendix A of [9]. Its absolute inner products are $0, 1/4, 1/3, 1/2$, whereas those of the 24-cell deletion are only $0, 1/2$; the classes are distinct. These computations also verify feasibility and complete the eleven-line classification, including the initially possible block pattern $5 + 5 + 1$.

For twelve lines in $\mathbb{R}^4$, at least three singular blocks occur. They must all have size four. After fixing one basis, all eight flat lines must occur, giving the 24-cell uniquely. This proves Theorem 2.2.

Remark 3.4. More generally, for $d \geq 2$, Proposition 3.2 gives $N \geq dr \geq d(N - D)$, and hence $N \leq d(d + 2)/2$. For even d, equality forces a union of $d/2 + 1$ mutually unbiased orthonormal bases. Levenshtein constructed systems attaining this size when d is a power of four [22]. Calderbank, Cameron, Kantor, and Seidel proved the basis decomposition for extremal line sets with absolute inner products 0 and $1/\sqrt{d}$ [7, Proposition 3.12]. This structural statement does not classify all such basis systems, nor their deletion-size equality cases. Those higher-dimensional questions are outside the present classification.

4. Exact constructions for the remaining three-dimensional cases

4.1. **How an algebraic Gram matrix specifies a code.** Let c be an isolated real root of a rational polynomial P. All identities below can be checked by polynomial division modulo P. To prove a strict sign, evaluate on a rational isolating interval, refining it by bisection until the interval has one sign. If a rational denominator occurs, verify separately that it is nonzero. No irreducibility assertion about P is used.

Here is a precise coefficient-certificate implementation of these checks. Represent a polynomial by its rational coefficient list in increasing degree order. Addition pads the shorter list with zeros; multiplication is the usual convolution, or recursively

$$(a :: p)q = aq + X(pq).$$

To certify that a polynomial R vanishes at a root of P, supply a quotient Q and check that every coefficient of $R - PQ$ is zero. Evaluation then proves the assertion. Thus polynomial division is a way to find a certificate, not an additional trusted operation. The Lean implementation `LinePackings/Arithmetic/PolynomialCertificates.lean` interprets lists using Mathlib's `Polynomial.ofCoeffList` and proves that these executable operations agree with polynomial arithmetic.

For signs on a nonnegative interval $[l, u]$, use Horner evaluation. The empty list has bounds $[0, 0]$. If the tail has bounds $[L, U]$, the list with constant coefficient a has bounds

$$[a + \min(lL, uL),\ a + \max(lU, uU)]\,.$$

Indeed $x \geq 0$ preserves the tail bounds on multiplication, and each endpoint multiple lies between its values at l and u. This proves the recursion by induction and reduces every asserted interval bound to rational arithmetic.

A symmetric matrix G with unit diagonal is a Gram matrix of rank three if its leading 3×3 block B is positive definite and

$$G_{ij} = G_{i,I} B^{-1} G_{I,j}, \qquad I = (0, 1, 2). \tag{4.1}$$

Indeed the columns in this formula give vectors in the positive definite inner product B^{-1}. An orthonormal basis transfers them isometrically to the ordinary Euclidean space. The same argument realizes any matrix $A^T H A$ when H is positive definite; it is formalized in `LinePackings/Geometry/Gram/GramRealization.lean`.

For clarity, the leading-minor test needed here is just square completion. For

$$B = \begin{pmatrix} 1 & a & b \\ a & 1 & d \\ b & d & 1 \end{pmatrix}, \qquad \Delta = 1 - a^2, \qquad D = 1 + 2abd - a^2 - b^2 - d^2,$$

the exact identity

$$v^T B v = (v_0 + a v_1 + b v_2)^2 + \Delta \left(v_1 + \frac{d - ab}{\Delta} v_2 \right)^2 + \frac{D}{\Delta} v_2^2$$

shows positive definiteness when $\Delta, D > 0$. The three squares can vanish simultaneously only for $v = 0$. This test is formalized in `LinePackings/Geometry/Gram/GramThree.lean`. For $c < 1$, checking $|G_{ij}| \le c$ for all $i \ne j$ proves feasibility. If the bound is attained, the equality pairs are exactly the contacts.

4.2. **Eight lines.** Mixon and Parshall [25] recovered an exact Gram matrix from the numerical eight-line packing of Conway, Hardin, and Sloane [11]. The following rational functions considerably shorten the expanded degree-eight entries of a Gram matrix over $\mathbb{Q}(c_8)$. Define

$$\begin{gathered} F_2(c) = \frac{4c^2 - c - 1}{c + 1}, \qquad F_3(c) = \frac{c(9c^2 - 2c - 3)}{(c + 1)^2}, \\ F_4(c) = \frac{16c^4 - 7c^3 - 5c^2 + 3c + 1}{(c + 1)^3}. \end{gathered} \tag{4.2}$$

At $c = c_8$, put

$$\begin{aligned} A &= -\frac{57c^4 - 498c^3 - 196c^2 + 98c + 43}{1537c^4 + 914c^3 + 96c^2 + 62c + 31}, & B &= -F_2(c), \\ D &= -\frac{(c - 1)(13c^3 + 3c^2 - 3c - 1)}{2c(c + 1)(3c + 1)}, & E &= \frac{c(31c^3 + 11c^2 - 7c - 3)}{(c + 1)^2(3c + 1)}, \\ F &= \frac{1537c^5 + 419c^4 - 582c^3 - 186c^2 + 29c + 15}{8(65c^3 + 31c^2 - 4c - 2)}, \\ H &= \frac{1537c^5 - 51c^4 - 1020c^3 - 284c^2 + 75c + 31}{2(5c + 3)(35c^2 + 10c - 1)}, & J &= -F_3(c), \qquad K = F_4(c). \end{aligned}$$

The required matrix is

$$G_8 = \begin{pmatrix} 1 & A & A & c & c & c & -c & -D \\ A & 1 & -c & c & -c & D & A & -c \\ A & -c & 1 & -c & c & c & F & -J \\ c & c & -c & 1 & B & -B & -c & B \\ c & -c & c & B & 1 & E & H & K \\ c & D & c & -B & E & 1 & J & -c \\ -c & A & F & -c & H & J & 1 & -c \\ -D & -c & -J & B & K & -c & -c & 1 \end{pmatrix}. \tag{4.3}$$

Polynomial reduction verifies (4.1) and all packing inequalities, with fourteen contacts and degrees $(4, 4, 4, 4, 3, 3, 3, 3)$. For a short reproducible positivity check, reduce each displayed rational function N/D to a polynomial q of degree at most eight by the extended Euclidean algorithm modulo P_8, and retain the quotient $(Dq - N)/P_8$. Coefficient certificates check these eight identities; Horner bounds on the stated isolating interval show that every denominator is positive, $0 < A < 17/100$, and each of A, B, D, E, F, H, J, K has absolute value less than $61/100 < c$. The leading block $B_0 = G_{I,I}$ has determinant

$$(1 + c)(1 - c - 2A^2) > 0,$$

since $c < 13/20$, and its second leading minor is $1 - A^2 > 0$. Finally check the polynomial identities $\det(B_0)G_{ij} - G_{i,I}\operatorname{adj}(B_0)G_{I,j} = 0$ by the same quotient certificates. These steps require only polynomial arithmetic and the preceding Gram-realization lemma. Lean checks the coefficient identities and realizes the resulting matrix in `LinePackings/DimensionThree/Eight/Construction.lean`.

4.3. **Nine lines.** Conway, Hardin, and Sloane described two inequivalent nine-line configurations whose minimum angles agreed numerically [11, § 3]. To give their Gram matrices, put $c = c_9$ and

$$a = \frac{13c^2 - 4c - 3}{2}, \qquad b = \frac{13c^2 - 6c - 1}{2}.$$

Exact sign checks give $0 < a < b < c < 1$. The two Gram matrices are

$$\begin{pmatrix} 1 & -c & -a & -c & a & c & -c & -c & -a \\ -c & 1 & c & c & a & -c & a & a & -c \\ -a & c & 1 & c & c & a & -c & -a & -c \\ -c & c & c & 1 & c & -a & -a & c & -a \\ a & a & c & c & 1 & c & -c & b & a \\ c & -c & a & -a & c & 1 & -c & a & b \\ -c & a & -c & -a & -c & -c & 1 & b & b \\ -c & a & -a & c & b & a & b & 1 & c \\ -a & -c & -c & -a & a & b & b & c & 1 \end{pmatrix} \tag{4.4}$$

and

$$\begin{pmatrix} 1 & c & c & c & a & b & a & b & b \\ c & 1 & a & c & c & c & -a & -b & -a \\ c & a & 1 & -a & -c & b & c & c & a \\ c & c & -a & 1 & c & -a & -c & a & c \\ a & c & -c & c & 1 & a & -c & -c & a \\ b & c & b & -a & a & 1 & c & -b & -c \\ a & -a & c & -c & -c & c & 1 & a & -c \\ b & -b & c & a & -c & -b & a & 1 & c \\ b & -a & a & c & a & -c & -c & c & 1 \end{pmatrix}. \tag{4.5}$$

Both satisfy (4.1) and the packing inequalities. The Lean proof in `LinePackings/DimensionThree/Nine/Construction.lean` distinguishes their congruence classes by the sums of squared Gram entries, which are

$$9 + 38c^2 + 26a^2 + 8b^2, \qquad 9 + 36c^2 + 24a^2 + 12b^2.$$

Their difference is $2(c^2 + a^2 - 2b^2) > 0$, since the root interval gives $c > 2/3$ and $0 < b < 21/50$. This sum is preserved by an orthogonal map, a permutation, and representative sign changes. Their minimum contact degrees are three.

4.4. **Ten lines: construction and the complete extra-line region.** Set

$$c = c_{10}, \qquad t = \sqrt{2c - 1}, \qquad r = \sqrt{2 - 2c}.$$

The nine-line core consists of the six representatives

$$h_k = (r\cos(k\pi/3), r\sin(k\pi/3), t), \quad k = 0, \ldots, 5,$$

and the three equatorial lines at azimuths $\pi/6, \pi/2, 5\pi/6$. The equation $2c^2+3c-3 = 0$ gives $r\sqrt{3}/2 = c$. Direct scalar products show that the core is feasible, has eighteen contacts, and has degree four at every vertex. The pole supplies a strictly noncontacting tenth line. Conway, Hardin, and Sloane observed that this line can move while the minimum angle stays fixed [11, § 3].

Represent any additional line in the northern hemisphere as

$$z = (\sin\theta\cos\phi, \sin\theta\sin\phi, \cos\theta), \qquad 0 \le \theta \le \pi/2.$$

Core symmetries reduce ϕ to $[0, \pi/6]$. Pairing h_k and h_{k+3} shows that all six latitude constraints are equivalent to

$$a\sin\theta + t\cos\theta \le c, \quad a = r\cos\phi, \qquad \sin\theta\cos(\pi/6 - \phi) \le c \tag{4.6}$$

where the second inequality collects the equatorial constraints. The symmetry reduction is also checked for arbitrary feasible vectors in Lean. Rotation by $\pi/3$ sends h_k to h_{k+1} and (e_0, e_1, e_2) to $(e_1, e_2, -e_0)$; reflection $(x, y, z_3) \mapsto (x, -y, z_3)$ sends h_k to h_{-k} and e_j to $-e_{2-j}$. These are actual ambient isometries applied to the extra vector as well as the core. After choosing its northern representative, take $\theta = \arccos z_3$ and the complex argument of $x + iy$ for an initial azimuth. The norm-times- argument identities include the pole without division by the horizontal radius. An integer multiple of $\pi/3$, followed if necessary by reflection, puts the azimuth in the closed sector. Thus the sector conditions used below are produced from the original unit vector. Here $c \le a \le r$ and $t < c$. Here is an algebraic way to

isolate the correct sublevel component, including its boundary. Put $u = \tan(\theta/2)$ and

$$Q(u) = (c+t)u^2 - 2au + c - t, \qquad s = \frac{a - \sqrt{a^2+t^2-c^2}}{c+t}.$$

Since $0 < t < c \le a$, the square root is at least t and less than a. Rationalizing gives

$$0 < s = \frac{c-t}{a+\sqrt{a^2+t^2-c^2}} \le \frac{c-t}{c+t} < 1, \qquad Q(s) = 0.$$

For $0 \le \theta < \pi/2$, we have $0 \le u < 1$ and

$$c - a\sin\theta - t\cos\theta = \frac{Q(u)}{1+u^2}, \qquad Q(u) = (u-s)\big((c+t)(u+s) - 2a\big).$$

The second factor is strictly negative: $(c+t)u < c+t$, $(c+t)s \le c-t$, and $c \le a$. Thus the latitude inequality holds exactly when $u \le s$. At $\theta = \pi/2$, the equatorial constraint fails because $\cos(\pi/6 - \phi) \ge \sqrt{3}/2 > c$. Consequently the exact feasible region is

$$0 \le \phi \le \pi/6, \quad 0 \le \theta \le \Theta(\phi), \qquad \Theta(\phi) = 2\arctan\frac{a - \sqrt{a^2+t^2-c^2}}{c+t}. \tag{4.7}$$

There is no other component. To verify that all equatorial inequalities are strict on this component, the rough rational bounds $17/25 < c < 7/10$ and $3/5 < t < c$ suffice. They imply $(c-t)/(c+t) < 1/12$, whence

$$0 < \Theta(\phi) < 1/6, \qquad \sin\theta \le \theta \le \Theta(\phi) < 1/6 < c.$$

We used only $\arctan s \le s$ for $s \ge 0$; also $s < 1$ gives $\Theta(\phi) < \pi/2$. The same inequalities prove feasibility on the entire closed region: in the sector, $|\cos(\phi - k\pi/3)| \le \cos\phi$ for every k, so the latitude constraints follow by the triangle inequality, and the equatorial ones follow from $|\cos x| \le 1$.

Before symmetry reduction the northern component is a closed curvilinear hexagon. Its interior points have no contacts, an open boundary arc has one, and a corner has two: the maximizing latitude cosine has respectively no active equality, one maximizer, or two adjacent maximizers. The equatorial constraints remain strict. All values of ϕ represent the same point when $\theta = 0$.

There are no further identifications in this parameter region. A useful proof uses the same Gram-moment invariant that distinguished the two nine-line constructions, and avoids identifying the core from contact degrees. For any unit extension $X = C \cup \{z\}$ of the fixed core, put

$$S_m(z) = \sum_{x\in C} \langle x, z\rangle^m, \qquad I_m(X) = \sum_{x,y\in X} \langle x, y\rangle^m.$$

For even m, I_m is unchanged by rigid motions, permutations, and representative sign changes. Since $I_m(X) = I_m(C) + 2S_m(z) + 1$, congruent extensions have equal S_m. Here are all the moment calculations needed. For $z = (x, y, z_3)$, write $u = x^2 + y^2$ and $H = x^6 - 15x^4y^2 + 15x^2y^4 - y^6$. Expanding the nine scalar products gives

$$\begin{aligned} S_2 &= (3r^2 + 3/2)u + 6t^2 z_3^2, \\ S_6 &= 6t^6 z_3^6 + 45r^2t^4 u z_3^4 + \frac{135}{4} r^4 t^2 u^2 z_3^2 \\ &\quad + \left(\frac{15}{8} r^6 + \frac{15}{16}\right) u^3 + \frac{3}{32}(2r^6 - 1)H. \end{aligned}$$

In polar coordinates, $u = \sin^2\theta$ and $H = \sin^6\theta\cos(6\phi)$, the latter following by the double- and triple-angle cosine formulas. Thus

$$S_2 = (15/2 - 6c) + (18c - 27/2)\cos^2\theta.$$

Its coefficient of $\cos^2\theta$ is negative, and $0 \le \theta < \pi/2$, so equality of S_2 forces equality of θ. In S_6, all remaining azimuthal dependence is $(3/32)(2r^6 - 1)\sin^6\theta\cos(6\phi)$. We have $r^2 < 16/25$, hence $r^6 < 1/2$. For $\theta > 0$, this coefficient is nonzero. The cosine is injective on $0 \le 6\phi \le \pi$, so equality of S_6 then forces equality of ϕ. For $\theta = 0$, all azimuths give the identical pole. Conversely, these parameter identifications plainly give identical codes. This proves exactly

$$X(\theta,\phi) \cong X(\theta',\phi') \quad \Longleftrightarrow \quad \theta = \theta' \text{ and } (\theta = 0 \text{ or } \phi = \phi').$$

Section 13.3 proves the separate global assertion that every optimum contains the core and therefore belongs to this family.

4.5. **Eleven and twelve lines.** For the eleven-line configuration in [11, Table 1], put $c = c_{11}$, $v = (1+\sqrt{5})/4$, and

$$a = \sqrt{\frac{1+\sqrt{5}-4c}{5+\sqrt{5}}}.$$

Take the pole and the representatives

$$z_k = (\sqrt{1-a^2}\cos(2k\pi/5), \sqrt{1-a^2}\sin(2k\pi/5), a),$$
$$y_k = (\sqrt{1-c^2}\cos((2k+1)\pi/5), \sqrt{1-c^2}\sin((2k+1)\pi/5), c), \qquad k = 0,\dots,4.$$

The five pole-to-y contacts, ten nearest-ring contacts, and five outer diagonals have respective scalar products $c, c, -c$. The defining equations are

$$a^2 - (1-a^2)v = -c, \qquad ac + v\sqrt{(1-a^2)(1-c^2)} = c.$$

Eliminating a, with the displayed positive signs, gives

$$5c^3 + (100+45\sqrt{5})c^2 - (45+20\sqrt{5})c - 20 - 9\sqrt{5} = 0.$$

For completeness, the following identities check the converse without assuming any radical signs. Write $s = \sqrt{5}$, $A = 5c^3+100c^2-45c-20$, and $B = 45c^2-20c-9$. Then $(A+sB)(A-sB) = 5P_{11}(c) = 0$. The root interval gives $357/500 < c < 143/200$, hence $A > 0$ and $B < 0$. Thus $A - sB > 0$, which selects $A + sB = 0$, the displayed cubic. Rationalizing the formula for a^2 gives

$$a^2 = \frac{s(c+1)}{5} - c, \qquad \frac{1}{5} < a < \frac{1}{4};$$

these bounds follow already from $223/100 < s < 224/100$ and the preceding bounds for c. Define

$$T = \frac{5c^3s - 15c^3 + 5c^2s + 25c^2 - cs - 5c - s - 5}{20}.$$

Expansion, using $s^2 = 5$, gives

$$T = c^2(1+a^2) - v^2(1-a^2)(1-c^2),$$
$$T^2 - 4c^4a^2 = \frac{(c+1)^2((35-15s)c + 15 - 7s)}{200}(A+sB) = 0.$$

The first identity gives $T \geq 2c^2 - 1 > 0$, since $0 < a < 1$ and $0 < v < 1$. Therefore $T = 2c^2 a$, and

$$v^2(1-a^2)(1-c^2) = c^2(1-a)^2.$$

Both square roots and $c(1-a)$ are positive, proving the required nearest-ring contact equation with its displayed signs.

The remaining pairs admit uniform bounds. Put $q = (s-1)/4 < 1/3$. For distinct vertices of one regular pentagon, the azimuthal cosine is either q or $-v$; between staggered pentagons it is at most v and at least -1. The outer-ring lower bound is the diagonal contact $-c$, and its upper bound is $a^2 + (1-a^2)/3 < c$. The inner-ring products lie between $2c^2 - 1 > 0$ and $c^2 + (1-c^2)/3 < c$. For cross-ring pairs let $h = \sqrt{1-a^2}\sqrt{1-c^2}$. Since $h \leq \sqrt{1-c^2} < c$, their products lie between $ac - h > -c$ and $ac + vh = c$. Pole products are $a < c$ and c. This proves feasibility and exact coherence for the displayed coordinate list. Lean uses these representatives in `LinePackings/DimensionThree/Eleven/Construction.lean`. The contact degrees are $(5, 4, 4, 4, 4, 4, 3, 3, 3, 3, 3)$.

For the twelve rhombicuboctahedral lines we use the coordinates given by Fickus, Jasper, and Mixon [18, § 6.1]. Put $a = 1 + \sqrt{2}$, $D = a^2 + 2 = 5 + 2\sqrt{2}$. Take the normalized permutations of $(\pm a, \pm 1, \pm 1)$, identifying antipodes. There are twelve lines. Their common shortest Euclidean chord before normalization has length two, hence the contact scalar product is

$$1 - \frac{2}{D} = \frac{a^2}{D} = \frac{7 + 4\sqrt{2}}{17} = c_{12}.$$

There are twenty-four projective contacts, four at every vertex. The supporting planes with normals of types $(\pm 1, \pm 1, \pm 1)$, coordinate axes, and permutations of $(\pm 1, \pm 1, 0)$ give eight triangles and eighteen squares on the antipodal sphere. These coordinates and every pairwise inequality are checked directly in $\mathbb{Q}(\sqrt{2})$. Lean proves attainment for the normalized coordinate list in `LinePackings/DimensionThree/Twelve/Rhombicuboctahedron.lean`. Section 12.4 classifies every realization of their signed contact map. For 24 points free to move independently on S^2, Robinson proved that the vertices of the snub cube maximize the minimum separation [36].

5. One isolation-and-selection principle

The same argument handles an isolated optimum, finitely many isolated optima, and a fixed rigid core with an admissible extra line. It is important to prove isolation among *all* competitive configurations, including those with fewer contacts than the reference.

5.1. **An algebraic isolation certificate for five lines.** For five lines there is a shorter alternative to the stress calculation below. Put $c = 1/\sqrt{5}$, order the ten pairs lexicographically as $01, 02, 03, 04, 12, 13, 14, 23, 24, 34$, and put

$$\sigma = (-1, 1, -1, 1, 1, -1, -1, -1, 1, 1).$$

For $z \in \mathbb{R}^{10}$, let $G(z)$ be the symmetric matrix with diagonal entries one and upper-triangular entries $\sigma_i z_i$, and set

$$F(z) = -\sum_{r=0}^{4} \det G(z)_{\widehat{r},\widehat{r}}, \qquad p = (c, \ldots, c).$$

For a configuration $(x_a)_{a=0}^4$, its signed coordinates are $z_i = \sigma_i\langle x_a, x_b\rangle$, where i indexes the pair ab. The Gram matrix of the five-line reference, after choosing its signs and order, is $G(p)$. Every unit configuration in $\mathbb{R}^3$ satisfies $F(z) = 0$, since each displayed minor has order four. Every competitive configuration satisfies $z_i \le c$, regardless of the signs of its actual scalar products.

Here is a purely algebraic way to check local isolation. Let $z^{[i]}$ denote z with its first i coordinates replaced by c. The polynomial

$$q_i(c, z) = \frac{F(z^{[i]}) - F(z^{[i+1]})}{z_i - c}$$

means polynomial division, not a function with an exceptional value at $z_i = c$: the numerator is divisible by $z_i - c$. Telescoping gives

$$F(z) - F(p) = \sum_{i=0}^{9} (z_i - c) q_i(c, z).$$

Expansion of the five determinants gives

$$F(p) = -5(c-1)(c+1)(5c^2-1) = 0,$$
$$q_i(c,p) = \begin{cases} -2c(c-1)(5c+3), & i \in \{0,2,4,8,9\}, \\ -2c(c+1)(5c-3), & i \in \{1,3,5,6,7\}. \end{cases}$$

Both values are positive for $0 < c < 3/5$. Continuity therefore makes all ten coefficients positive in some neighborhood of p. If $z_i \le c$ and $F(z) = F(p)$ there, every term in the sum is nonpositive and their sum is zero, so each $z_i = c$. Thus the labelled Gram matrix is locally fixed. Equality of Gram matrices gives an ambient orthogonal map, and signed permutations transport these neighborhoods to every member of the reference congruence class. This proves that the whole class is relatively open in the competitive set. It does not require preservation of contacts or a choice of coordinate frame.

This calculation is reconstructed by forming the displayed matrix, expanding its five order-four determinants, and doing the ten exact polynomial divisions above. The self-contained Lean files `LinePackings/DimensionThree/Five/IsolationPolynomial.lean` and `LinePackings/DimensionThree/Five/Isolation.lean` check the identities and the neighborhood argument. The general algebraic observation is in `LinePackings/Geometry/OrthantIsolation.lean`.

5.2. **Quantitative isolation from a positive stress.** Tarnai studied rigidity of antipodal circle packings through their contact graphs [41]. Cohn, Jiao, Kumar, and Torquato used the infinitesimal rigidity criterion of Connelly, Roth, and Whiteley to test spherical codes by linear programming [8, § 2]. Here a positive stress and a rank estimate give an explicit neighborhood in which every competitive core is congruent to the reference core.

Let $p_0, \dots, p_{m-1} \in \mathbb{R}^3$ be reference representatives of a rigid core, all of a common norm $\rho > 0$, with contact signs s_{ij} and contact scalar products $s_{ij}c\rho^2$. Suppose positive weights w_{ij} on the unordered contact edges satisfy

$$\sum_j w_{ij}(s_{ij}p_j - cp_i) = 0, \qquad \Delta_i = \sum_j w_{ij}. \tag{5.1}$$

Align a nearby competitive configuration, in the same scale, and write its representatives as $p_i + \eta_i$. Set $T^2 = \sum_i \|\eta_i\|^2$. Use either the fixed frame

$$p_0 = (\rho, 0, 0), \quad p_1 = (u, v, 0), \quad v > 0,$$

for both configurations, or a best orthogonal alignment. The corresponding three linear gauge equations are respectively $\eta_{0,2} = \eta_{0,3} = \eta_{1,3} = 0$, or $\sum_i p_i \times \eta_i = 0$. For the latter, minimize the squared alignment error over the entire congruence orbit, including representative signs and labels. A minimizer exists: the orbit is bounded and is closed by the finitely many signed Gram-matrix equations. Here is an algebraic proof of its gauge equations. For orthonormal vectors u, v, compose reflection in $\mathbb{R}u$ with reflection in $\mathbb{R}(u + tv)$, calling the resulting isometry R_t. Writing $q_i = p_i + \eta_i$, put

$$\alpha = \sum_i (\langle p_i, u\rangle\langle u, q_i\rangle + \langle p_i, v\rangle\langle v, q_i\rangle), \qquad \beta = \sum_i (\langle p_i, v\rangle\langle u, q_i\rangle - \langle p_i, u\rangle\langle v, q_i\rangle).$$

The reflection formula $x \mapsto 2\langle w, x\rangle w/\|w\|^2 - x$ gives

$$\sum_i \langle p_i, R_t q_i\rangle - \sum_i \langle p_i, q_i\rangle = \frac{2}{1+t^2}(t\beta - t^2\alpha).$$

Minimality of the alignment error implies $t\beta \le t^2\alpha$ for every real t. Taking $t = 1, -1$ gives $\alpha \ge 0$, and then $t = \beta/(\alpha+1)$ forces $\beta = 0$. Apply this to the three coordinate planes and use $p_i \times p_i = 0$ to obtain $\sum_i p_i \times \eta_i = 0$.

Define the norm and contact linear forms

$$N_i = \langle p_i, \eta_i\rangle, \qquad L_{ij} = s_{ij}(\langle p_i, \eta_j\rangle + \langle p_j, \eta_i\rangle).$$

Equal norms and the packing inequalities give

$$\begin{aligned} N_i &= -\tfrac{1}{2}\|\eta_i\|^2, \\ L_{ij} &\le -s_{ij}\langle \eta_i, \eta_j\rangle \le \tfrac{1}{2}(\|\eta_i\|^2 + \|\eta_j\|^2) \le \tfrac{1}{2}T^2. \end{aligned} \tag{5.2}$$

Summing over the unordered contact edges gives the stress identity

$$\sum_{ij} w_{ij} L_{ij} = c\sum_i \Delta_i N_i = -\frac{c}{2}\sum_i \Delta_i \|\eta_i\|^2. \tag{5.3}$$

Bounding every other contact from above gives, for each edge,

$$L_{ij} \ge -\frac{(1+c)\max_i \Delta_i}{2w_{ij}} T^2.$$

Thus every norm or contact form is bounded in absolute value by MT^2, where

$$M \ge \max\left\{\tfrac{1}{2}, \frac{(1+c)\max_i \Delta_i}{2\min_{ij} w_{ij}}\right\}.$$

Put the norm, contact, and three gauge rows in a matrix A. It may be rectangular; selecting an invertible square submatrix is optional. For any rational matrix B, a certified residual $\varepsilon = \|I - BA\|_\infty < 1$ gives

$$\|\eta\|_\infty \le \frac{\|B\|_\infty}{1-\varepsilon}\|A\eta\|_\infty. \tag{5.4}$$

This follows immediately by moving the residual term to the left; it assumes neither a numerical inverse nor a singular-value estimate. If the quotient is at most K, then

$$T \le \sqrt{3m}\, KM\, T^2.$$

Consequently either $T = 0$, or $T \geq 1/(\sqrt{3m}KM)$. This is uniform local isolation.

One useful strengthening avoids replacing every row of $A\eta$ by the same coarse bound. For either sign of a row of B, write its norm/contact coefficients as b_i, b_e. Choose $\lambda \geq 0$ so that $b_e + \lambda w_e \geq 0$ for every contact. Adding λ times $\sum_e w_e L_e - c\sum_i \Delta_i N_i = 0$ and using (5.2) shows that the signed row is at most DT^2, where it suffices that

$$D \geq \frac{1}{2} \max_i \left(\sum_{e \ni i} b_e - b_i + \lambda(1+c)\Delta_i \right). \tag{5.5}$$

Verify this for both signs of every row. Then $\|\eta\|_\infty \leq CT^2$ for $C \geq D/(1-\varepsilon)$. For unit representatives, coordinate differences at most $1/(6mC)$ force $T = 0$. The identities with nonconstant weighted degrees, the signed-row estimate (5.5), and this last nonlinear displacement implication are checked in `LinePackings/Optimality/VariableStress.lean`, `LinePackings/Optimality/StressRows.lean`, and `LinePackings/Geometry/InverseRowBounds.lean`. These general lemmas require the actual stress, row, and residual certificates; they do not assume local isolation.

Stress and inverse certificates. Use the displayed Gram matrices for eight and nine lines. For ten lines, let e_j be the equatorial representative at azimuth $\pi/6 + j\pi/3$, and order the nine core representatives as

$$(h_0, -h_2, -h_1, -h_5, e_1, -e_2, -h_3, -e_0, -h_4).$$

For eleven lines use the order

$$(P, z_0, z_2, z_1, z_3, z_4, y_2, -y_3, -y_1, y_4, y_0)$$

from Section 4.5. These orders fix only the numerical coordinate tolerances below. Their Gram entries require no trigonometric approximation: the hexagon cosines are $1, 1/2, -1/2, -1, -1/2, 1/2$, and, with $q = (\sqrt{5}-1)/4$, the pentagon cosines are $1, q, -v, -v, q$, while the staggered cosines are $v, -q, -1, -q, v$. For the eleven-line arithmetic the identities

$$\sqrt{5} = -\frac{5c^3 + 100c^2 - 45c - 20}{45c^2 - 20c - 9}, \qquad a = \frac{c^2 - (1-c^2)v^2}{c^2 + (1-c^2)v^2},$$
$$\sqrt{(1-a^2)(1-c^2)} = \frac{c(1-a)}{v}$$

put every Gram entry in $\mathbb{Q}(c)$. Polynomial reduction and the positive signs verify these identities. For ten lines, use the root interval $(0.686140, 0.686141)$.

List contacts in lexicographic order of their endpoint pairs. Construct the $3m$-by-E equilibrium matrix U, using the first three Gram columns as coordinates: in column ij, its three entries at vertex i are $s_{ij}G_{jk} - cG_{ik}$, $k = 0, 1, 2$, and similarly at j. All other entries vanish. These coordinates are related to Euclidean coordinates by an invertible linear map, so the kernel is unchanged. To propose a stress, find a kernel basis K by exact Gaussian elimination. Projecting the all-ones vector onto the kernel gives

$$w = K(K^T K)^{-1} K^T \mathbf{1}. \tag{5.6}$$

The projection is independent of the chosen basis. The Lean certificates check positivity and equilibrium of the explicit weights described below.

For eight lines, the stress certificate sets one free edge weight to one. Exact elimination from the displayed Gram formulas supplies its fourteen polynomial weights. Their signs are checked on the refined root interval

$$\frac{647588978734}{10^{12}} < c < \frac{647588978735}{10^{12}}.$$

All sixty-four full Gram-column equilibrium identities are checked modulo P_8, not merely the first three columns. For any realization, the equilibrium residual is orthogonal to every reference representative and is itself a linear combination of them. Its squared norm is therefore zero; no seed-spanning assumption is needed for this step. `LinePackings/DimensionThree/Eight/StressData.lean` and `LinePackings/DimensionThree/Eight/Stress.lean` prove positive vector equilibrium for every realization of (4.3) and supply such a stressed configuration from the proved construction.

The positive-height seed frame and its normalization are also checked. For seed Gram entries a, b, d, put

$$q = \sqrt{1-a^2}, \qquad h = \frac{d-ab}{q}, \qquad t = \sqrt{1-b^2-h^2}.$$

The public parameter domain is $1 - a^2 > 0$ and $1 + 2abd - a^2 - b^2 - d^2 > 0$; these imply $q, t > 0$. In the frame $(1,0,0), (a,q,0), (b,h,t)$, the unique vector with prescribed scalar products r_0, r_1, r_2 is

$$\left(r_0, \frac{r_1 - ar_0}{q}, \frac{r_2 - br_0 - h(r_1 - ar_0)/q}{t}\right).$$

Existence and uniqueness are proved before defining this solver. Applying it to the actual seed scalar products gives a normalization induced by an ambient orthogonal map; it preserves the full Gram matrix. Its explicit formula is continuous throughout the independent unit-seed domain, without choosing a continuous family of orthogonal maps. For the eight-line reference, every sufficiently near unit configuration therefore has a congruent representative in the three frame gauges, with the same coherence and coordinate errors less than any prescribed $\delta > 0$. The neighboring Gram matrix and contacts may change. These assertions are checked in `LinePackings/Geometry/Frames/SeedFrames.lean`, `LinePackings/Geometry/Frames/SeedFrameContinuity.lean`, `LinePackings/Geometry/SeedNormalization.lean`, `LinePackings/Geometry/SeedNeighborhoods.lean`, `LinePackings/DimensionThree/Eight/Frames.lean`, and `LinePackings/DimensionThree/Eight/FrameNeighborhoods.lean`. They supply the geometric normalization step used by the numerical certificate below.

For the eight-line numerical certificate, all twenty-four actual reference coordinates are enclosed by rational intervals with denominator 10^8, using the proved Gram polynomials, rational comparisons for the two square roots, and positive division. The matrix A has eight norm rows, fourteen contact rows, and the three fixed-frame coordinate rows, hence size 25 by 24. A rational midpoint calculation proposes B with denominator 2^{40}. Integer endpoint arithmetic proves every residual row sum strictly less than $1/1024$. For both signs of each of the twenty-four rows of B, the checked compensation coefficients have denominator 10^6; the shifted contact coefficients are nonnegative, and the vertexwise bound in (5.5) is at most $467 \cdot 1023/1024$. Thus $\|\eta\|_\infty \le 467T^2$. The closed coordinate condition $|\eta_{ik}| \le 1/22416$ forces $\eta = 0$. No reference contact is required to persist in the competitor. `LinePackings/`

`DimensionThree/Eight/LocalIsolation.lean` proves this fixed-frame statement and, using the continuous normalization, relative openness of the entire signed and relabeled Gram class in the competitive set. `LinePackings/DimensionThree/Eight/Selection.lean` applies the geometric selector to the actual compact, relatively open class. The census and case proofs use this selection to classify all competitive eight-line configurations.

The same argument supplies isolation for both nine-line forms with different constants. Their seed Gram triples are $(-c, -a, c)$ and (c, c, a), where $a = (13c^2 - 4c - 3)/2$, and the root is refined to

$$\frac{669362319281}{10^{12}} < c < \frac{669362319282}{10^{12}}.$$

Exact elimination supplies nineteen and eighteen candidate stress weights; Lean checks all thirty-seven signs and all eighty-one full Gram-column identities for each form. The actual frames have fifty-four checked coordinate enclosures. Their fixed-frame matrices have sizes 31 by 27 and 30 by 27; all fifty-four residual row tests and all one hundred eight signed-row tests are checked against the actual reference configurations. The resulting constants are $C = 22$ and $C = 15$, giving the closed framed radii $1/1188$ and $1/810$, respectively. No competitor contact is assumed to persist. The two `LinePackings/DimensionThree/Nine/ALocalIsolation.lean` and `LinePackings/DimensionThree/Nine/BLocalIsolation.lean` proofs give ambient local congruence; `LinePackings/DimensionThree/Nine/LocalIsolation.lean` proves compactness and relative openness of the full union of the two signed and relabeled Gram classes. `LinePackings/DimensionThree/Nine/Selection.lean` uses that union to select a hypothetical counterexample.

For eleven lines the same argument applies to the prescribed pole-and-two-pentagons construction. With its parameters a, c, use the three positive stress values

$$\alpha = \frac{2(c^2 - a)}{1 - c^2}, \qquad \beta = \frac{c(1 - a)}{a(1 + c)}, \qquad \gamma = 1$$

on the pole-to-inner, outer-diagonal, and nearest cross-ring contacts, respectively. The root and latitude bounds prove positivity. Exact pentagon cosine tables identify the complete Gram matrix in the signed ordering above. Polynomial identities prove all 121 Gram-column equilibrium equations for these weights. The refined interval is

$$\frac{714434497394}{10^{12}} < c < \frac{714434497395}{10^{12}}.$$

The first three vectors in this ordering have seed Gram triple $(a, a, -c)$, whose positive minors follow from the construction bounds. Their continuous normalization produces the actual reference frame and all nearby unit competitors. All 33 frame coordinates have rational enclosures with denominator 10^8. The fixed-frame derivative has 34 rows and 33 columns; its proposed inverse has 1122 integer numerators and denominator 2^{40}. Lean checks all 33 strict residual-row bounds below $1/1024$, all 66 signed-row compensations, and the vertex bounds at $6 \cdot 1023/1024$. Thus $C = 6$ gives the closed framed radius $1/396$, allowing contacts to be lost. `LinePackings/DimensionThree/Eleven/LocalIsolation.lean` transports this result to ambient local congruence and relative openness of the entire signed and relabeled class of `elevenLines`. The radius $1/396$ is for the normalized seed frame.

For the ten-line family, the isolated object is its fixed nine-line core. The signed ordering above has seed triple $(2 - 3c, -c, c)$, with $c = c_{10}$, and the refined interval

is

$$\frac{686140661634}{10^{12}} < c < \frac{686140661635}{10^{12}}.$$

The seed determinant is $57c - 39 > 0$, using $2c^2 + 3c - 3 = 0$. One positive stress assigns $(63 + 40c)/67$ to latitude–latitude contacts and $(40 + 2c)/67$ to latitude–equator contacts. Lean checks all eighteen signs and all eighty-one full Gram-column equilibrium equations against the actual core. All twenty-seven frame coordinates are enclosed with denominator 10^8. The fixed-frame matrix has size 30 by 27; its inverse witness has 810 integer numerators and denominator 2^{40}. The twenty-seven strict residual-row tests below $1/1024$ and fifty-four signed-row tests give $C = 8$ and the closed framed tolerance $1/432$, with no contact-persistence requirement. `LinePackings/DimensionThree/Ten/CoreIsolation.lean` transports this to local congruence of the original nine-line core.

The extra vector remains free in its entire closed feasible region. `LinePackings/DimensionThree/Ten/SectorReduction.lean` proves that every unit feasible extra vector yields an admissible family member, including the pole and the boundary. `LinePackings/Geometry/ConfigurationExtensions.lean` extends an actual core congruence using the same ambient isometry on the tenth vector. Pulling back the core neighborhood through restriction to nine labels, then applying this extension and the sector reduction, proves relative openness of the full ten-line family in `LinePackings/DimensionThree/Ten/LocalFamily.lean`. The common selector in `LinePackings/Geometry/Peeling/LargePeelingSelection.lean` uses that openness and compactness to select a hypothetical nonmember. The packed census and case proofs exclude it in `LinePackings/DimensionThree/Ten/Completeness.lean`.

Construct the unit Euclidean frame from the first three Gram rows by (9.8), with positive third coordinate, and obtain each remaining point by solving its three scalar-product equations. Use all norm rows, all contact rows, and the three frame gauges in A, in that order. Refine the root interval to width less than 2^{-200}; enclose the frame entries by outward arithmetic at 80 binary fractional bits. If A_0 is the rational midpoint matrix, calculate

$$B_0 = (A_0^T A_0)^{-1} A_0^T, \qquad B = 2^{-40}\,\mathrm{round}(2^{40} B_0)$$

entrywise, rounding ties to the even integer. All operations defining B_0 are rational Gaussian elimination. Verify $\varepsilon = \|I - BA\|_\infty < 1/1024$. For each signed row of B, choose $\lambda = \max(0, \max_e(-b_e/\underline{w}_e))$, using positive lower bounds $\underline{w}_e$; evaluate (5.5) with upper bounds for c and Δ_i. This gives the constants in the following table. The residual and positive-weight checks, not the midpoint construction, prove the assertions.

Finite calculation 5.1. The constructions above have positive stresses and the inverse certificates just described. The verified unit-coordinate neighborhoods are as follows:

core	contacts	C	coordinate tolerance
8	14	467	1/22416
9, matrix (4.4)	19	22	1/1188
9, matrix (4.5)	18	15	1/810
10, nine-line core	18	8	1/432
11	20	6	1/396
12	24	see below	1/3000

For the first five rows the norm and contact derivative has rank $3m-3$, and the frame gauges complete it to rank $3m$. The Lean isolation proofs check the stress and inverse data and apply the bounds to the exact constructions. The five-line proof uses the polynomial argument of Section 5.1.

For twelve lines a particularly simple certificate uses the unnormalized coordinates of Section 4.5. Triangular contact edges have weight 1, and the other contacts have weight $b = 2 - \sqrt{2}/2$. Then

$$\Delta_i = 6 - \sqrt{2}, \qquad c_{12}\Delta_i = 2 + \sqrt{2}, \qquad (1 + c_{12})\Delta_i = 8.$$

Hence $|L_e| \le 4T^2$. The best-alignment gauge and a rational inverse certificate give $K = 4$. Thus $T \le 96T^2$. Since $\rho = \sqrt{5 + 2\sqrt{2}} < 3$, a competitive configuration at positive distance from the reference orbit has unit product-space distance at least $1/288$. Unit-coordinate errors below $1/3000$ have scaled product distance below $18/3000 < 1/96$, so they force congruence. In particular, a unit configuration X of coherence at most c_{12} satisfying $\sum_i \|X_i - p_i/\rho\|^2 < 1/100000$ is congruent to the reference: its best aligned scaled squared error is below $9/100000 < 1/9216$, whereas a nonzero error has $T^2 \ge 1/9216$. The congruence class is therefore relatively open in the competitive set; transport this neighborhood by the isometry, labels, and signs of any reference congruence. All entries in this calculation lie in $\mathbb{Q}(\sqrt{2})$; the square roots needed for unit normalization need only the bound $\rho < 3$. The following small-integer recipe reconstructs the stronger inverse bound. Order the twelve representatives by the position of the positive coordinate $1 + \sqrt{2}$, and within each group order the other two signs as $(++), (+-), (-+), (--)$. Order contacts lexicographically. Use the twelve norm rows, the twenty-four signed contact rows, and the three coordinates of $\sum_i p_i \times \eta_i$, in that order, with columns ordered by vertex and then coordinate. Thus $A = A_0 + \sqrt{2}A_1$ for integer matrices A_0, A_1. Set

$$H = A_0 + \frac{169}{120}A_1, \qquad D = 10^6, \qquad Z = \operatorname{round}\big(D(H^T H)^{-1}H^T\big), \qquad B = Z/D,$$

again rounding ties to the even integer. Define integer residuals $R_0 = DI - ZA_0$ and $R_1 = -ZA_1$. For every row i, check

$$\sum_k |Z_{ik}| \le 3D, \qquad 4\sum_j \max\{|60(R_0)_{ij} + 84(R_1)_{ij}|, |60(R_0)_{ij} + 85(R_1)_{ij}|\} \le 60D.$$

Since $7/5 \le \sqrt{2} \le 17/12$, the endpoint bound for an affine function gives $\|B\|_\infty \le 3$ and $\varepsilon = \|I - BA\|_\infty \le 1/4$; hence $K = 4$. The integer data and residual checks are in `LinePackings/DimensionThree/Twelve/IsolationData.lean`. The proof in `LinePackings/DimensionThree/Twelve/LocalIsolation.lean` applies them to the actual construction.

5.3. **The common classification principle.**

Proposition 5.2. *Fix $N \ge 4$ and a target coherence $0 < c_* < 1$. Let $F \subset (S^2)^N$ consist of configurations with coherence at most c_*, and let $\mathcal{C} \subset F$ be a compact family of proposed optima, all with coherence c_*. Suppose the preceding isolation argument makes $\mathcal{C}$ relatively open in F. If $F \setminus \mathcal{C} \ne \varnothing$, there is a configuration X outside $\mathcal{C}$ with these properties:*

1. *X is a local minimum of coherence.*
2. *At every nonisolated contact vertex, the tangent contact directions are not contained in a closed semicircle.*

(3) *Write* $c = \mu(X)$ *and* $E_c(Z) = \{ij : |\langle z_i, z_j\rangle| = c,\ i < j\}$. *There is no* $Y \in F \setminus \mathcal{C}$ *with* $\mu(Y) \le c$ *and* $E_c(Y) \subsetneq E_c(X)$.

Proof. Both F and $F \setminus \mathcal{C}$ are compact. Sort the $\binom{N}{2}$ absolute scalar products in nonincreasing order. Each order statistic is continuous: the k-th largest is the maximum over k-element subsets of their minimum. Successively minimize these finitely many continuous functions on the remaining compact minimizer sets. This gives a lexicographic minimum X. Small perturbations of X remain outside the closed set $\mathcal{C}$. A sufficiently small improvement of coherence would therefore contradict the first minimized coordinate, proving local minimality.

At a contact vertex x, orient the contact neighbors y so that $\langle x, y\rangle = c = \mu(X) > 0$; positivity follows because $N \ge 4$ lines in $\mathbb{R}^3$ cannot be mutually perpendicular. If their tangent directions lie in a closed semicircle, choose a unit tangent u with $\langle u, y\rangle \le 0$ for all of them. Use the unit motion

$$x(t) = \frac{x + tu}{\sqrt{1 + t^2}}.$$

This is the great-circle motion with angular parameter $\arctan t$. For $t > 0$, it gives $\langle x(t), y\rangle \le c/\sqrt{1 + t^2} < c$. For sufficiently small t, continuity also keeps this scalar product above $-c$, and all noncontacts retain strict slack. At least one contact is lost and none is added, strictly improving the sorted list. This is impossible.

For the third assertion, the sorted list for such a Y would have fewer entries equal to c and all other entries below c. It is therefore lexicographically smaller. Lean carries these three properties of the selected packing through the cut and into the case proofs in `LinePackings/Geometry/GeometricSelection.lean` and `LinePackings/Geometry/Peeling/SelectedPeeling.lean`. □

The compactness and relative openness hypotheses hold for every family used here. For an isolated code, its full congruence class is closed: the signed Gram characterization expresses it as a finite union, over permutations and representative signs, of sets defined by scalar-product equalities. It lies in the compact product of unit spheres, so is compact. This argument also covers configurations that do not span the ambient space. The same argument proves compactness for the full congruence closure of any compact family C of unit configurations. In the product of the compact unit-configuration space and C, the relation $X \cong Y$ is closed, again by the finite signed-Gram equations. Its projection onto X is therefore compact. For ten lines, Θ is continuous, and the admissible parameter region is a closed subset of $[0, 1/6] \times [0, \pi/6]$, hence compact. The coordinate map is continuous, so its image and then its full congruence closure are compact. Uniform isolation of its nine-line core applies independently of the extra line: once that core is fixed, every competitive remaining line is already an allowed extension. Thus the same proposition treats the boundary of the rattler region as well as its interior.

The finite move used with the proposition is Danzer's reflection [12], applied simultaneously at antipodes as in [31, § 4]. If $\langle x, y\rangle = \langle x, z\rangle = c$ and $-1 < g = \langle y, z\rangle < 1$, reflecting x across $\operatorname{span}(y, z)$ gives

$$x' = \frac{2c}{1 + g}(y + z) - x. \tag{5.7}$$

A certificate must check strict slack with *every* other line. An efficient exact check can also use

$$\langle x', x_j\rangle - \langle x, x_j\rangle = -\frac{2\det(x,y,z)\det(x_j,y,z)}{1-g^2}.$$

A known nonzero sign makes one of the old weak packing inequalities strict after reflection; the other is checked directly. The reflection rule requires a position for every line, so the slack checks cover the entire configuration. The moved line then has exactly two contacts. For five, eight, nine, eleven, and twelve lines it cannot belong to a listed optimum, whose minimum contact degree is at least three. For ten lines, if the endpoint belonged to the stated family, the moved line would be its extra line; the nine unchanged lines were already the required core, so the starting configuration was also a family member. This too is impossible. These checks justify all finite reflections used below; local minimality alone would not justify them.

6. Preliminary bounds and contact geometry

6.1. **Small exact polynomial bounds.** Let μ_N be the minimum coherence of N lines in $\mathbb{R}^3$. The following coarse lower bounds restrict the domains of the exhaustive geometric calculations; they apply to every packing, independently of the proposed values c_N:

$$\mu_5 \ge \tfrac{1}{\sqrt{6}}, \quad \mu_8 > \tfrac{121}{200}, \quad \mu_9 > \tfrac{63}{100}, \quad \mu_{10} > \tfrac{13}{20}, \quad \mu_{11} > \tfrac{69}{100}, \quad \mu_{12} > \tfrac{181}{250}. \tag{6.1}$$

The first is the trace bound (3.1) with $N = 5$. For the others use even Legendre polynomials P_k, defined by

$$P_0 = 1, \quad P_1(t) = t, \quad (k+1)P_{k+1}(t) = (2k+1)tP_k(t) - kP_{k-1}(t).$$

If $f = \sum a_k P_k$ has $a_k \ge 0$, $a_0 > 0$, $f(t) \le 0$ for $|t| \le s$, and $f(1) < Na_0$, then coherence at most s is impossible:

$$a_0 N^2 \le \sum_{i,j} f(\langle x_i, x_j\rangle) \le Nf(1) < a_0 N^2. \tag{6.2}$$

This is the two-point linear programming bound for spherical codes [15]. Even polynomials give bounds on unoriented lines, as in the projective-code bounds of Delsarte, Goethals, and Seidel [14] and Levenshtein [22]. An exploratory calculation for twelve lines also tested sampled three-point bounds, following the spherical semidefinite method of Bachoc and Vallentin [2] and its projective application by Cohn and Woo [9].

For completeness, the positivity of each kernel needed here has a finite algebraic proof. Write $P_k(t) = \sum_n p_n t^n$, and homogenize:

$$K_k(x,y) = \sum_n p_n(\langle x,y\rangle)^n(\|x\|^2\|y\|^2)^{(k-n)/2}.$$

In the monomial vector $v_k(x) = (x^\alpha)_{|\alpha|=k}$, this is $v_k(x)^T M_k v_k(y)$. With $j = (k-n)/2$, the multinomial theorem puts the rational contribution

$$p_n\binom{n}{\gamma}\binom{j}{\delta}\binom{j}{\epsilon}$$

in entry $(\gamma+2\delta, \gamma+2\epsilon)$. For every degree used below, rational square completion proves $M_k \succeq 0$: at a positive pivot p, replace the remaining block B by $B - rr^T/p$;

at a zero pivot require its remaining row to be zero. The identity

$$pt^2 + 2tr^T z + z^T Bz = p(t + r^T z/p)^2 + z^T(B - rr^T/p)z$$

proves the test by induction. Thus $\sum_{i,j} b_i b_j P_k(\langle x_i, x_j\rangle) \geq 0$ for all real weights, proving the first inequality in (6.2).

The Lean proof writes each vector using a complex coordinate and a height. Define

$$R_0(s,t) = 1, \quad R_1(s,t) = s, \quad R_{m+2}(s,t) = 2sR_{m+1}(s,t) - tR_m(s,t).$$

The identity $z\bar{z} = |z|^2$ gives $R_m(\Re z, |z|^2) = \Re(z^m)$, including $z = 0$. Let $D_{km} = P_k^{(m)}$, $\lambda_{k0} = 1$, and $\lambda_{km} = 2(k-m)!/(k+m)!$ for $1 \leq m \leq k$. For each $k \in \{0, 2, 4, 6, 8, 10, 12, 14\}$, the finite identity

$$P_k(s + ab) = \sum_{m=0}^{k} \lambda_{km} D_{km}(a) D_{km}(b) R_m\big(s, (1-a^2)(1-b^2)\big)$$

is checked by exact polynomial arithmetic. For unit vectors $x = (\Re z, \Im z, a)$ and $y = (\Re w, \Im w, b)$, put $s = \Re(w\bar{z})$. Then $1 - a^2 = |z|^2$, and each summand is a positive multiple of the real Gram kernel of $D_{km}(a)z^m$. Weighted double sums are therefore nonnegative squared norms. No polar angle or division by a radius occurs, so the poles are included. The recurrence, these eight complete identities, and their actual unit-vector and finite-sum consequences are checked in `LinePackings/Arithmetic/LegendrePolynomials.lean`, `LinePackings/Arithmetic/PowerKernels.lean`, `LinePackings/Arithmetic/LegendreKernels.lean`, the degree modules in `LinePackings/Arithmetic/Legendre/`, and `LinePackings/Arithmetic/LegendreBounds.lean`. For degrees four through fourteen, the Lean checker constructs the coefficients of each derivative from the finite binomial formula for P_k. It clears rational denominators by least common multiples and compares normalized integer polynomials. A single proof identifies evaluation of those polynomials with the two sides of the identity at every real triple (a, b, s). Each degree then requires one closed coefficient check. When applying the linear programming inequality, only degrees with nonzero coefficients require a kernel positivity proof.

For $N = 8, 9, 10, 11$, take $a_0 = 1$, with the following other nonzero coefficients; omitted coefficients are zero:

N	s	a_2	a_4	a_6	a_{10}	a_{12}
8	121/200	3.80875514	2.64475560	0	0.41936724	0
9	63/100	4.079016	3.068878	0	0.492260	0
10	13/20	4.396873	3.556380	0	0.568691	0
11	69/100	4.055090	4.018152	1.630229	0	0.133362

The terminating decimals are exact rationals. Each row has $f(1) < N$. Negativity on $[-s, s]$ is checked by rational Bernstein subdivision in $y = t^2$: on an interval, express the polynomial in the Bernstein basis, whose nonnegative functions sum to one; negative coefficients imply negativity. Explicitly, for $q(y) = \sum_{i=0}^{d} q_i y^i$ on $[0, L]$, its coefficients in $\binom{d}{k}(y/L)^k(1-y/L)^{d-k}$ are

$$b_k = \sum_{i=0}^{k} q_i L^i \frac{\binom{k}{i}}{\binom{d}{i}}.$$

Start with $L = s^2$. To bisect, repeatedly replace a row by the averages of adjacent entries. The first entries of the successive rows give the left child's coefficients, and the last entries in reverse order give the right child's. Check every terminal interval.

For $N = 12$, set $s = (181/250)^2$ and take

$$f(t) = (t^2 - s)(t^2 - 23/1250)^2(t^2 - 731/5000)^2(t^4 - (20129/10000)t^2 + 10798/10000).$$

The last factor is positive by completing the square. Expansion by the recurrence gives nonnegative even Legendre coefficients and $f(1)/a_0 < 12$. These inequalities concern the full N-line packing even when its contact core has fewer vertices. In Lean, a single sign test covers the four rows. For each interval $[l, u]$ in the squared inner product, substitute $y = (l + ux)/(1 + x)$ and multiply by $(1 + x)^{d+1}$, where $d = \deg q$. Nonpositive coefficients of the resulting polynomial give the bound for every $x \geq 0$, and the test checks $q(u) \leq 0$ separately. Bisecting only when the test fails gives respectively $5, 7, 7, 6$ closed pieces. The resulting universal bounds are proved in `LinePackings/DimensionThree/Eight/CoherenceBound.lean`, `LinePackings/DimensionThree/Nine/CoherenceBound.lean`, `LinePackings/DimensionThree/Ten/CoherenceBound.lean`, `LinePackings/DimensionThree/Eleven/CoherenceBound.lean`, and `LinePackings/DimensionThree/Twelve/CoherenceBound.lean`. None assumes a contact graph, a minimizer, or the correctness of an external computation.

6.2. **The contact graph is embedded and connected.** Tammes posed the problem of maximizing the minimum separation of points on S^2 [40]. Schütte and van der Waerden [37] and Danzer [12] used contacts between closest pairs to solve small cases. In the line-packing problem each point moves together with its antipode.

In the rest of the three-dimensional proof let $\delta = \arccos c \in (0, \pi/2)$. Lift each line to its two antipodal points, and join contacting lifted points by their short great-circle arcs of length δ. Two nonincident edges cannot cross: take an endpoint of each within $\delta/2$ of the crossing; the strict triangle inequality gives two packing points less than δ apart. Collinear overlap or a vertex in an edge interior likewise violates separation. Thus this is an embedded antipodal graph. Delete only its isolated vertices, retaining them as packing points to be placed later.

Here is a purely algebraic verification of the same embedding assertion. For unit vectors p, q, the short arc is the set of unit vectors $ap + bq$, with $a, b \geq 0$. Equivalently it is the image of $[0, 1]$ under

$$t \longmapsto \frac{(1-t)p + tq}{\|(1-t)p + tq\|}.$$

When $-1 < \langle p, q\rangle < 1$, this is a continuous injective parametrization, hence a closed embedding. The denominator never vanishes: the scalar product of its numerator with $p + q$ is $1 + \langle p, q\rangle > 0$. That identity also shows that equality of two normalized points forces equality of the denominators and then equality of the parameters.

More generally, suppose $\langle p, q\rangle, \langle r, s\rangle \geq c$, while all four cross scalar products are at most c, where $0 \leq c < 1$. A putative intersection $z = ap + bq = dr + es$, with all coefficients nonnegative and $\|z\| = 1$, would satisfy

$$(1 + c)(a + b)^2 \leq 2, \qquad (1 + c)(d + e)^2 \leq 2, \qquad 1 \leq c(a + b)(d + e).$$

The first two follow by expanding the squared norms and using $(1 - c)(a - b)^2, (1 - c)(d - e)^2 \geq 0$. They imply $(1 + c)(a + b)(d + e) \leq 2$, contradicting

the third inequality because $c < 1$. Taking $r = s$ excludes every other packing vertex from an edge. If two edges share p, compare the coefficients of p in $ap + bq = dp + er$. Unless the common point is p, both b, e are positive; according to whether $a \geq d$ or $d \geq a$, this places r on the arc pq or q on the arc pr, already excluded. Thus incident edges meet only at their common endpoint. These statements, their compactness and topology, and their application to the actual vertices $(i, \pm)$ are formalized in `LinePackings/Geometry/Spherical/SphericalSegments.lean`, `LinePackings/Geometry/Spherical/SphericalArcTopology.lean`, and `LinePackings/Geometry/Contact/LiftedContacts.lean`. The strict-star condition from the selector is transported to these actual lifted neighbors in `LinePackings/Geometry/Contact/LiftedContactStars.lean`.

Lemma 6.1. *A nonempty finite embedded geodesic graph on S^2, without isolated vertices, is connected if at every vertex the incident tangent directions are not contained in a closed semicircle.*

Proof. For two distinct graph components, let A, B be their geometric traces, the finite unions of their closed edge arcs. These traces are nonempty and compact, and embeddedness makes them disjoint. Maximize $h = \langle x, y \rangle$ over $x \in A, y \in B$. Equality $h = 1$ would give $x = y$, contradicting disjointness. The other strict inequality uses the absence of isolated vertices: A contains two distinct points of an edge. If $h = -1$, maximality and the unit-vector scalar-product bound would force both points to equal $-y$. Thus $-1 < h < 1$. Neither point is a vertex: the nonzero tangent projection $y - hx$ has positive scalar product with some incident direction, along which h increases. At interior edge points, stationarity gives unit tangents u, v perpendicular to both x and y. Their common orthogonal complement is one-dimensional, since x, y are independent in $\mathbb{R}^3$. Hence $u = \pm v$; reverse one interior parameter so $u = v$. Moving both points a small common distance gives scalar product

$$h \cos^2 t + \sin^2 t = h + (1 - h) \sin^2 t > h,$$

a contradiction. □

Proposition 5.2 supplies the hypothesis. The lifted core is therefore connected, as is its projective quotient. It is nonempty because some pair attains $c > 0$.

For the actual contact graphs, the formal proof defines a component trace directly as the union of arcs whose initial vertex is reachable from the chosen vertex. The previously proved arc intersections give disjointness of distinct traces, without assuming a separate graph-realization theorem. The local variations can use the same rational parameter as the selector:

$$R_{x,u}(s) = \frac{x + su}{\sqrt{1 + s^2}}, \qquad R'_{x,u}(0) = u.$$

At an interior arc point $x = ap + bq$, both coefficients are positive. For a tangent $u = \alpha p + \beta q$, the coefficients of $x + su$ are $a + s\alpha, b + s\beta$, so both signs of a sufficiently small parameter stay on the actual arc after normalization. At an endpoint, the outgoing tangent $q - \langle p, q \rangle p$ gives the corresponding one-sided statement. Thus a positive first derivative excludes a vertex, whereas an interior maximum gives zero first derivative. No positivity assumption on the maximizing scalar product h is

used. The common-tangent identity is

$$\langle R_{x,u}(s), R_{y,u}(s)\rangle = \frac{h+s^2}{1+s^2} > h \quad (s \neq 0).$$

One algebraic check of the dimension-three tangent alignment uses the Gram matrix of x, y, u, v: its zero determinant is $(1-h^2)(1-\langle u,v\rangle^2) = 0$, so $\langle u, v\rangle = \pm 1$. These steps are verified in `LinePackings/Geometry/Topology/ArcVariations.lean`, `LinePackings/Geometry/Topology/ArcTangents.lean`, `LinePackings/Geometry/Contact/ContactComponents.lean`, `LinePackings/Geometry/Contact/ContactComponentMaxima.lean`, and `LinePackings/Geometry/Contact/ContactConnectedness.lean`. The actual induced graph on the nonisolated vertices is proved connected, including nonemptiness from positive coherence. Projection to the original line labels then gives the projective-core conclusion in `LinePackings/Geometry/Spherical/ProjectiveContacts.lean`. Finally, `LinePackings/Geometry/Peeling/ConnectedSelection.lean` applies both conclusions to the very same configuration produced by the compact-family selector, retaining its local and contact-loss minimality.

6.3. **Convex hemispherical disk faces.**

Lemma 6.2. *Suppose a nonempty finite embedded graph on S^2 has short geodesic edges, no isolated vertices, and every consecutive tangent gap is less than π. Every complementary component is the interior of a convex spherical polygon whose closure lies in an open hemisphere. Its boundary is simple and its closure is a disk.*

Proof. We first avoid assuming that the boundary is simple. Extend all edges to great circles, add three mutually perpendicular great circles, and triangulate the resulting cells. For a chosen component U, glue the closed triangles belonging to it across edges not in the graph, keeping distinct occurrences of a boundary vertex separate. This gives a compact intrinsic completion F. Its local models are spherical disks and spherical wedges of angle less than π, with artificial straight subdivisions of angle π. It has the same interior as U. Any two points of F have a shortest intrinsic path: uniformly Lipschitz paths of bounded length have a uniformly convergent subsequence in the finite compact gluing, by a diagonal subsequence on a countable dense parameter set. Length, as a supremum of sums over partitions, is lower semicontinuous.

A shortest path between interior points cannot meet a genuine corner: two rays in a wedge of angle less than π can be shortened. At a smooth boundary point it would be tangent to the boundary great circle and continue along it until a corner, also impossible. Thus the path is an interior great-circle arc. It has length at most π. Otherwise take an interior subarc of length $\ell \in (\pi, 2\pi)$, with endpoints A, B, midpoint M, and normal n. Replacing the midpoint by $M_\epsilon = \cos\epsilon M + \sin\epsilon n$ increases both endpoint scalar products from $\cos(\ell/2)$ to $\cos\epsilon\cos(\ell/2)$. The two shorter joining arcs stay inside U for small ϵ and have smaller total length.

There are no antipodal interior points. If $p, -p \in U$, at least one great semicircle between them lies in U. The set of its allowed initial directions is open by compactness of the semicircle. It is also closed. A limiting semicircle cannot meet a corner, because opposite tangent rays cannot fit in a wedge of angle less than π; after a subsequence, the neighboring semicircles use the same one of the finitely many wedges. If it touches an edge interior it must be tangent, and continuation along that edge reaches a genuine corner before either endpoint, since the edge is

shorter than π. This is again impossible. The circle of initial directions is connected, so all semicircles would lie in U, covering the sphere and contradicting the nonempty graph. It follows that the unique short arc between any two points of U lies in U.

Let $C = \{rx : r > 0, x \in U\}$ and $D = \overline{C}$. Then C is an open convex cone not containing zero, D is proper and has nonempty interior, and $C = \operatorname{int} D$. For the last equality, if $b \in C$ and $y \in \operatorname{int} D$, write $y = (1-t)b + tz$, with $t < 1$ sufficiently close to one and $z \in D$. Approximate z by $z_j \in C$ and replace b by $(y - tz_j)/(1-t) \in C$. Convexity gives $y \in C$. Properness follows because a point of C and an approximation in C to its negative would, by openness, force zero into C.

The cone D contains no line. If it contained $\mathbb{R}p$, then

$$D = \mathbb{R}p + (D \cap p^{\perp}).$$

The planar factor is a proper closed convex sector with nonempty interior, of angle at most π. Thus U would be the interior of a spherical lune or hemisphere. A semicircular side of length π, subdivided into graph edges shorter than π, has an interior graph vertex where the face angle is π. This contradicts the strict tangent-gap hypothesis.

Set $K = D \cap S^2 = \overline{U}$. Its Euclidean convex hull does not contain zero: a positive linear relation among its points would put a point and its negative in D. This convex hull is compact. Indeed every convex combination reduces to at most four points by eliminating coefficients along an affine dependence, and the combinations of four points form a compact set. Its minimum-norm point $a \neq 0$ satisfies $\langle a, x\rangle \geq \|a\|^2 > 0$ for all $x \in K$. Thus K lies in an open hemisphere.

Gnomonic projection onto $\langle a, z\rangle = 1$ sends K to a compact planar convex set with nonempty interior and boundary in finitely many straight edges. It is a convex polygon with simple boundary. Radial parametrization from an interior point identifies it with a closed disk. Projection back proves the lemma. □

Face closures contain no antipodal pair, so quotienting by antipodes is injective on each closure. The projective faces are therefore disks with simple boundaries too. An isolated packing point lies in a face interior: it cannot lie on a contact edge, where it would be too close to an endpoint.

6.4. **The convex-hull proof and the face rotations.** The proof of Lemma 6.2 uses intrinsic shortest paths. For the actual packing there is a finite alternative, which is the proof used in Lean. It identifies the faces by merging facets of a convex hull and produces their ordered boundaries at the same time.

The hull and its contact edges. Let S be the nonisolated lifted vertices and $H = \operatorname{conv} S$. The strict-star condition forces S to span $\mathbb{R}^3$, since a unit normal to a proper span would be orthogonal to every tangent direction at a core vertex. Antipodal symmetry then puts zero in the interior of H. Each ray from zero meets ∂H exactly once, giving a radial homeomorphism $\partial H \to S^2$. For a contact p, q, the functional $\langle p + q, \cdot\,\rangle$ has value $1 + c$ at p, q and at most $2c < 1 + c$ at every other generator. It exposes precisely the chord $[p, q]$, which projects to the whole contact arc.

For any supporting form $f \leq 1$, the height-one section is the convex hull of the generators with $f(x) = 1$. This follows by examining equality in the weighted average of the support values. Supporting hyperplanes and finiteness give a cover of ∂H by maximal proper exposed faces. Such a face has affine dimension two. Otherwise a nonzero form g annihilating its active generators would allow a tilt

$f + tg$, where

$$t = \min_{\substack{x \in S \\ g(x) > 0}} \frac{1 - f(x)}{g(x)}.$$

The tilt retains every active generator and adds at least one. Full span and antipodality make the minimum positive and attained. The resulting facets are convex polygons with all their generators on a circle. Distinct facets have at most two common generators, since three unit vectors of common positive height are linearly independent and hence determine the normalized support. Their intersection is empty, a vertex, or a whole ridge. At a ridge $[p, q]$, the supports of height one at p, q form a one-parameter pencil. Starting from a support exposing the ridge, the positive and negative slack minima give the two endpoints of its supporting interval. Exactly these endpoints add a third generator, so exactly two facets contain the ridge. Their support difference separates the two cones and vanishes on $\operatorname{span}(p, q)$. These arguments are formalized in `LinePackings/Geometry/Contact/ContactCoreHull.lean`, `LinePackings/Geometry/Contact/ContactExposedEdges.lean`, `LinePackings/Geometry/Contact/ContactCoreFacets.lean`, and `LinePackings/Geometry/Contact/ContactFacetIncidence.lean`.

Merging across noncontact ridges. For a facet F let Q_F be its radial image and K_F its nonnegative cone. The normalized supporting plane $f = 1$ maps homeomorphically onto the hemisphere $f > 0$ by radial projection, with inverse $z \mapsto z/f(z)$. Thus facet interiors and frontiers map to the corresponding sphere-relative sets. At the interior of a ridge the two incident facets are the only ones present. A noncontact ridge has no trace in its open arc, since intersecting the interior of an exposed contact chord would force the same endpoints. Consequently the closures of the contact faces are precisely the unions of the Q_F's over components of the graph of facets joined across noncontact ridges. To see completeness, group the facets whose interiors belong to a given contact face. Their closures cover the face closure by density of the facet interiors and finiteness of the cover. If the group split into disconnected sets of facets, the two finite closed unions would have to meet in the open contact face by connectedness. Such an intersection is an open noncontact ridge and gives a joining edge. See `LinePackings/Geometry/Contact/ContactFaceFacetReachability.lean`.

Grow one reachable group of facets by adding one incident facet at a time, always across a noncontact ridge. The induction maintains convexity of the union of the cones and absence of trace in the interior of its unit section. Suppose the attachment is across $[p, q]$. The open interior of the new facet cone is disjoint from the old convex cone, so separation gives opposite weak signs for their whole cones on a form with kernel $\operatorname{span}(p, q)$. Both cones contain p, q and zero, which fixes this kernel and the zero threshold. Near p, use the tangent chart $z \mapsto z/\langle p, z\rangle - p$. The incident contact arcs are straight rays, and the other arcs stay away from a sufficiently small ball. The old and new interior patches in this ball are convex and connected. Their closures meet on the open ridge off the trace, so the patches lie in one common open sector between consecutive contact rays. The same holds at q. The closed sectors confine the two cone sections locally and have widths less than π.

The local sector at p bounds the tangential projection of every x in either cone. Indeed

$$p + t(x - \langle p, x\rangle p) = (1 - t\langle p, x\rangle)p + tx$$

belongs to that cone for small $t > 0$, and normalization followed by the tangent chart gives $t(x - \langle p, x\rangle p)$. The sum of the two unit boundary tangents of the sector is strictly positive on every nonzero vector of the closed sector. It gives a linear form f_p nonnegative on both cones with $f_p(p) = 0$ and $f_p(q) > 0$. The analogous form f_q has $f_q(q) = 0$ and $f_q(p) > 0$. On the separating plane these inequalities force a point $ap + bq$ of either cone to have $a, b \geq 0$. Thus their intersection is exactly the cone of the shared ridge, and a segment joining points in opposite cones crosses the separating plane in that intersection. This proves convexity of the actual union. The form $f_p + f_q$ is positive on every nonzero point of the union, giving a common open hemisphere. Only points of the shared ridge could introduce trace into the enlarged interior. Its open arc is a noncontact, and the local sectors exclude both endpoints from the interior.

The finite induction therefore gives a compact convex spherical polygon in one open hemisphere for each component of the facet graph. Its sphere-relative interior is the actual contact face. Gnomonic projection makes its closure a planar convex polygon. Radial parametrization from a planar interior point gives a disk chart taking the open disk, closed disk and circle to the face, closure and frontier. In particular antipodal face closures are disjoint. The cone attachment and the disk chart are proved in `LinePackings / Geometry / Convex / FacetBlockAttachmentGeometry . lean`, `LinePackings/Geometry/ReachableFacetBlockGeometry.lean`, `LinePackings/ Geometry / Contact / ContactFaceConeGeometry . lean`, and `LinePackings / Geometry/Contact/ContactFaceDisks.lean`.

From faces to rotations. At a boundary vertex the whole face occupies one of the strict tangent sectors. Its intersection with a small tangent-chart ball is connected by convexity, and its frontier there consists of the two rays of that sector. An open point of a contact arc in the frontier puts the entire arc in the frontier by the facet incidence argument. Conversely, a contact arc joining two frontier vertices stays in the face closure by convexity and cannot meet its open interior. Hence the induced contact graph on all frontier vertices has degree two and traces the whole frontier. A disconnected graph would split the circle frontier into disjoint compact arc unions. It is therefore a single simple cycle. Its projective labels are distinct because the entire face lies in one open hemisphere. Every contact arc has two distinct incident faces, since otherwise the two hull facets at that edge would belong to the same merged region and put the open contact arc in its interior.

Orient the tangent planes using the ambient determinant. At p the positive rotation ρ of outgoing directed edges, or *darts*, moves to the next tangent in the positive direction. The positive sectors have pairwise disjoint interiors and exhaust the tangent circle apart from finitely many rays. Their angles therefore sum to 2π. For the measure calculation, a short sector on the unit tangent circle is a metric ball centered at the normalized sum of its boundary tangents, of radius half the angle. Write $\bar{e}$ for reversal of a dart e and A for its antipode. For $e : p \to q$ the face $L(e)$ on its positive side has $\det(p, q, z) > 0$ in its interior. The other face is $L(\bar{e})$. The two rays of the positive corner at q give the successor $\phi(e) = \rho^{-1}(\bar{e})$ around $L(e)$. The entire orbit of ϕ is its boundary cycle. Antipodes reverse the tangent rotations, $A\rho = \rho^{-1}A$, and $A\bar{e}$ lies in the oppositely traversed boundary of the antipodal face. These identifications, including the closing corner, are supplied by `LinePackings/Geometry/Contact/ContactFaceBoundaryCycles.`

`lean`, `LinePackings/Geometry/Contact/ContactTangentAngleSums.lean`, and `LinePackings/Certificates/Geometry/RotationFaceOrbitsPacking.lean`.

One can recover the sphere directly from these finite data. For each dart take a square with coordinates $(r,t) \in [0,1]^2$, collapse $r=0$, join its $t=1$ seam to the $t=0$ seam of $\phi(e)$, and identify $(1,t)$ with $(1,1-t)$ on $\bar{e}$. Use the same normalized chord parameter on the two sides of each edge. Pull it back to the boundary of a disk chart for $L(e)$, and use the radius r in that chart. Within each face, equality of the resulting sphere points means either two centers or equal radii and equal boundary points. On the trace, equality means the same edge point or a common original vertex. All dart occurrences at a vertex are identified by following its full rotation. These are exactly the stated seams, so the evaluation is a continuous bijection from a compact quotient to the sphere. Paired face charts can be taken to satisfy $g_{-C}(z) = -g_C(\bar{z})$, where here $\bar{z}$ is complex conjugation. Then the combinatorial map $(e,r,t) \mapsto (A\bar{e}, r, 1-t)$ realizes the antipode on the whole sphere. Quotienting by it gives the projective cellulation. Each closed face remains an embedded disk, and every isolated line remains in an open face. The census uses the actual disk faces and corner orders established above.

6.5. **Common local inequalities.** We use the spherical cosine rule, obtained by taking scalar products of tangent projections of unit vectors, and the spherical area formula. The latter has an elementary proof: a lune of angle θ has area 2θ, by rotation invariance and subdivision of the sphere. The three pairs of lunes of a triangle cover the sphere once and the triangle and its antipode three times. Thus $4(A+B+C) = 4\pi + 4E$, where E is the triangle's area and A, B, C its angles. Triangulating a convex k-gon gives angle sum minus $(k-2)\pi$.

Put

$$\alpha = \arccos \frac{c}{1+c}.$$

Two contact directions at a vertex are separated by at least α, by the cosine rule applied to their neighbors. Since $c < 1$, $\alpha > \pi/3$, giving degree at most five; the strict-star condition gives degree at least three.

Here is an algebraic proof of the upper degree bound, avoiding angular ordering. Suppose a unit vector p has six distinct lifted contact neighbors q_j, so $\langle p, q_j \rangle = c$, and set

$$u_j = \frac{q_j - cp}{\sqrt{1-c^2}}, \qquad s = \frac{c}{1+c} < \frac{1}{2}.$$

They are unit vectors in the real two-dimensional plane $p^\perp$, and

$$\langle u_i, u_j \rangle = \frac{\langle q_i, q_j \rangle - c^2}{1-c^2} \le s \quad (i \ne j).$$

Identify this plane isometrically with $\mathbb{C}$, writing its unit vectors as z_j. For the first-kind Chebyshev polynomials $T_0 = 1, T_1 = t, T_{k+2} = 2tT_{k+1} - T_k$, the unit equation gives

$$z^{k+2} + z^k = 2\,\mathrm{Re}(z) z^{k+1}, \qquad T_k(\mathrm{Re}\, z) = \mathrm{Re}(z^k).$$

Consequently their real inner products satisfy

$$\sum_{i,j} T_k(\langle z_i, z_j \rangle) = \left| \sum_i z_i^k \right|^2 \ge 0.$$

Now take $f_s(t) = (t+1)(t+1/2)^2(t-s)$. Its Chebyshev coefficients for degrees zero through four are, respectively,

$$\frac{4-5s}{4}, \quad \frac{7-8s}{4}, \quad \frac{9-8s}{8}, \quad \frac{2-s}{4}, \quad \frac{1}{8}.$$

All are positive for $s < 1/2$, while $f_s(t) \le 0$ on $[-1, s]$, and

$$f_s(1) = \frac{9}{2}(1-s) < 6\frac{4-5s}{4}.$$

For six points the ordered double sum would therefore obey

$$36\frac{4-5s}{4} \le \sum_{i,j} f_s(\langle z_i, z_j\rangle) \le 6f_s(1) < 36\frac{4-5s}{4},$$

a contradiction. This proves the lifted degree bound. Projection of the lifted neighbor set onto the original line labels proves the projective bound as well. The calculation itself also allows $c = 0$: opposite lifts may then both be neighbors, but their scalar product is -1 and satisfies the required upper bound. No bijection between the two neighbor sets is assumed at that endpoint. The kernels, certificate, actual plane isometry, and degree bounds are formalized in `LinePackings/Geometry/Circles/CircleKernels.lean`, `LinePackings/Geometry/Circles/CircleDegree.lean`, `LinePackings/Geometry/Circles/TangentCircleBound.lean`, and `LinePackings/Geometry/Contact/ContactDegree.lean`.

A triangular face has all angles α. For a nontriangular face, each corner angle is strictly larger than α, since equality would add a diagonal contact.

For $c > 1/2$, $\alpha < 2\pi/5$. An equilateral convex spherical quadrilateral has alternating angles p, q satisfying

$$\cot(p/2)\cot(q/2) = c, \qquad \alpha < p, q < 2\alpha, \qquad p + q > 3\alpha. \tag{6.3}$$

Here is a derivation. Its diagonals bisect opposite angles, by the two-circle description or congruence of the triangles cut by a diagonal. The spherical cosine rule for those triangles gives the cotangent identity. Its decreasing involution

$$h_c(p) = 2\arctan\frac{1}{c\tan(p/2)}$$

takes α to 2α, so the noncontact diagonals give the indicated strict range. Differentiation gives

$$h_c'(p) = -\frac{\sin q}{\sin p}, \qquad h_c''(p) = \frac{\sin q(\cos q + \cos p)}{\sin^2 p} < 0.$$

The sign follows from $p + q > \pi$, the positive area of the rhombus. Strict concavity above the chord between $(\alpha, 2\alpha)$ and $(2\alpha, \alpha)$ gives the last inequality. All other face angles are less than π. Thus, if t, q, r count the incident triangles, quadrilaterals, and larger faces at a vertex,

$$2t + 4q + 5r > 10. \tag{6.4}$$

The Lean proof assigns each outgoing dart at a fixed lift to its positive face. That face or its antipode occurs in the completed disk list, exactly at a word whose projected labels contain the vertex. The assignments are injective because the positive outgoing dart of a face at a vertex is unique, and the same lift cannot belong to both antipodal copies. Summing the strict corner inequalities and using

the positive rotation's exact angle sum proves the weight bound for the literal stored words.

A convex hemispherical polygon has perimeter less than 2π. One elementary proof takes the inward normals to its successive edge planes: the polar polygon has interior angles $\pi - \ell_i$, where ℓ_i are the original side lengths. Triangulation and the spherical triangle area formula give polar area $2\pi - \sum_i \ell_i > 0$. Consequently a k-face obeys $k\delta < 2\pi$. For the eight- and nine-line searches the weaker bound $k\delta \le 2\pi$ already gives $k \le 7$, since both candidate coherences are below $1/\sqrt{2}$. The Lean proof obtains the strict bound directly from the oriented face. Project its vertices from the origin onto a plane of height one and let d_i be the forward direction of projected edge i. On the sphere the edge endpoint lies on the arc from its starting vertex to the normalized horizontal direction d_i. Adding these arc lengths and applying the angular triangle inequality at successive vertices bounds the perimeter strictly by $\sum_i \angle(d_i, d_{i+1})$. Indeed, successive horizontal edge directions are independent at a strict corner, and the common vertex has positive height. The three vectors are therefore independent, which excludes equality in the angular triangle inequality. At each projected corner, every direction strictly between the two inward normals exposes that corner uniquely. The open normal sectors therefore have disjoint interiors and their angles sum to at most 2π.

Since all upper coherences used for $N \ge 8$ are less than $3/4$ and $\arccos(3/4) > 2\pi/9$, these faces have at most eight sides. For example, $2\pi/9 < 7/10$ and $\cos x \ge 1 - x^2/2$ give $\cos(2\pi/9) > 3/4$. For five lines, projective simplicity and at most five vertices give at most five sides per face and degree at most four.

A negative closed walk in the projective map lifts to a path between antipodes, of length at least π. Thus there are at least four edges for eight through eleven lines and five for twelve lines. For five lines, simplicity already forces a negative closed walk to have at least three edges. These are the only changes of negative-girth parameter in the common census.

The short negative-walk exclusions also have direct algebraic proofs. For a three-edge lift $p, q, r, -p$, expansion gives $0 \le \|p - q + r\|^2 = 3 - 6c$, so $c \le 1/2$. For a four-edge lift $p, q, r, s, -p$, Cauchy–Schwarz gives

$$4c^2 = \langle q, p + r\rangle^2 \le \|p + r\|^2, \qquad 4c^2 = \langle s, r - p\rangle^2 \le \|r - p\|^2.$$

Adding yields $c^2 \le 1/2$. A two-edge lift would force $c = -c$. Hence $c > 1/2$ excludes all negative walks of length at most three, and $c^2 > 1/2$ excludes those of length at most four. The proofs allow repeated vertices and are checked for actual walks in the lifted graph in `LinePackings/Geometry/Contact/NegativeContactCycles.lean`. For $N \ge 7$, the already proved orthoplex bound gives $c \ge 1/\sqrt{3} > 1/2$, so the four-edge cutoff needs no further preliminary bound; this is checked in `LinePackings/Geometry/Contact/ContactGirth.lean`. For twelve lines, the proved universal lower bound $c > 181/250$ gives $c^2 > 1/2$. Thus the five-edge cutoff also applies without an additional numerical premise; this composition is checked in `LinePackings/DimensionThree/Twelve/ContactGirth.lean`.

The executable short-path test is also linked to these actual walks. A realized list of signed contact records has valid distinct labels and the stated signed scalar product on every stored edge. Induction on its depth shows that `pathWithin` returning true produces an actual lifted contact walk of at most that depth, including its length-zero case. The canonical list built from the configuration's contact pairs supplies such a realization. A path to the opposite sign of a proposed neighbor,

followed by the antipode of the proposed contact, gives a negative walk one edge longer. Thus the four-edge cutoff justifies the depth-two insertion test, and the five-edge cutoff justifies the depth-three test under its stronger coherence premise. These implications are checked in `LinePackings/Census/ContactEdges.lean` and `LinePackings/Census/ContactPaths.lean`. They require neither completeness nor uniqueness of the partial edge list; they establish soundness of this filter, not coverage of the face-peeling search or the separate degree-count invariants for lists with no repeated edge records.

7. One exhaustive census of signed contact maps

Musin and Tarasov enumerated irreducible spherical contact graphs [30] and used graph enumeration and geometric exclusions to solve the thirteen- and fourteen-point Tammes problems [29, 32]. Mixon and Parshall applied this approach to the antipodal lift of eight lines [26].

Barnette gave a construction generating all triangulations of the projective plane [3]. In the initial investigation of twelve lines we used Sulanke and Lutz's catalogue of 114,478 twelve-vertex triangulations of the projective plane [39, Table 4]. We first generated the contact maps for that problem with Sulanke's `surftri` [38], which extends the `plantri` generator of Brinkmann and McKay [6]. The disk recursion in Section 7.3 generates the signed contact maps directly.

7.1. **Objects and the elementary cutting lemma.** A signed rotation system records, at each projective vertex i, the cyclic list of its neighbors and the signs s_{ij} of their contact scalar products. The lift has vertices (i, ϵ), $\epsilon = \pm 1$, with edges to $(j, \epsilon s_{ij})$. The rotation at the negative lift is the reverse of that at the positive lift. A walk is *negative* when the product of its edge signs is -1, equivalently when it lifts to a path between antipodes. The full rotations are essential: an abstract contact graph would omit the faces and the antipodal gluing. A spherical cover means the finite polygonal cell surface encoded by the rotations. In the printed encoding, letters $a, b, \ldots$ stand for vertices $0, 1, \ldots$; lowercase denotes a positive edge and uppercase a negative edge. The initial integer is the number of vertices, and the comma-separated words give their cyclic neighbor lists. To trace lifted faces, from the directed edge $u \to v$ take the neighbor immediately preceding u in the rotation at v, and continue until that directed edge returns. Project each face to vertex names and choose the lexicographically smallest cyclic rotation in either direction. Sorting these keys gives a fixed projective face order; each key occurs twice in the lift.

The cut along a shortest negative walk. The nonempty connected lifted core has a walk from a vertex to its antipode. Choose such a walk of minimum length k over all starting vertices. It has no repeated lifted vertex. A repeated projective label among its first k vertices would be either a repetition or a shorter antipodal subwalk. Thus its projection is a simple negative cycle, with $3 \le k \le N$. Concatenating the walk with its antipodal image gives a simple lifted cycle of length $2k$. Its contact arcs form a simple closed curve Γ: arcs meet only at their common endpoints. Parametrize each complete arc by its normalized chord on a unit interval and glue the interval ends in cyclic order. This gives an embedding $\Phi : \mathbb{R}/(2k\mathbb{Z}) \to S^2$ with $\Phi(t + k) = -\Phi(t)$. In particular the antipode preserves the traversal order of this curve. The projected curve is parametrized by the circle of period k. The full marked parametrizations and the shortest-walk argument are in

`LinePackings/Geometry/Topology/CyclicSelection.lean` and `LinePackings/Geometry/Spherical/AntipodalCycleEmbeddings.lean`.
Drawing all contact arcs as segments. For the separation and subsequent cuts we can use a single Schlegel diagram. Use the hull H from Section 6.4 and its height-one facet supports a_F. Choose one facet F_0, with support $f = a_{F_0}$, and let u be the average of all its generators. We have $f(u) = 1$ and $a_F(u) < 1$ for every other facet F, since each of them misses at least one of those generators. With

$$M = \max_{F \neq F_0} a_F(u), \qquad v = (1 + (1 - M)/2)u,$$

the point v lies beyond F_0 and strictly inside all the other supporting halfspaces. Central projection from v maps the closed patch $B = \partial H \setminus \operatorname{relint}(F_0)$ homeomorphically onto F_0. Its formula is

$$x \longmapsto v + \frac{f(v) - 1}{f(v) - f(x)}(x - v).$$

For $y \in F_0$ the ray $v + t(y - v)$ exits the hull at

$$t = \left(\max_{F \neq F_0} \frac{a_F(y - v)}{1 - a_F(v)} \right)^{-1}.$$

The maximum is positive by the opposite facet and at most one by the halfspace inequalities at y. These formulas give continuous inverses on the entire closed patches, also on their common boundary. Projection sends a whole chord in B to a whole straight segment: its convex weights are multiplied by the positive endpoint denominators and renormalized. Every contact chord is in B, since it belongs to two facets.

Identify the plane of F_0 with the complex plane. To extend the coordinates over the omitted cap, normalize the convex polygon F_0 to the unit disk by a plane homeomorphism. Invert in the unit circle, interchanging zero and infinity, then undo the plane homeomorphism. This identifies the cap with the closed exterior of the planar polygon in the one-point compactification and fixes its whole boundary. The two compact patch maps agree precisely there and glue to a homeomorphism of ∂H onto the compactified plane. Composing with inverse radial projection gives one sphere-to-plane chart T under which the original marked curve and every contact arc have their whole straight segment images. We keep the original edge parameters even when their planar speed is nonuniform. See `LinePackings / Geometry / Contact / ContactSchlegelRealization . lean`, `LinePackings / Geometry / Contact / ContactCapExtension . lean`, and `LinePackings/Geometry/ContainedStraightCyclicSelection.lean`.
The two marked disks. Here is a finite polygon separation argument that also keeps the marks needed in the recursion. Choose a planar direction in which all vertex heights are distinct. Off the polygon, count horizontal ray crossings modulo two, counting each edge at its lower endpoint and omitting its upper endpoint. The incident edges account for the change at each vertex height, so the count is locally constant off the curve. It is even outside a large rectangle. The odd and even regions have the whole marked curve as frontier. At an open edge they occupy opposite sides. At a vertex a small affine chart exhibits two connected local sides, also at a reflex corner or a straight mark. For a component of one parity region, the portion of the curve in its closure is nonempty and both open and closed in the curve, by

this local description. Connectedness of the curve then makes each parity region connected. Thus there is one bounded component and one unbounded component.

For the bounded disk, choose a corner minimizing a generic linear functional. In its corner triangle abc, take the diagonal ac if there is no other vertex in the closed triangle. Otherwise join b to the other vertex nearest it in height measured from ac, allowing vertices on ac. An edge crossing the open chosen segment would cross one of the two incident sides or have an endpoint in the triangle at smaller distance in height from b. Thus the open diagonal avoids the whole boundary. The corner sector on this side is in the bounded component, by the supporting line at b, so the diagonal lies there. Splitting the boundary into its two old intervals and the opposite copies of the diagonal gives two smaller simple polygons. Their bounded regions lie in the old bounded region, have disjoint interiors, and occupy opposite local sides of the open diagonal. Their closed union therefore fills the old closed bounded region and their closures intersect in precisely the diagonal.

Induct from triangles. A homeomorphism of the unit circle extends to the closed disk by $ru \mapsto r\,h(u)$. This lets a triangular disk chart match every prescribed boundary parameter. In the induction step use the two halves of a diamond as reference triangles, with matching parameters on the shared segment. The two smaller disk charts glue there, and the radial extension adjusts the parent boundary to its original cyclic parameter. All old edge intervals, including straight marks and the closing seam, are retained. The bounded side lies in the Schlegel polygon, since a point outside that convex polygon can be separated from it by a whole unbounded halfplane. These constructions are in `LinePackings/Geometry/ConnectedPolygonRegions.lean`, `LinePackings/Geometry/Topology/FilledPolygonSplits.lean`, and `LinePackings/Geometry/Topology/PolygonBoundedDiskCharts.lean`.

Antipodes permute the two complementary components of Γ. If the bounded-side disk transported back to the sphere were preserved, its closure would have a fixed point by the fixed-point theorem for the closed disk. The elementary proof of that theorem sends x along the ray from its distinct image to x and on to the circle, giving a retraction if the map has no fixed points. The boundary loop of winding number one cannot contract in the circle. Thus the antipode exchanges the two sides. Composing the first disk chart with the antipode and shifting its boundary parameter by k gives the other disk chart, with the same original boundary values. This yields exactly one lift of each nonboundary projective vertex in the chosen open disk, including any isolated marks. Each face lies on one side, and exactly one face from each antipodal pair is in the chosen disk. See `LinePackings/Geometry/Topology/DiskFixedPoint.lean` and `LinePackings/Geometry/ExchangedCyclicSelection.lean`.

Cutting off a face. A simple polygonal arc with distinct boundary marks as endpoints and all other points inside a marked polygonal disk cuts it in two. Form the two closed boundaries from the old intervals and the arc in opposite directions. Apply the bounded-polygon argument to each. The old exterior is outside both children. Neither child can surround the other, since each retains an open interval of the old boundary. The interiors are disjoint and meet the two local sides of the interior of the arc. Their closures fill the parent and intersect exactly in the whole arc. This gives marked disks with every old and new parameter in the same chart T. The argument applies to any proper arc made of contact edges, including a single edge. See

`LinePackings/Geometry/Topology/FilledArcSplits.lean` and `LinePackings/Geometry/Spherical/SphericalArcCuts.lean`.

In the current disk expose the inside face at its rooted boundary edge. The edge-point incidence theorem supplies that face, whose connected interior lies wholly in the disk. Read its full boundary starting in the same direction as the rooted edge. The visits to the old boundary are exactly its vertices on that boundary. Between consecutive visits the path is either one old edge or a proper arc: an interior edge point on the old boundary would identify the entire edge as old. The proper arc cuts off the interval of the old boundary that avoids the rooted edge. The inside face stays on the side containing the rooted edge, so no intermediate old mark of the cut-off interval belongs to that face. The same conclusion holds when a visit is traversed in reverse. It forces the old visits to be increasing in boundary order: the first two visits are the root and its successor, and the first reversal would put a visit strictly between the endpoints of another visit interval. Simplicity precludes a repeated visit. Append the closing pair of indices representing the return to the root.

Write the parent and face vertices as $b_0, \dots, b_n = b_0$ and $v_0, \dots, v_m = v_0$, starting with the common edge. Drop the visit $(0, 0)$. For consecutive visits $(r, j), (s, l)$ in face and parent positions, the gap has the boundary word

$$(b_j, \dots, b_l,\ v_{s-1}, \dots, v_{r+1}).$$

An old single edge gives a length-two word and no gap. To see that the gaps are disjoint and exhaustive, after visit (r, j) keep the disk with rooted dart word consisting of the first r face darts and the parent darts from j to $n-1$. The next cut preserves this form and discards precisely the displayed gap. At (m, n) the retained disk is the exposed face, since it has the same frontier and contains that face. The same construction therefore proves both the order and the exact gap inventory. See `LinePackings/Geometry/Contact/ContactFaceOrderedVisits.lean`, `LinePackings/Geometry/Peeling/OrderedGapPeeling.lean`, and `LinePackings/Geometry/Contact/ContactPeelingTraversals.lean`.

7.2. **Parameters and one additional necessary filter.** The common enumerated class consists of simple signed maps with a connected spherical cover, simple disk faces, degree at least three, and the following parameters. The five-line row records the analogous bounds for the separate signed-graph argument of Section 12.1.

(7.1)

N	Maximum order	Maximum degree	Maximum face size	Minimum negative cycle length
5	5	4	5	3
$8, 9, 10, 11$	N	5	8	4
12	12	5	8	5

For $N \geq 8$, also impose (6.4). For $N = 5$ do not impose that inequality, whose coherence hypothesis is unavailable.

For eleven lines we can further require: if two vertices have common neighbors giving length-two paths of both signs, they have exactly two common neighbors. To prove it, suppose there are three. Two paths have the same sign; orient the endpoints so their scalar product is A and these paths are positive. If B is the scalar

product of their corresponding common neighbors, the two-circle identity gives

$$(1+A)(1+B) = 4c^2, \qquad A \geq \frac{4c^2}{1+c} - 1.$$

The opposite-signed path gives $A \leq 1-2c^2$. Together these imply $c^3+3c^2-c-1 \leq 0$, impossible for $c > 69/100$: the polynomial is positive at $69/100$ and its derivative is positive thereafter. The identity used here follows by solving the two contact plane equations, as in (9.3) below. This forbidden pattern is monotone under adding edges, so it is also a valid intermediate pruning rule. It automatically holds when the negative girth is at least five.

7.3. **The exhaustive recursion.** Tutte counted rooted planar maps [42], and Bender, Canfield, and Robinson counted rooted maps on the projective plane by number of edges [4]. In our recursion, cutting along a shortest negative cycle exposes a disk. A distinguished boundary edge then determines which face to expose next.

For each permissible $k \leq N$, initialize the boundary disk $(0, 1, \ldots, 2k-1)$ and allow at most $N-k$ interior vertices. A state consists of the processed faces and an ordered list of unfilled disks with simple boundary walks, together with the exposed disk edges, their projective signed codes, and the fresh-name counter. In its first disk $B = (b_0, \ldots, b_{L-1})$, expose the face at edge b_0b_1. Its remaining path goes from b_1 back to b_0. Its old boundary visits increase from 1 to L, where index L denotes b_0. The waiting open disks are the components of the initial open disk after removing the closures of the processed faces. The processed closures together with the waiting closures cover the whole closed cut disk. The gap construction proves these invariants after each step.

An exposed vertex in a waiting closure must be on its boundary, since it is on the original cut or on a processed face. The same test applies to the vertex's projective label. The opposite of a cut vertex is another cut vertex, and the opposite of an interior vertex is outside the whole closed cut disk. So a vertex of the new face that is absent from the current boundary has a fresh projective label. One can construct all the names at once by listing the first half of the initial boundary and then the successive face words, keeping the first occurrence of each projective label. Complete the signed permutation on unused labels at the end. The fresh-name counter before each insertion is exactly the length of this prefix of projective names plus k.

Try every such path of a permitted face length. At each step either close at b_0, visit any later unused boundary position, or insert the next unused interior vertex. Name fresh vertices in order of first appearance, losing only irrelevant labels. If consecutive old positions are $i < j$ with fresh vertices P between them, the remaining gap is the disk

$$(b_i, b_{i+1}, \ldots, b_j, \text{reverse } P).$$

A consecutive boundary edge with no fresh vertex leaves no gap. The arc-cut lemma proves that all other gaps are precisely the remaining disks. Process them in boundary order, followed by the other waiting disks.

Boundary position $i < k$ has projective name i and sheet 0; position $k \leq i < 2k$ has name $i-k$ and sheet 1. A new interior name $i \geq 2k$ has projective name $i-k$ and sheet 0. Edge transition bits are the xor of endpoint sheets. The two boundary copies of each cut-cycle edge are initialized as one projective edge. The face recursion uses the following necessary conditions.

(1) Reject a loop or a new repeated projective endpoint pair. An existing disk edge can be reused only on the current unfilled boundary.
(2) Reject a degree above the maximum in (7.1).
(3) Before adding an edge uv of sign $(-1)^s$, reject an old path from $(u, 0)$ to $(v, 1-s)$ of length at most $k-2$. It would create a negative cycle shorter than k. Conversely every newly created shorter negative cycle contains the new edge exactly once, and is found by this test.
(4) Reject a face repeating a projective vertex or exceeding the maximum face size.
(5) If C_v corners have already been processed at v, reject C_v above the degree bound. When the weight filter is active, also reject $W_v + 5(5 - C_v) \leq 10$, where processed triangular, quadrilateral, and larger corners have weights $2, 4, 5$.
(6) If a vertex is absent from all remaining boundaries, its incident faces are complete. Require its final degree to be at least three, its corner count to equal its degree, and, when active, its final weight to exceed ten.
(7) For eleven lines, reject the common-neighbor obstruction above.

Fresh names enforce the maximum order. All degrees, corner counts, and forbidden-pattern counts used in pruning are monotone in the required direction.

The geometry justifies the guards on a partial face as well as on a completed one. An old edge of the current face in the disk must be on the current boundary, by the whole-arc incidence and waiting-region identities. Two disk edges with the same projective endpoints are equal or antipodal, since the packing fixes their sign. Both antipodal copies can be in the closed disk only on the original cut, where both were already initialized. The stored degree counts distinct actual neighbors, so a genuinely new edge leaves room under the degree bound. The short-path test uses only actual stored contacts, and appending the new edge would shorten the original antipodal walk.

Each processed projective corner corresponds to an outgoing dart at one fixed lift, using the antipodal face if necessary. Two different processed faces cannot give the same dart. At a used vertex with complete incidence every incident face pair has been processed, since a remaining incident face would put that vertex on a waiting boundary. Thus both the stored degree and the corner count equal the actual degree there. The same argument gives its final weight, which exceeds ten when (6.4) applies. The weight bound for an unfinished vertex follows by allowing weight five for each remaining corner. These facts justify the closure test without assigning positive degree to an unused isolated line. The geometric trace and its acceptance by the list recursion are proved in `LinePackings/Geometry/Contact/ContactPeelingTraversals.lean`, `LinePackings/Geometry/FirstAppearanceVertexNames.lean`, `LinePackings/Geometry/Contact/ContactPeelingEdgeInsertions.lean`, and `LinePackings/Geometry/Peeling/BoundedContactPeelingSearch.lean`.

Theorem 7.1 (Census completeness)**.** *The recursion just specified, for all permitted k, enumerates every map in the stated class, up to signed map isomorphism. It terminates without a state or time limit.*

Proof. Cut any target map along a shortest negative cycle and assign first-appearance names to its interior vertices. Its next exposed face is among the paths tried. None of the necessary pruning rules rejects that target completion. The arc-cut rule

gives exactly its remaining disks. Induction on the unprocessed faces reaches its completed disk and recovers the target by gluing.

Each recursive visit adds at least three corners, while there are at most N projective vertices and at most five corners at each. Path lengths and available vertex names are bounded. Thus the recursion is finite. A budget-limited implementation is not an exhaustive run and is never used to assert this theorem's finite output. □

To glue a disk, add each oriented face and its antipodal copy in reverse order. Its corners determine the cyclic links of the lifted vertices. Check reciprocal edges, one cyclic link at each vertex, the faces and Euler characteristic of the sphere, and all stated filters. These are assertions that abort on failure, not silent extra pruning criteria.

Deduplicate only at completed maps. Try every rooted directed edge of the connected cover in both sphere orientations. Start a queue with its initial vertex, starting that cyclic neighbor list at the terminal vertex of the root edge. Whenever a projective vertex is first encountered, assign it the next label, choose the encountered lift as representative, append it to the queue, and start its later neighbor list at its parent. Process the queue in insertion order; record a negative sign exactly when a neighbor is the opposite of its chosen representative. Record the complete signed rotations. The smallest such encoding is canonical. Each encoding is an explicit signed relabelling, so equal encodings imply isomorphism. Conversely every isomorphism maps a tried root and orientation to one tried on the other map; the traversals then agree. No unproved isomorphism pruning occurs inside the recursion.

7.4. **Checking the census in Lean.** For the Kepler conjecture, Nipkow, Bauer, and Schultz verified the enumeration of tame plane graphs [34], and Nipkow verified an efficient enumeration up to isomorphism [33]. In the present census an isomorphism must also preserve the antipodal lift.

There are three interfaces to the finite proof. The geometric construction supplies a path through the list recursion to a terminal state containing the actual signed edges and ordered face words. The numerical census supplies a checked match for every eligible terminal state. Finally the match transports the edge, face and corner data back to the packing for the case proof.

In the first interface, the edge lists record the initial boundary and the sides of the processed faces, keeping the first occurrence of each raw edge and of each signed projective edge. At termination the processed faces give one representative of every antipodal face pair. Therefore every contact occurs in the signed list, and every stored contact has the correct sign. The used projective labels are exactly the contact core. To obtain the rotation, join the predecessor and successor around each corner. For the directed version use both lifted copies of every word, reversing the antipodal copy. Each waiting edge either inherits its direction from the original boundary or runs opposite the processed edge it borders. This invariant follows from the forward old interval and reversed face interval in the gap word. No two waiting disks can share such an edge, since its processed or exterior side would give a third incident face. Consuming an old edge in its inherited direction therefore gives at most one predecessor assignment for each directed key. Terminal face coverage gives all the assignments. The original boundary, whose antipode preserves its cyclic direction, is paired with the opposite direction in the second disk. The two copies therefore give the complete rotations of the same packing. See `LinePackings/`

`Geometry/Contact/ContactTerminalLinks.lean` and `LinePackings/Geometry/Peeling/BoundedContactPeelingDirections.lean`.

The packed search uses the same signed adjacency and face recursion, storing positive and negative neighbor masks separately. One integer row per vertex carries degree, number of completed corners, and weight. Boundary words store a base-32 label sequence and a second sequence of single-bit position masks. The path-state transitions read one additional vertex or close the current face. The simulation keeps the original path, the last old-boundary position, the fresh-name counter, the gap list, and the partial signed edge inventory. The final corner weight of the actual disk bounds each prefix, and equality of the corner and degree counts identifies completed vertices in the packed guard. The two terminal encodings have the same order, signed edges and ordered faces. The bridge theorem `bounded_leaf_matched_by_census` returns this correspondence together with the in-range catalogue index and its signed match. The list simulation and the finite kernel are in `LinePackings/Census/PackedDiskBridge/WholeFaces.lean` and `LinePackings/Census/PackedDisk/Kernel.lean`.

For each terminal, a proposed table index, signed label map and one orientation are enough to check the match. The map must be a bijection on projective core labels and send paired cut vertices to opposite lifts. The checker uses all face corners and both antipodal copies. It verifies the successor at each directed key, checks that the corner keys are distinct, and compares their mask with the full table dart mask. Thus a missing contact or a wrong face cannot pass by matching only the supplied edges. The geometric adapters check, in particular, that each face follows a genuine sequence of darts and closes at its initial dart with distinct projective vertices. Across joined face words the direction convention must be common. These checks are in `LinePackings/Census/PackedDisk/Leaf.lean`, `LinePackings/Census/PackedDisk/Statement.lean`, and `LinePackings/Certificates/Geometry/RotationMatch.lean`.

The finite checker regenerates the children at each address. One certificate may cover a group of children of a checked size using a mask. A successful group proves coverage of every child it selects, and the complementary children must be checked by other groups or by recursion. Each leaf consumes a checked match, and exhausted depth at a nonterminal cannot return success. Induction on the checker and the partition of the children proves the universal statement about reachable terminals. The soundness theorem in `LinePackings/Census/PackedDisk/Sound.lean` turns the finite checks into a match for every reachable terminal.

The eight-line proof uses the packed match on all 86 indices. The nine-line proof uses the list-census implementation in `LinePackings/Census/NineFullCensus/Coverage.lean`. Its cycle-four branch uses the seven-sided perimeter bound. Once all vertex names have been introduced, the remaining mass of a polygon of length l is $l-2$. Cutting off an old-vertex m-gon consumes $m-2$ of this mass, by the gap-word length formula. A vertex can gain at most $2(m-2)$ from that corner. Thus twice the sum of the masses of the waiting polygons containing either lift of a projective vertex bounds its future weight. When the current weight plus that bound is at most ten, the whole branch is excluded. The applicable cycle-five terminal histories match a single row, which is excluded by a grounded stress. Longer cycles have no eligible terminals. See `LinePackings/DimensionThree/Eight/CatalogueCoverage.lean`, `LinePackings/DimensionThree/Nine/ShortestCycle.lean`, and `LinePackings/DimensionThree/Nine/Completeness.lean`.

For ten, eleven, and twelve lines, `LinePackings / Geometry / Peeling / LargePeelingSelection . lean` supplies actual disks with at most eight sides per face. The packed censuses cover $4 \le k \le N$ for $N = 10, 11$ and $5 \le k \le 12$ for $N = 12$, where k is the length of the selected antipodal walk. For eleven lines the bridge checks the mixed-sign common-neighbor filter when adding an edge. For twelve lines the bound $c > 181/250$ gives $c^2 > 1/2$ and hence the five-edge cutoff. The resulting catalogue sizes are 13473, 37289, and 30861, respectively. The coverage theorems are in `LinePackings/Census/PackedDisk/Order10.lean`, `LinePackings/Census/PackedDisk/Order11.lean`, and `LinePackings/Census/PackedDisk/Order12.lean`.

8. Area and angle certificates

8.1. **Isolated lines and cap area.** An isolated point x in a convex contact face of a packing with $c > 1/2$ requires at least six sides. For consecutive boundary vertices u, v, put $a = \langle x, u\rangle$, $b = \langle x, v\rangle$, and $t = c/(1+c)$. If their directions from x made an angle θ with $\cos\theta \le t$, then

$$c = ab + \sqrt{1-a^2}\sqrt{1-b^2}\cos\theta \le t + (1-t)\frac{a^2+b^2}{2} < t + (1-t)c^2 = c,$$

using $|a|, |b| < c$. Thus every such $\theta < \alpha$. They sum to 2π, and $\alpha < 2\pi/5$, proving the assertion.

Let a k-face have angle sum $S\pi$ and contain r isolated points. Set $C = \cos(\delta/2)$. The caps of radius $\delta/2$ about packing points have disjoint interiors. The isolated points contribute whole caps inside the face, and a boundary vertex contributes a cap sector with its face angle. To justify containment, if x is at distance at least δ from both endpoints of a contact edge, every point of that edge has scalar product with x at most $c/C < C$. Indeed normalize a nonnegative linear combination of the endpoints; its norm is at least C times the sum of its coefficients. So the distance to that edge is greater than $\delta/2$. Apply this to all nonincident edges and all isolated points. Comparing cap-sector areas with the polygon area gives

$$\pi(S-k+2) \ge \pi(S+2r)(1-C), \qquad S \ge \frac{k-2}{C} + 2r\left(\frac{1}{C} - 1\right). \tag{8.1}$$

Allowing the r's to be nonnegative real numbers, with total $N-n$ over the projective faces, is a necessary relaxation of the integer placement problem.

8.2. **The regular-polygon area bound.** The spherical polygon isoperimetric theorem, used by Maehara in the thirteen-spheres problem [23], says that the regular k-gon maximizes area at fixed perimeter. On S^2 the angle sum exceeds the area by $(k-2)\pi$, giving the following bound.

Lemma 8.1. *A convex hemispherical equilateral spherical k-gon of side δ, with $k\delta < 2\pi$, has angle sum at most*

$$k\gamma_k, \qquad \gamma_k = 2\arcsin\frac{\cos(\pi/k)}{\cos(\delta/2)}.$$

Proof. We give the maximization argument, including its degeneracies. For a spherical triangle with two fixed sides r, s and third side e, put $A = \cos r$, $B = \cos s$, $z = \cos e$, and

$$D = 1 + 2ABz - A^2 - B^2 - z^2, \qquad H = 1 + A + B + z.$$

The area is $E = 2\operatorname{atan2}(\sqrt{D}, H)$, as follows from the spherical cosine and half-angle formulas. The identities

$$H^2 + D = 2(1+A)(1+B)(1+z), \quad (AB - z)H - D = (1+A)(1+B)(A+B-z-1)$$

give

$$\frac{dE}{de} = \tan(e/2)\frac{1+z-A-B}{\sqrt{D}}. \tag{8.2}$$

If u, v are the endpoints of side e, let $m = (u+v)/\|u+v\|$ and let n point normally towards the third vertex. The circumcenter chosen with positive common scalar product is $O = \eta m + \xi n$, $\eta > 0$, with

$$\frac{\xi}{\eta} = \sin(e/2)\frac{1+z-A-B}{\sqrt{D}}.$$

For a convex quadrilateral split along a diagonal, the two triangle normals are opposite. Stationarity of its area with four boundary sides fixed therefore equates their circumcenters. Every stationary such quadrilateral is cyclic.

A maximizing sequence of equilateral convex k-gons has a convergent vertex subsequence. Its limiting perimeter is $k\delta < 2\pi$. Taking a limit of hemisphere centers puts it in a closed hemisphere; antipodal points, necessarily on its boundary, would give two boundary paths each of length at least π. Thus a nondegenerate limit has no antipodal pair. A compact geodesically convex set without antipodal points is in an open hemisphere: its Euclidean convex hull avoids zero (a minimal positive dependence would generate an antipode by positive combinations), and its minimum-norm point separates it. Area is continuous, by triangulation and the displayed triangle formula. A one-dimensional limit has zero area and cannot maximize against the regular polygon.

Nor can a maximum have a flat corner. Temporarily collapse straight boundary chains; there are at least three genuine corners. Choose a chain from a genuine corner a to c, containing a flat vertex b, and let d be the next genuine corner. Keep a, d fixed and shorten $ac = ab + bc$ by $\epsilon > 0$, preserving ab, bc, cd. The nondegenerate triangle acd changes area by $O(\epsilon)$. Place b on the other side of ac; the new triangle abc gains $K\sqrt{\epsilon} + O(\epsilon)$ with $K > 0$. Explicitly at $e = r + s - \epsilon$,

$$D(0) = 0, \qquad D'(0) = 2\sin r \sin s \sin(r+s) > 0,$$
$$H(0) = 4\cos(r/2)\cos(s/2)\cos((r+s)/2) > 0.$$

The gain dominates the loss. Convexity persists at the genuine corners, and reinserting the original side-δ subdivisions preserves all side lengths, a contradiction.

At a strictly convex maximum, vary any four consecutive vertices while preserving their three boundary sides and the chord joining the first and last. Their quadrilateral is stationary and hence cyclic. Overlapping quadruples share three noncollinear vertices, so the whole polygon is cyclic. Equal chords on its circle give angular gaps θ or $2\pi - \theta$. A large gap together with the other $k-1$ equal-chord gaps would exceed 2π; thus all gaps equal $2\pi/k$. The maximum is regular. Its isosceles center triangles give the stated angle formula. For $k = 3$ regularity is immediate. □

8.3. **A single linear relaxation.** Musin and Tarasov used linear relaxations of the face-angle constraints to eliminate spherical contact graphs [29, 32]. Mixon and Parshall used the same strategy for eight lines [26]. Here the relaxation also includes area constraints for faces containing isolated points.

Measure angles in units of π. Use one triangle angle α/π, two alternating variables per quadrilateral, and one per corner of every larger face. Impose: vertex sums equal two; the triangle bounds; all inequalities in (6.3); larger corner angles in (α, π); positive face area; (8.1); and Lemma 8.1. Counts for missing isolated points are zero on faces of fewer than six sides and sum to $N - n$ on the others. For five lines the separate Gram argument below makes this relaxation unnecessary.

To linearize the regular-polygon upper bounds, put $A_k = 4\cos^2(\pi/k)$. In terms of α,

$$\gamma_k(\alpha) = \arccos(1 - A_k + A_k \cos\alpha), \qquad \gamma_k''(\alpha) = \frac{A_k^2(A_k - 1)(1 - \cos\alpha)^2}{\sin^3 \gamma_k} > 0.$$

The chord through certified upper endpoint values therefore lies above the graph. If its domain ends before the proposed right endpoint, take an endpoint inside the domain with upper value π; the increasing line exceeds π thereafter and still bounds every convex face angle. All needed endpoints and bounds for $1/C$ in (8.1) are rational, verified by alternating Taylor bounds for cosine. A rational enclosure for π follows from $\pi = 16\arctan(1/5) - 4\arctan(1/239)$: the tangent formulas give tangent one for the quarter-angle, and its range fixes the branch. The alternating arctangent series supplies the enclosure.

A certificate is a nonnegative rational linear combination of these rows for which all variable coefficients cancel and the constant is negative. A zero constant also gives a contradiction if a positively weighted row was strict. Equalities can be added with either sign. This is a direct arithmetic proof of inconsistency, requiring no optimization theorem or trusted linear-programming solver.

Explicit constants and certificate generation. Here are all endpoint constants used by the angle calculations. Write $a = \alpha/\pi$, and choose $L < a < U$ and $1 < \kappa < 1/C$. The entries headed L, U in this table are integers in units of 10^{-6}; κ is unscaled. The row 11_4 is used when a negative four-cycle is present. The row 12_s uses a tighter upper angle bound on the same twelve-line coherence interval.

N	L	U	κ
8	371419	376974	1101769/1000000
9	368673	373683	6841/6250
10	366599	371112	10891/10000
11	363180	366128	270019/250000
11_4	364056	366128	135299/125000
12	359649	364057	500/467
12_s	359649	362047	500/467

For each k, the next table gives (y_L, y_R), again in units of 10^{-6}. Put

$$\ell_k(a) = y_L + \frac{y_R - y_L}{E - L}(a - L).$$

Use $E = U$ except for the eight-line heptagon, which uses $E = 0.374531$, and the octagons in rows 11 and 12, which use $E = 0.364056$. Then $\gamma_k(\pi a)/\pi < \ell_k(a)$ throughout the required domain. A dash means that perimeter already excludes that face size.

N	$k=4$	$k=5$	$k=6$	$k=7$	$k=8$
8	(568616,579153)	(700483,717428)	(806497,835341)	(922818,1000000)	–
9	(563465,572891)	(692392,707291)	(793629,817735)	(893976,959745)	–
10	(559599,568039)	(686394,699570)	(784380,805019)	(876511,919089)	–
11	(553268,558723)	(676704,685045)	(769873,782329)	(852045,872870)	(958340,1000000)
11_4	(554885,558723)	(679164,685045)	(773510,782329)	(857925,872870)	–
12	(546784,554886)	(666931,679166)	(755707,773513)	(830315,857931)	(906433,1000000)
12_s	(546784,551181)	(666931,673542)	(755707,765244)	(830315,844755)	(906433,936889)

The checks are short rational inequalities. For a coherence interval $[l,u]$, verify

$$\cos(\pi L) > \frac{u}{1+u}, \quad \cos(\pi U) < \frac{l}{1+l}, \quad \kappa^2(1+u) < 2.$$

At $x = L, E$, verify

$$\cos(\pi y_x) < 1 - 4\cos^2(\pi/k)(1-\cos(\pi x)).$$

For $y_x = 1$, this says that x lies strictly inside the domain; the continuation beyond E was justified above. Use the lower bounds (6.1) and the printed upper root endpoints; for 11_4, replace the upper endpoint by $707107/10^6 > 1/\sqrt{2}$. For twelve lines an upper enclosure $(7 + 4 \cdot 1.414213562374)/17$ suffices. Machin's formula with the first 26 arctangent terms, and the first 24 cosine terms, followed by their alternating remainders, verify all these comparisons.

To generate the linear system, give a triangle the repeated corner variable a, a quadrilateral the cyclic list (p,q,p,q), and a larger face independent corner variables. Add the corner, rhombus, vertex-sum, cap-area, and polygon inequalities specified above, replacing $1/C$ by κ. For a k-face with $k \geq 4$ and corner sum S, the two area rows are explicitly

$$-S + 2(\kappa-1)r \leq -\kappa(k-2), \qquad S - k\ell_k(a) \leq 0.$$

For triangles use the first row only, with $S = 3a$ and $r = 0$. Set $r = 0$ when $k < 6$; otherwise introduce $r \geq 0$, and impose $\sum r = N - n$. These allocation constraints are weak. The basic corner and rhombus bounds are strict for a full contact map; the rounded endpoint bounds above have strict slack too. For eight through eleven lines the added area and endpoint rows can be weakened. Lean's local checker uses the triangle and quadrilateral cap rows and the quadrilateral secants. The larger-face secants give the numerical bounds for the full relaxation above.

One practical way to find a certificate is to maximize a common slack ϵ in $A_j x + e_j\epsilon \leq b_j$, where $e_j = 1$ for strict rows and zero otherwise. A numerical dual solution merely suggests a support. On that support solve $A^T\lambda = 0$, $e^T\lambda = 1$ over $\mathbb{Q}$, and check $\lambda \geq 0$, $b^T\lambda \leq 0$ exactly. Thus the linear solver is replaceable, and none of its output is trusted. A solver-free alternative is to enumerate supports and solve either

$$A^T\lambda = 0,\ b^T\lambda = -1, \qquad \text{or} \qquad A^T\lambda = 0,\ b^T\lambda = 0,\ e^T\lambda = 1,$$

with $\lambda \geq 0$. Supports of size at most the number of equations suffice: a dependence among supported columns permits motion until a coefficient first vanishes, preserving the target. Repeated elimination gives an independent support. This describes both certificate generation and exact verification without an external optimization theorem. The proofs in `LinePackings/Certificates/Angles/Bounds.lean` check the parameter domains, cap bounds, and all thirty-one secants by exact rational inequalities.

For a worked exclusion, consider the eight-line map

`8 bcd,ade,aefg,aFGb,bhfc,cehD,cDH,eGf`.

It has a triangular face $(0,1,3)$, a quadrilateral $(0,1,4,2)$, and larger faces at the remaining sectors of vertices $0,1$. Let p,q be the quadrilateral angles at these vertices, in units of π, and $u,v<1$ the larger face angles there. The vertex equations give $a+p+u=a+q+v=2$, and hence

$$p+q>2-2a\geq 2-2(0.376974)=1.246052.$$

The quadrilateral secant, increasing in a, instead gives $p+q\leq 2\ell_4(a)\leq 2(0.579153)=1.158306$. This is exactly the kind of rational weighted contradiction stored by the general angle calculation; its certificate contains no geometric assertion beyond the specified rows.

8.4. **Local angle certificates in Lean.** Many of the linear contradictions use only a few complete vertex stars and positive contact quadrilaterals. The Lean checker stores those rows and a sparse list of rational multipliers. The realization proof identifies the stars and face words in the matched disk, so the variables are actual angles. It supplies the full vertex-angle sums and the necessary bounds for the indicated face corners. For eight lines the local certificate can use the strict quadrilateral inequality

$$2p+2q+4a<4. \tag{8.3}$$

with the full vertex sums and the triangle rows. Multipliers 1 and 2 give zero weighted column sums and zero right side. The strict row then gives the contradiction. The catalogue incidences for these exclusions are checked in `LinePackings/DimensionThree/Eight/CatalogueAngleExclusions.lean`. The angle rules for larger packings are in `LinePackings/Certificates/Angles/PackingBounds.lean`.

Here is a direct proof of the quadrilateral inequality used in (8.3). Let x_0,x_1,x_2,x_3 be the actual four unit vectors in $\mathbb{R}^3$, with successive inner products equal to $0\leq c<1$, and distinct opposite vertices. Write $A=x_0\cdot x_2$ and $B=x_1\cdot x_3$. The vanishing four-vector Gram determinant factors as

$$(1-A)(1-B)\big((1+A)(1+B)-4c^2\big)=0.$$

Distinct unit vectors have inner product strictly below one, so

$$(1+A)(1+B)=4c^2. \tag{8.4}$$

This identity is derived from the actual vectors inside the Lean theorem. It is not supplied as a certificate premise.

Let $P,Q\in[0,\pi]$ be the successive actual angles between the contact tangent projections at x_0,x_1. Their cosines are

$$\cos P=\frac{B-c^2}{1-c^2},\qquad \cos Q=\frac{A-c^2}{1-c^2}.$$

The same formulas prove equality of opposite corner angles. Equation (8.4) gives

$$(1+\cos P)(1+\cos Q)=c^2(1-\cos P)(1-\cos Q).$$

Put $U=\cos(P/2)\cos(Q/2)$ and $V=\sin(P/2)\sin(Q/2)$. Both are nonnegative, and the last identity implies $U=cV$. Consequently

$$(c+1)V=\cos((P-Q)/2)\leq 1,\qquad \cos((P+Q)/2)=(c-1)V\geq\frac{c-1}{c+1}.$$

The principal angle ranges now give

$$P + Q \le 2\beta, \qquad \beta = \arccos \frac{c-1}{c+1}.$$

For $c > 1/2$, comparison of the cosine arguments gives

$$\alpha + \beta < \pi, \qquad \alpha = \arccos \frac{c}{1+c},$$

and hence $P + Q + 2\alpha < 2\pi$. Dividing by π and doubling gives (8.3). All these claims, including the actual four-vector corner bound, are proved in Lean without a polygon-area premise.

Three of the angle cases admit a still more direct contact-graph exclusion. At a lifted vertex u with precisely the three possible lifted neighbors a, b, t, the original strict contact star implies

$$a \cdot b + a \cdot t \le 2c^2. \tag{8.5}$$

Here the letters denote their actual unit vectors and every incident inner product with u equals c. To prove the inequality, use the explicit tangent $w = 2cu - b - t$. Then $u \cdot w = 0$, and

$$\|w\|^2 = 2(1 + b \cdot t - 2c^2), \qquad w \cdot b = w \cdot t = 2c^2 - 1 - b \cdot t \le 0.$$

If (8.5) failed, then $w \cdot a < 0$, so $w \neq 0$. Its normalization would have nonpositive inner product with every actual lifted neighbor, contradicting the original strict star. The theorem derives this tangent and its properties internally. If a, t also form a contact, it follows that $a \cdot b \le 2c^2 - c$. The same conclusion holds if the triangle instead uses the neighbor b.

Suppose two adjacent vertices of a contact quadrilateral each have three contacts and each meet a contact triangle along one of their quadrilateral edges. Applying the preceding estimate at these two vertices bounds both opposite inner products by $2c^2 - c$. Unit vectors give $1 + A, 1 + B \ge 0$, whereas for $1/2 < c < 1$,

$$0 \le 1 + 2c^2 - c < 2c.$$

Thus $(1 + A)(1 + B) \le (1 + 2c^2 - c)^2 < 4c^2$, contradicting (8.4). This exclusion uses only the actual signed contact graph and the original strict stars, with no angle assignment, rotation-row reconstruction, or Euler assertion.

The three original angle cases $0, 1, 5$ have this obstruction. The exact lifted quadrilaterals and their two additional neighbors are

case	(u_0, u_1, u_2, u_3)	(t_0, t_1)
0	$(0^+, 1^+, 4^+, 2^+)$	$(3^+, 3^+)$
1	$(1^+, 4^+, 6^-, 3^+)$	$(0^+, 7^+)$
5	$(0^+, 2^+, 6^+, 3^+)$	$(1^+, 4^-)$.

Lean checks the required local edges and signs, and tests every entry of each relevant matrix row to verify the complete three-neighbor lists. The underlying matrices retain all eight vertices, every signed edge and every nonedge. For every original eight-line packing, the already-proved preliminary bound gives $c > 121/200 > 1/2$, while the packing property gives $c < 1$. These bounds are supplied inside the exclusion theorem, not added to its inputs. The theorem consumes the original packing, its strict stars and the indicated contact-graph case. A strengthened counterexample selector calls the original selector once, retains every previous

conclusion and its exact minimum antipodal walk, and excludes all three patterns on the same packing.

Two adjacent trivalent stars. A single corner of an actual contact quadrilateral is at most 2α, where $\alpha = \arccos(c/(1+c))$. For four successive unit vertices x_0, x_1, x_2, x_3, put $A = \langle x_0, x_2\rangle$, $B = \langle x_1, x_3\rangle$. The already checked Gram identity and the original packing bound give

$$(1+A)(1+B) = 4c^2, \qquad A \le c, \qquad 4c^2 \le (1+c)(1+B).$$

The cosine of the corner at x_0 is $(B-c^2)/(1-c^2)$. For $0 < c < 1$, the last inequality therefore implies

$$\cos\angle(x_1 - cx_0, x_3 - cx_0) \ge 2\left(\frac{c}{1+c}\right)^2 - 1 = \cos(2\alpha).$$

Both angles lie in $[0,\pi]$, so the corner is at most 2α. Every diagonal estimate and the Gram identity are derived inside the original-packing consumer.

The full tangent-star angle sum specializes to all three pairwise angles at a vertex with exactly three named neighbors. The entire actual tangent partition has at least three entries, while completeness of the three-neighbor list injects it into a three-element set. Thus it has exactly three entries. Each possible order gives the same three unordered pairs, whose sum is 2π. No ordering is assumed as an additional geometric input.

Here is the resulting four-quadrilateral obstruction. Let the complete neighbors of u be v, a, b, and those of v be u, c, d. Assume the contact four-cycles are

$$(u,v,c,a), \quad (u,v,d,b), \quad (u,a,e,b), \quad (v,c,f,d),$$

with the eight displayed lifted vertices distinct. Writing μ for the coherence, put $\Theta_x(y,z) = \angle(p_y - \mu p_x, p_z - \mu p_x)$ for the actual corner of the lifted packing. Put

$$R = \Theta_u(a,b), \qquad S = \Theta_v(c,d),$$
$$t_1 = \Theta_u(v,a), \quad t_2 = \Theta_u(v,b), \quad s_1 = \Theta_v(u,c), \quad s_2 = \Theta_v(u,d).$$

The complete three-contact stars give $R + t_1 + t_2 = S + s_1 + s_2 = 2\pi$. The first two quadrilaterals give

$$t_1 + s_1 + 2\alpha < 2\pi, \qquad t_2 + s_2 + 2\alpha < 2\pi,$$

and the other two give $R, S \le 2\alpha$. Adding these inequalities contradicts the sum 4π of the two star identities.

The literal original signed graphs supply this patch as follows:

case	u	v	a	b	c	d	e	f
6	3^+	6^+	0^+	4^+	2^+	7^+	1^+	5^-
7	6^+	7^-	2^+	3^+	4^-	5^-	0^+	1^-

Lean checks every required contact edge and both complete neighbor lists against the full signed matrices, including every nonedge and both lifts. For each original eight-line packing, the necessary bound $\mu > 1/2$ is derived internally from the universal bound $\mu > 121/200$; the bound $\mu < 1$ follows from the packing property. No numerical, angle, Gram, map or Euler certificate is added to the case statement.

Two quadrilaterals with opposite diagonals. In original angle case 8, the signed contact graph has positive lifted cycles $(0,1,6,2)$ and $(1,4,-2,5)$. Write c for the actual coherence and set $g = G_{12}$, $h = G_{06}$, and $t = G_{45}$. The quadrilateral identity gives

$$(1+h)(1+g) = 4c^2, \qquad (1-g)(1+t) = 4c^2.$$

The packing bound gives $h \le c$ and $|g| \le 1$. The two other signed contacts $G_{34} = c$ and $G_{35} = -c$ give $2c = x_3 \cdot (x_4 - x_5)$, so $4c^2 \le 2 - 2t$ by Cauchy–Schwarz. Therefore

$$4c^2 \le (1+c)(1+g), \qquad 4c^2 \le (1-g)(2-2c^2).$$

Multiplying the first bound by $2(1-c)$ and adding yields $4c^2 - 2c^3 \le 1$. Its left side exceeds $126/125$ because $3/5 < c \le 1$ and

$$4c^2 - 2c^3 - 126/125 = (c - 3/5)\big(2c(1-c) + (4/5)c + 42/25\big).$$

Lean proves the exclusion on arbitrary distinct labels and checks the required contacts against the case matrix.

9. Metric and orientation identities

The angle relaxation must be supplemented by the requirement that all corners belong to one configuration in $\mathbb{R}^3$. The following identities are shared by the Gram and coordinate calculations.

9.1. **Paths, fans, and determinants.** When $c > 1/2$, a signed contact path of $j \le 3$ edges with sign product s gives

$$s\, G_{uv} \ge T_j(c), \quad T_1(c) = c, \quad T_2(c) = 2c^2 - 1, \quad T_3(c) = 4c^3 - 3c.$$

Indeed its spherical length is $j\delta < \pi$. These polynomials increase for $c > 1/2$. Paths of both signs give both bounds. Across j consecutive triangular sectors the exact scalar product of the oriented neighbors is

$$F_j(c) = c^2 + (1-c^2)T_j\left(\frac{c}{1+c}\right).$$

Here $F_1 = c$, and F_2, F_3, F_4 were given in (4.2). Their derivatives are

$$1, \quad \frac{4c(c+2)}{(c+1)^2}, \quad \frac{(c+3)(3c-1)(3c+1)}{(c+1)^3}, \quad \frac{16c(c^3+4c^2-c-1)}{(c+1)^4}.$$

They are positive on $[3/5, 3/4]$: the last cubic equals $7/125$ at $3/5$ and has positive derivative thereafter. Thus endpoint evaluation is valid for all cases $N \ge 8$. At a degree-k vertex, let j be the smaller of the two numbers of sectors between a pair of directions, so $1 \le j \le \lfloor k/2 \rfloor \le 2$. Both angular arcs contain at least j sectors, so the smaller angle is at least $j\alpha$. If $k - j \ge 3$, the opposite arc is greater than π, and the smaller angle is at most $2\pi - (k-j)\alpha < \pi$. These give upper bound $F_j(c)$ and, in the latter case, lower bound $F_{k-j}(c)$; otherwise $2c^2 - 1$ is a valid lower bound. The Lean readout checks the complete signed neighbor row and an actual face containing each consecutive corner. The positive rotation follows this row in one of its two directions. Composing the tangent-plane rotations gives the cosine of an arc sum, and the two complementary arc sums add to 2π. The rational forms of $F_1, \dots, F_4$ and their monotonicity on the computational interval are checked. Across two contact triangles the equilateral quadrilateral reflection also gives the exact scalar product and transfers the first triangle's determinant sign to the two-step determinant.

Write $[abc] = \det(x_a, x_b, x_c)$. Every positively ordered triple of a strictly convex contact face has positive determinant in its consistent lift, by gnomonic projection. At a degree-five vertex any two consecutive sectors have sum less than π, giving further determinant signs. Lean proves the two-step sign on the actual positive rotation. Each of the other three angles exceeds $\pi/3$, and the rotation sums to 2π, so the two angles add to less than π. The determinant of the two-turn tangent pair is the sine of their sum in the oriented unit tangent plane, and rescaling to the original lifts preserves its sign. For the eight-line key `8bcd,ade,afg,aFGhb,bhf,ceD,cDH,dGe`, the checked face words are transported to the original packing's boundary darts, including the reversed antipodal copies. The heptagon $(0^+, 2^+, 6^+, 7^-, 4^-, 5^-, 3^+)$ puts 6^+ on the closed face side of the edge 3^+0^+. Its corner and that of the quadrilateral $(2^-, 6^-, 3^+, 5^-)$ force two successive turns between 0^+ and 6^- through 5^- at the degree-five vertex 3^+. Reversing the turn reverses both determinant signs. In either direction, the two-turn strict inequality, after switching 6^- to 6^+, contradicts the closed-side inequality. This excludes the map on the selected packing. The circle certificate also uses the weak side inequalities of the lifted face words. Two different faces with opposite copies of a boundary edge must use the same orientation convention, since each oriented dart has one positive face. Checked joins propagate the convention to every word of the matched entry. A normalized reconstruction with both a strictly positive and a strictly negative directed side determinant violates the common convention in either ambient orientation. Each test checks its edge and third vertex against the same stored face. For a contact-losing reflection leaf, the reconstructed Gram entries hold for the same packing before the seed isometry. The checker uses the two signed parent contacts and strict slack against all five other lines. The reflected packing has a degree-two vertex and so is outside the attaining class, while its strictly smaller contact set contradicts the selected packing's contact minimality. For three contact neighbors in their cyclic order, oriented as

$$y_\theta = (\sqrt{1-c^2}\cos\theta, \sqrt{1-c^2}\sin\theta, c),$$

direct expansion gives, for $\alpha_0 < \beta_0 < \gamma_0 < \alpha_0 + 2\pi$,

$$\det(y_{\alpha_0}, y_{\beta_0}, y_{\gamma_0}) = 4c(1-c^2)\sin\frac{\beta_0-\alpha_0}{2}\sin\frac{\gamma_0-\beta_0}{2}\sin\frac{\gamma_0-\alpha_0}{2} > 0. \tag{9.1}$$

Convert signs back by multiplying representative signs. Propagate any of these strict signs with the rank-three identity

$$[abc][ade] - [abd][ace] + [abe][acd] = 0. \tag{9.2}$$

Here a term includes its displayed coefficient $+1$ or -1. Two terms of the same strict sign force the remaining signed term to have the opposite sign. Divide this sign by its coefficient and one known determinant sign to determine the other determinant's sign. Three terms of the same strict sign give a contradiction. Unknown determinants may be zero; no general-position assumption is made.

9.2. **Two-circle reconstruction and four-cycles.** For unit y, z, let $g = \langle y, z\rangle$, $|g| < 1$. The unit vectors with scalar product c with both are

$$x = \frac{c}{1+g}(y+z) \ \pm \sqrt{\frac{1+g-2c^2}{(1+g)(1-g^2)}}(y\times z). \tag{9.3}$$

This follows by resolving x along $y+z$ and $y\times z$. A known strict determinant sign selects the branch and forces a positive radicand. If the other intersection t is already a distinct packing line, then

$$x=\frac{2c}{1+g}(y+z)-t. \tag{9.4}$$

Distinctness is essential here; a plan cannot simply discard one intersection.

For a positive signed four-cycle, its two compatibly oriented diagonal entries A,B therefore satisfy

$$(1+A)(1+B)=4c^2,\qquad A,B\geq F_2(c). \tag{9.5}$$

The second assertion uses $A,B\leq c$. Taking the scalar product of (9.4) with every other vector gives linear relations between four Gram entries; all their rearrangements are valid interval contractions. For a negative four-cycle, with consecutive contacts $c,c,c,-c$ and diagonals x,y, the rank-three determinant equation gives

$$(1-x^2)(1-y^2)=4c^2(1-c^2),\qquad |x|,|y|\leq 1-2c^2. \tag{9.6}$$

The latter bounds follow from the two-step paths of both signs. Lean proves these bounds by applying Cauchy–Schwarz to the sum of the two unit vectors with equal contact inner products. It derives the positive reflection by squaring the norm of $(1+g)(x+t)-2c(y+z)$ and substituting the positive diagonal identity. The corresponding vector equality and its inner product with any test vector are in `LinePackings/Geometry/SignedQuadrilateralIdentities.lean`. A negative four-cycle requires $c\leq 1/\sqrt{2}$. The equality case, which can be planar, is retained. This also supplies a simple perimeter exclusion: if $N\leq 10$, or if the map has a negative four-cycle, then $c\leq 1/\sqrt{2}$ and $\delta\geq\pi/4$. An eight-sided face would have perimeter at least 2π, which is impossible. The census deliberately keeps this weaker combinatorial bound separate from its resolution.

More generally the unit vector with $\langle x,y\rangle=p,\langle x,z\rangle=q$ has the form

$$x=\frac{p-gq}{1-g^2}y+\frac{q-gp}{1-g^2}z+\sigma\sqrt{\frac{R}{1-g^2}}(y\times z),\quad R=1-p^2-\frac{(q-gp)^2}{1-g^2}. \tag{9.7}$$

Each use requires a justified branch σ, or explicit coverage of both branches, including zero when its determinant is not forced to be strict.

Three unit seed vectors with Gram entries g_{12},g_{13},g_{23} and $|g_{12}|<1$ can be written

$$\begin{aligned} x_1&=(1,0,0),\qquad x_2=(g_{12},\sqrt{1-g_{12}^2},0),\\ x_3&=(g_{13},h,\sigma\sqrt{1-g_{13}^2-h^2}),\quad h=\frac{g_{23}-g_{12}g_{13}}{\sqrt{1-g_{12}^2}}. \end{aligned} \tag{9.8}$$

A reconstruction plan successively uses (9.7) or (9.4), with contact values, known fan values, or additional Gram parameters. Every extra parameter receives its full necessary range, initially within $[-c,c]$. The checker verifies each plan step and every unused contact, noncontact, norm, and orientation condition. Induction shows that every possible realization occurs in this parameterization up to an orthogonal transformation. Lean's two-axis gauge lemma retains both possible third coordinates, including zero. A separate rational square-root rule proves the outward endpoints by scaling to an integer square-root computation. The checked circle evaluator uses the cross-product and reflection formulas after verifying their contact and distinctness

hypotheses. It tests the unit norm and the known scalar products of each enclosed vector, with strict bounds at noncontacts. One may split on a Gram entry as well as on coherence, carrying earlier restrictions into both children. The circle proofs and the scalar proofs below can share these enclosures.

For a Gram calculation without reconstruction, impose the unit diagonal, symmetry, all packing and path bounds, the identities above, and the nonnegative principal determinants

$$\Delta(x,y,z) = 1 + 2xyz - x^2 - y^2 - z^2 \geq 0.$$

Whenever a seed triple is certifiably independent, (4.1) supplies all remaining rank-three conditions. If independence cannot be certified, that particular test gives no conclusion.

9.3. **Tangent-circle contractions and alternate coordinates.** For oriented contact neighbors y_u, y_j, y_k of x_v, set $r^2 = 1 - c^2$, $A = \langle y_u, y_j\rangle - c^2$, and $B = \langle y_u, y_k\rangle - c^2$. Resolving their tangent projections along that of y_u gives

$$\langle y_j, y_k\rangle = c^2 + \frac{AB + \sigma\sqrt{(r^4 - A^2)(r^4 - B^2)}}{r^2}, \tag{9.9}$$

where σ is the product of the two known determinant signs. The squared radical factors as $r^4 - (g - c^2)^2 = (1 - g)(1 + g - 2c^2)$. For three such neighbors with mutual scalar products x, y, z, the 4×4 Gram determinant, or a direct circle-area calculation, gives

$$(1 - c^2)\Delta(x,y,z) = 2c^2(1 - x)(1 - y)(1 - z). \tag{9.10}$$

For $1/2 < c < 3/4$, this implies $\Delta \geq 2c^2(1 - c)^2/(1 + c) \geq 9/224$. Thus neighbor triples are uniformly independent and can provide well-conditioned seed frames. Lean checks the identity by the vanishing four-vector Gram determinant in $\mathbb{R}^3$, then proves the lower bound using the three packing inequalities on x, y, z.

An auxiliary Gram parameter can instead be a tangent-angle cosine. For $\langle v, u\rangle = p$ and a reference w with $\langle u, w\rangle = g$,

$$v = pu + \sqrt{\frac{1 - p^2}{1 - g^2}}\,\big(t(w - gu) + \sigma\sqrt{1 - t^2}(u \times w)\big), \quad -1 \leq t \leq 1.$$

This describes the entire circle with the selected orientation. When $1 + \epsilon t$ is bounded away from zero, the half-angle coordinate

$$z = \sqrt{\frac{1 - \epsilon t}{1 + \epsilon t}}, \quad t = \epsilon\frac{1 - z^2}{1 + z^2}, \quad \sqrt{1 - t^2} = \frac{2z}{1 + z^2}$$

gives the same full domain by monotone endpoint conversion. These coordinate changes do not add geometric assumptions. Norm equations and linear scalar-product equations can further contract coordinate intervals, and every resulting Gram enclosure can be intersected with the earlier ones.

10. Variational certificates and sparse stress supports

Connelly and Whiteley developed the relation between equilibrium stresses and second-order flexes for tensegrity frameworks [10]. Here a contact constrains a signed scalar product, and each velocity is tangent to the sphere.

This section provides all implications used by certificates that exclude local optimality rather than geometric realizability. The full contact set is required

throughout. Isolated lines are kept fixed, and their strict slack persists under sufficiently small motions.

10.1. **A strict linear alternative and normalized motions.** For tangent velocities $v_i \perp x_i$, define

$$(Rv)_{ij} = s_{ij}(\langle x_i, v_j\rangle + \langle x_j, v_i\rangle), \qquad q_{ij}(v) = 2s_{ij}\langle v_i, v_j\rangle - c(\|v_i\|^2 + \|v_j\|^2).$$

Equivalently, on arbitrary ambient velocities use the row matrix

$$(Au)_{ij} = \langle s_{ij}x_j - cx_i, u_i\rangle + \langle s_{ij}x_i - cx_j, u_j\rangle.$$

Projecting u_i tangentially leaves Au unchanged. The paths normalize$(x_i + tu_i)$ have first contact derivatives Au. Thus $Au < 0$ componentwise contradicts local minimality. Full row rank of A suffices.

The elementary strict alternative says that either $Rv < 0$, or there is a nonzero $\lambda \geq 0$ with $\lambda^T R = 0$. One direct proof tests whether zero belongs to the convex hull of the finitely many rows of R. If not, its minimum-norm point strictly separates them from zero and its negative is a descent direction. If so, the convex coefficients give λ. Hence local minimality forces the equilibrium equations

$$\sum_j \lambda_{ij}(s_{ij}x_j - cx_i) = 0, \qquad \lambda_{ij} \geq 0. \tag{10.1}$$

Assign the same weight to the two spherical edges above each projective contact. The displayed equations then give equilibrium at both lifts of every vertex. This is the antipodally invariant stress used by the geometric theorem below. The Lean necessity theorem proves a convex combination of the gradients of half the squared contact inner products vanishes. At a contact that gradient is c times the corresponding row of A, so $c > 0$ gives the equilibrium equations above. The simultaneous path uses tangent velocities and normalizes each original representative, including zero velocities at fixed lines. The proof controls the two signs of every contact using the quadratic inner-product numerator and controls every noncontact by continuity.

We also need its affine version:

$$Ra + q < 0 \text{ is solvable} \iff \lambda^T q < 0 \text{ for every nonzero } \lambda \geq 0,\ \lambda^T R = 0. \tag{10.2}$$

The Lean proof also obtains this alternative by appending a column with entries q and the additional row $(0, -1)$. A homogeneous descent has positive last coordinate, by the extra row, so dividing by that coordinate gives an affine descent. Otherwise the homogeneous alternative gives nonnegative equilibrium weights. The weight of the added row equals the sum $\lambda^T q$, contradicting the strict inequality for λ. For completeness, project onto $(\operatorname{im} R)^\perp$. The image of the open negative orthant is an open convex cone in that space. If the projected q is outside it, separation gives a nonzero functional nonnegative on q and nonpositive on the cone. Such a functional is a vector $\lambda \geq 0$ orthogonal to $\operatorname{im} R$. The finite-dimensional separation used here follows by taking the nearest point of a closed convex set to an exterior point: differentiation along segments gives its separating normal. For a boundary point of an open convex set, take limits of unit separating normals at exterior points. The identity $\operatorname{int}\overline{C} = C$ for an open convex set is proved by the convex-combination argument in Lemma 6.2. This proves the required separation and (10.2).

If $Rv = 0$ and (10.2) supplies a, the paths

$$x_i(t) = \text{normalize}\left(x_i + tv_i + \tfrac{1}{2}t^2 a_i\right)$$

have zero first contact derivatives and second derivatives $(Ra)_{ij} + q_{ij}(v) < 0$. They improve coherence, a contradiction.

10.2. **Finite rank and second-order checks.** A common rational direction u can be certified by interval upper bounds $(Au)_e < 0$. Alternatively certify a square row minor M by $\|I - BM\|_\infty < 1$ for a rational B. Then every enclosed actual M is invertible, by (5.4). Interval Gaussian elimination with nonzero pivot intervals is another direct valid rank test.

If an $(E-1)$-square minor of A is invertible, hypothetical local minimality forces $\operatorname{rank} A = E - 1$. Its unique stress, normalized to be one on the omitted row, is nonnegative by the strict alternative. Solve for it with that minor; negative certified entries already give a contradiction. Prescribe free coordinates of u and solve the same minor to make $Au = 0$. Tangential projection gives $Rv = 0$. A certified $\lambda^T q(v) < 0$ now excludes local optimality by (10.2).

The inverse residual also rigorously encloses the solutions of these systems. For $Mx = b$, put $R_0 = I - BM$, $z = Bb$. For any rational center x_0,

$$\|x - x_0\|_\infty \le \frac{\|z - x_0 + R_0 x_0\|_\infty}{1 - \|R_0\|_\infty}.$$

Further intersections with $z + R_0 x$ remain valid. Approximate arithmetic may suggest B, selected rows, or free velocities; only these exact inequalities accept them.

There is also a Gram-only second-order test. Define the signed stress matrix

$$M_{ii} = c\sum_j \lambda_{ij}, \qquad M_{ij} = -s_{ij}\lambda_{ij} \ (ij \text{ a contact}), \qquad M_{ij} = 0 \text{ otherwise.} \tag{10.3}$$

Equilibrium is $MX = 0$, for the matrix X of position rows. Choose three independent position rows B, and let T be the other indices. If $M_{TT} > 0$, then $M \succeq 0$ and $\ker M = \operatorname{col} X$: subtract Xa from any vector to make its coordinates on B zero, and use $MX = 0$. Positive definiteness can be certified by a rational congruence whose diagonal lower bounds exceed the sums of off-diagonal absolute upper bounds; expanding the quadratic form and using $2|ab| \le a^2 + b^2$ proves that test.

If in addition the stress space is one-dimensional and $E \le 2n-3$, then $\dim\ker R = 2n - E + 1 \ge 4$, so choose a tangent flex v that is not a rotation. The quadratic identity

$$\lambda^T q(v) = -\sum_{\ell=1}^{3} (v^\ell)^T M v^\ell \tag{10.4}$$

is strictly negative. Indeed equality would give $v_i = Bx_i$ for one linear map B. Tangency and $Rv = 0$ imply

$$x_i^T \operatorname{Sym}(B) x_i = 0, \qquad x_i^T \operatorname{Sym}(B) x_j = 0 \quad (ij \text{ a contact}).$$

The strict contact star spans the tangent plane at each vertex; hence x_i and its neighbors span $\mathbb{R}^3$, forcing $\operatorname{Sym}(B)x_i = 0$ for all i, and thus $\operatorname{Sym}(B) = 0$. This would be a rotation. Equation (10.2) now supplies the improving acceleration.

10.3. **Cofactor reduction of equilibrium.** At a trivalent vertex orient the three neighbors to have scalar product c with it. Their tangent projections have a unique dependence with all coefficients positive, because the three cyclic gaps are less than π. The coefficient on edge vu, up to common scale, is

$$k_{vu} = \sqrt{(1 - g_{wz})(1 + g_{wz} - 2c^2)}, \qquad g_{wz} = s_{vw}s_{vz}G_{wz}, \tag{10.5}$$

where w, z are the other two neighbors. This is the magnitude of the oriented tangent area, since its square is $(1-c^2)^2-(g_{wz}-c^2)^2$. Every stress, even one of mixed sign, therefore has equal ratios λ_{vu}/k_{vu} at the three edges.

Join edges when they meet at such a vertex. In each resulting component, a spanning tree of these ratios writes $\lambda_e = r_e t_j$, with $r_e > 0$. Unused ratios and scalar products of (10.1) with contact tangents give a reduced homogeneous system $Kt = 0$, including the rows

$$\sum_{w\sim v} r_{vw} t_{\mathrm{component}(vw)} (s_{vu}s_{vw}G_{uw} - c^2) = 0.$$

Full column rank of K, or a strict separator of its columns from nonnegative kernel vectors, contradicts local optimality. If K has r columns, an invertible $(r-1)$-square minor bounds the stress space by one and permits the preceding second-order test. Explicitly, after permuting rows and columns write

$$K = \begin{pmatrix} D & a \\ B & b \end{pmatrix}, \qquad D \text{ invertible.}$$

A nonzero kernel vector must have a nonzero last coordinate, so local minimality forces $b - BD^{-1}a = 0$. These are the necessary equations used for parameter contraction.

All divisions require a strictly positive denominator enclosure. A directed forest of valid ratio divisions is sufficient: relations between its groups are retained as two-column equations, so no stress is lost. If the full trivalent-edge incidence graph is connected, every nonzero stress is nonzero on every edge. Products of ratios around any cycle may then be divided by their common scale and squared, giving the polynomial identities

$$\prod_v k_{v,\mathrm{out}}^2 - \prod_v k_{v,\mathrm{in}}^2 = 0.$$

Every selected cycle supplies its own necessary equation; no completeness of the selected cycle list is assumed.

10.4. **The geometric stress theorem, proved from volume.** We now remove the need to compute individual stress matrices in many sparse cases. The geometric input is a positive equilibrium stress on an embedded antipodal graph with convex hemispherical faces and strictly spanning stars. Geodesic edge lengths may vary within $(0,\pi)$, so equilibrium now means

$$\sum_j \lambda_{ij}\big(x_j - \langle x_i, x_j\rangle x_i\big) = 0.$$

Here a star is *strictly spanning* if its tangent directions are not contained in a closed semicircle.

Lemma 10.1 (The volume inequality needed here)**.** *For full-dimensional convex polytopes $A, B \subset \mathbb{R}^d$, $d = 2, 3$, and $0 < t < 1$,*

$$\mathrm{vol}((1-t)A + tB)^{1/d} \geq (1-t)\,\mathrm{vol}(A)^{1/d} + t\,\mathrm{vol}(B)^{1/d}.$$

In dimension two, if A, B have the same positive area and their Minkowski midpoint has that same area, they are translates.

Proof. We use Knothe's transport proof of the Brunn–Minkowski inequality [20]. First assume equal volumes. Transport uniform measure from A to B successively in the first coordinate, then the conditional second coordinate, and then, in dimension three, the conditional third coordinate, using increasing cumulative-distribution maps. This gives a triangular map T. On the piecewise smooth interiors of the projections and sections its diagonal derivatives d_i are positive, and differentiation of the distribution identities gives $\prod_i d_i = 1$; the conditional densities cancel. Exceptional section boundaries have measure zero. The map $S = (1-t)\,\mathrm{id} + tT$ is injective, successively by strict monotonicity in each coordinate, and its image lies in $(1-t)A + tB$. Change of variables and the weighted arithmetic-geometric mean inequality give

$$\mathrm{vol}((1-t)A + tB) \geq \int_A \prod_i (1 - t + t d_i) \geq \int_A \prod_i d_i^t = \mathrm{vol}(A).$$

The integrations can be carried out on the piecewise smooth interiors; their boundaries contribute zero. For arbitrary volumes set $a = \mathrm{vol}(A)^{1/d}$, $b = \mathrm{vol}(B)^{1/d}$, and $L = (1-t)a + tb$. Apply the equal-volume case to $A/a, B/b$ with coefficient tb/L, then dilate by L.

For planar equality, the arithmetic-geometric mean step forces $d_1 = d_2 = 1$ almost everywhere. After a horizontal translation, $T_1(x) = x$, the vertical sections have equal heights, and $T_2(x, y) = y + b(x)$. If $l(x), u(x)$ are the section endpoints of A, those of B are $l + b, u + b$. These functions are continuous piecewise affine on the common interior projection. The image $S(A)$ has endpoints $l + b/2, u + b/2$. Containment and equality of area force these to be the section endpoints of the midpoint sum as well. At a differentiability point, the permissible lower-boundary value

$$\tfrac{1}{2}\{l(x+\epsilon) + l(x-\epsilon) + b(x-\epsilon)\}$$

is minimized at $\epsilon = 0$, so its derivative $-b'(x)/2$ vanishes. Thus b is constant on every affine interval, hence everywhere by continuity. The polygons are translates. □

Izmestiev expressed the entries of the volume Hessian in terms of the faces of a polytope and determined its signature [19]. We use the following three-dimensional form.

Lemma 10.2 (Volume Hessian)**.** *Let $P(h) = \{y : \langle u_i, y\rangle \leq h_i\}$ be a bounded three-dimensional polytope with distinct unit facet normals and every listed facet of positive area A_i. Its volume Hessian H satisfies $f^T H f \leq 0$ whenever $\sum_i A_i f_i = 0$, and has kernel*

$$\{(\langle u_i, a\rangle)_i : a \in \mathbb{R}^3\}.$$

If adjacent facets i, j meet along an edge of length L_{ij} and their normals make angle θ_{ij}, its entries are

$$H_{ij} = \frac{L_{ij}}{\sin\theta_{ij}} \quad (i \neq j), \qquad H_{ii} = -\sum_{j\sim i} L_{ij}\cot\theta_{ij}, \tag{10.6}$$

where $j \sim i$ means adjacency; nonadjacent off-diagonal entries are zero. In particular opposite parallel facets do not enter the diagonal sum.

Proof. Translate the origin inside P, so $h_i > 0$. Moving plane i adds a slab, giving $\partial_i V = A_i$, its facet area. In facet i, moving plane j moves an edge through distance $dh_j/\sin\theta_{ij}$; moving plane i changes that relative support through $-\cot\theta_{ij}\,dh_i$.

The planar strip-area formula gives (10.6). These derivatives remain continuous at nonsimple vertices: newly created edges have lengths tending to zero. More explicitly the support domain splits into finitely many regions with vertices affine in h; the slab and strip formulas agree on their boundaries. Thus V is C^2 in a neighborhood where all listed facets remain present.

Since $P((1-t)h+tk)$ contains $(1-t)P(h)+tP(k)$, Lemma 10.1 makes $V^{1/3}$ concave locally. The Hessian H is therefore nonpositive on the hyperplane orthogonal to (A_i). Translations give the asserted subspace of the kernel.

Suppose $Hf=0$. For small positive t, the combinatorial type of each facet polygon of $P(h+tf)$ is fixed, and its area has the exact form

$$A_i(t)=A_i+\alpha_i t+\beta_i t^2, \qquad \alpha_i=(Hf)_i=0.$$

Its defining in-plane supports are affine in t. Here moving facet planes are identified with their original planes by translation in their normal direction. The two-dimensional volume inequality makes $\sqrt{A_i(t)}$ concave, hence $\beta_i \le 0$. The pyramid formula $3V(h+tf)=\sum_i (h_i+tf_i)A_i(t)$, together with $f^THf=0$, gives $\sum_i h_i\beta_i=0$. Since all $h_i>0$, every $\beta_i=0$. Thus each facet polygon has constant area for an interval of t. Its midpoint contains the Minkowski midpoint of the endpoint polygons; the planar equality case shows those polygons are translates. Every facet is therefore a translate of its original.

Adjacent facet translations agree. The relative interior of an original edge has positive slack in all other facet inequalities; for small t its corresponding segment in either translated facet is their common edge. A bounded segment has a unique translation to a given parallel segment. Facet adjacency is connected (join interior facet points by a generic path on the polytope boundary), so all translations agree. Their normal components are tf_i. Hence $f_i=\langle u_i,a\rangle$ for one a, proving the kernel assertion. □

Proposition 10.3 (Positive spherical stresses)**.** *For an antipodally invariant positive equilibrium stress on an antipodal embedded geodesic graph with convex hemispherical faces and strictly spanning stars, the projective signed stress matrix is positive semidefinite, with kernel spanned by the three position-coordinate columns.*

Proof. Work first on the spherical lift, with adjacent positions x_i, x_j. Write $M_{ij}=-\lambda_{ij}$ on edges and $M_{ii}=\sum_j \lambda_{ij}\langle x_i,x_j\rangle$. Equilibrium gives $MX=0$. On the dual graph prescribe gradient differences

$$Y_{\text{left}}-Y_{\text{right}}=\lambda_{ij}(x_i\times x_j) \tag{10.7}$$

across oriented edge $i\to j$. Their sum around a dual face is $x_i\times\sum_j\lambda_{ij}x_j=0$. Every dual closed walk splits into simple cycles. Each cycle is the sum of the consistently oriented face boundaries in either disk that it bounds, with internal edges cancelling. Thus the gradients Y_F exist, up to translation.

Define $h(z)=\langle Y_F,z\rangle$ on the cone over face F. The definitions agree across common cones. Equation (10.7) makes every fold convex and strict: $x_i\times x_j$ points towards the left-hand face, where its scalar product with z is positive. Along a line avoiding lower-dimensional cones, slopes are nondecreasing; perturbation proves the same on every line. Thus h is a convex homogeneous piecewise linear function, the support function of $P=\operatorname{conv}\{Y_F\}$. Strict folds give the prescribed normal fan: merging nonadjacent linear regions would force linearity across an intervening fold. The facet with normal x_i has cyclic edge vectors $\lambda_{ij}(x_i\times x_j)$. Their strict

spanning and positive weights give a convex polygon of positive area. Hence P is three-dimensional with all the prescribed facets.

Antipodes reverse left and right and preserve the stress. Equation (10.7) therefore makes $Y_{-F} + Y_F$ independent of F. Subtract half this common vector from every gradient to arrange $Y_{-F} = -Y_F$. Thus $P = -P$, and opposite facets have equal areas. The dual edge has length $\lambda_{ij} \sin\theta_{ij}$, so Lemma 10.2 gives $H = D^2V = -M$, with coordinate kernel. An odd vector f, meaning $f_{-i} = -f_i$, is orthogonal to the facet-area vector. Volume concavity therefore gives $f^T H f \le 0$. Also H preserves the odd subspace, by its displayed entries and antipodal symmetry. The kernel of that restriction is therefore $\ker H$ intersected with the odd subspace. The three position-coordinate columns are odd, so the odd restriction of $M = -H$ is positive semidefinite with exactly their span as kernel. Identifying odd values on antipodal pairs gives the projective signed stress matrix. □

The Lean proofs use case-specific tests for the stress-matrix properties, as described in the next two subsections. The variational identities use the matrix cM, where M is the projective signed stress matrix. The complete-contact equilibrium puts the position columns in its kernel. The weighted sum of $cq_{ij}(v)$ is minus the sum of the coordinate quadratic forms of cM. For a positive semidefinite stress, a velocity column outside its kernel therefore makes the weighted second variation strictly negative.

10.5. **Sparse-map exclusions, including vanishing stresses.** If the trivalent-edge incidence graph is connected, every nonzero nonnegative stress is positive on every edge. For $E \le 2n - 3$, $\operatorname{rank} R \le E - 1$ gives $\dim\ker R \ge 2n - E + 1 \ge 4$. Choose a nonrotational flex. Proposition 10.3 and the equality argument following (10.4) show that its quadratic expression is strictly negative for *every* nonzero nonnegative stress. The affine alternative gives an improving acceleration. Thus this purely combinatorial condition excludes local optimality.

For the eight-line catalogue key `7bcd,ade,afE,agFb,bCG,cGD,dEF`, Lean uses a specific positive principal block to establish the stress conclusion. The checked contact list has eleven edges on seven active labels and leaves the eighth line isolated. Trivalent incidence connects the entire edge set. Taking the scalar product of a tangent equilibrium with any one of its unit directions shows that the corresponding weight is at most half the incident total. The induced block on $0, 1, 5, 6$ consists of the edges 01 and 56. Since $c > 1/2$, both diagonal entries of each normalized two-vertex block strictly exceed its off-diagonal magnitude. The full scaled matrix is therefore positive semidefinite with kernel spanned by the three position columns and the isolated axis. The positive triangle $0, 1, 3$ spans $\mathbb{R}^3$. The eleven contact derivatives have rank at most ten on the fourteen-dimensional active tangent space, so three independent rotation coordinates can be fixed while retaining a nonzero flex. The gauge and the triangle equations fix its three triangle velocities, and the isolated velocity is zero by construction. If every velocity column lay in the stress kernel, its triangle entries would force its position component to vanish, and the isolated entry would force its remaining component to vanish. Thus the same flex gives strict negativity for every nonzero nonnegative equilibrium on this map. The normalized path given by the affine alternative contradicts the selected packing's local minimum, which is preserved by the checked signed relabelling.

For 34 eight-line and 198 nine-line catalogue entries there is a shorter stress argument. Work on the active contact core. Isolated lines may be held fixed during a sufficiently small variation of the core, since every pair involving an isolate has strict slack. Remove two labels p, q and switch signs on the remaining vertices so that every edge between them is positive. Denote by A the resulting principal block of the scaled stress matrix. Its off-diagonal entries are nonpositive. A list of contacts joined through trivalent stars leaves a forest of omitted contacts. Every endpoint of a positive-weight contact needs a second positive incident weight, by the half-incident-total bound above. Repeatedly removing leaf edges from the omitted forest shows that it cannot support a nonzero equilibrium by itself. Trivalent propagation then makes every listed weight positive. The list contains a spanning tree of the block, giving a connected graph of strictly negative entries.

Let h be the signed position column in direction $x_p \times x_q$, choosing either overall sign. Its omitted entries vanish, so $Ah = 0$. The positions span space and the two lines are distinct, giving $h \neq 0$. The checked face-side signs give $h_i \geq 0$ at the indicated vertices. The vertices with undetermined height induce a matching, possibly with isolated vertices. If a negative minimum occurred at a vertex i with an undetermined neighbour j, its row sum on this pair would be positive: $A_{ii} + A_{ij} = c^2 \sum_{e \ni i} w_e - c w_{ij} > 0$ by $c > 1/2$ and $2w_{ij} \leq \sum_{e \ni i} w_e$. The row equation would then have a strictly negative left side. At an isolated undetermined vertex the same argument uses $A_{ii} > 0$. A zero would propagate across every strictly negative entry. Thus $h_i > 0$ throughout the block. For $u_i = y_i/h_i$, symmetry and $Ah = 0$ give the identity

$$2y^T Ay = \sum_{i,j} (-A_{ij}) h_i h_j (u_i - u_j)^2.$$

Its right side is nonnegative and it vanishes only for constant u. Deleting one further coordinate therefore gives a positive definite block of order three less than the active core size. Together with the three position columns in the kernel this proves positivity and the exact kernel on the full space. The sparse-map flex bound then excludes local minimality. The finite certificates specify the deleted labels, sign switches, trivalent joins and oriented triples. At eight lines they include catalogue indices 13, 56, 65, 76 and 79.

For the stronger test let S be the vertex support of a nonzero nonnegative stress. There is no support-degree-one vertex. At a support-degree-two vertex, the tangents are opposite and the two edge weights equal. Its chains follow a great circle in steps δ. Throughout $1/2 < c < 3/4$,

$$T_4(c) + c = (c + 1)(1 - 8c^2(1 - c)) < 0.$$

Indeed $c^2(1 - c) > 1/8$ on that interval. Four steps with distinct projective endpoints would violate packing. Unless the chain closes projectively in four steps, it therefore has at most two internal degree-two vertices. Suppress these vertices. The resulting arcs have lengths $\delta, 2\delta, 3\delta < \pi$, and branch stars strictly span. Indeed a positive equilibrium on at least three distinct tangent directions cannot lie in a closed semicircle: taking its scalar product with an inward normal would force all directions onto the same diameter, which has only two available contact points. The connectedness and face lemmas apply to the suppressed graph. No loops or multiple edges arise in the spherical lift: short arcs between nonantipodal endpoints are unique, and the original graph was embedded. The projective quotient may have

parallel edges of opposite signs; their contributions are added in the odd restriction of the lifted stress matrix.

Eliminate the degree-two vertices by a Schur complement. For a two-step path the internal block is $2c\lambda$; for a three-step path it is $\lambda \left(\begin{smallmatrix} 2c & -1 \\ -1 & 2c \end{smallmatrix} \right)$. They are positive definite for $c > 1/2$. The new edge weights are, respectively,

$$\lambda, \qquad \frac{\lambda}{2c}, \qquad \frac{\lambda}{4c^2 - 1},$$

for one, two, and three steps; their diagonal contributions are the new weight times $\cos(r\delta)$. Thus Proposition 10.3, which allowed varying edge lengths, applies to the Schur complement. Congruence with the positive internal blocks makes the full support matrix positive semidefinite, with the same coordinate description of its kernel. For any full-contact flex, equality in $\lambda^T q(v) \leq 0$ holds precisely when its restriction to S is one common infinitesimal rotation. The branch stars give the symmetric-part argument, and the branch positions span $\mathbb{R}^3$, since a great circle cannot have a strictly spanning star. The coordinate-kernel representation includes the eliminated vertices.

There is one possible exception to suppression: a negative four-cycle at $c = 1/\sqrt{2}$. It is important not to omit it in the eleven-line problem. Normalize stresses to have total weight one. If a normalized stress is not unique on its positive support, move in both directions in that affine stress space until a coordinate becomes zero. This writes it as a convex combination of stresses on smaller supports. Iteration yields finitely many extreme stresses, at most one for each support. A four-step return through degree-two vertices has equal weights; the stress carried by that great-circle cycle alone is in equilibrium, and subtracting it leaves a nonnegative stress. An extreme stress containing the chain must therefore be exactly that cycle. The same reasoning treats a component with no branches.

For this exceptional cycle, its signed adjacency matrix satisfies $A^2 = 2I$ and $\operatorname{tr} A = 0$. The stress matrix $w(\sqrt{2}I - A)$ is positive semidefinite, with two-dimensional kernel given by the planar position coordinates. Equality in its quadratic expression gives $v_i = Bx_i$ for one map from the cycle plane to $\mathbb{R}^3$. Tangency at directions $0, \pi/4, \pi/2$ kills the symmetric part of its planar block; the normal component is an arbitrary linear form. These are precisely restrictions of a three-dimensional infinitesimal rotation. Thus the same equality characterization holds for every extreme stress.

To obtain one flex improving all stresses, let Z_S be the space of full-contact flexes vanishing on a possible support S. Suppose a finite calculation gives $\dim Z_S \leq b_S$. The flexes restricting to a rotation on S then have dimension at most $3 + b_S$. If

$$2n - E + 1 > 3 + b_S \tag{10.8}$$

for every possible extreme support, these are finitely many proper subspaces of $\ker R$. They cannot cover it: choose a nonzero linear form vanishing on each proper subspace; their product is a nonzero polynomial and cannot vanish identically on a real vector space, by induction on its variables. A flex outside this union has negative quadratic expression for every extreme stress, hence for every nonzero nonnegative stress. Equation (10.2) again gives improvement.

Here is the finite upper bound b_S, with no generic-rank assumption. Mark the support vertices fixed. A vertex with two fixed contact neighbors is fixed too whenever the corresponding three-vector determinant is proved nonzero: its two tangent

equations are independent. Repeat this propagation. Require every remaining vertex to have a fixed neighbor; otherwise this particular test is inconclusive. Such a vertex has a velocity parallel to its cross product with that neighbor, hence one scalar parameter. A contact from another unfixed vertex determines this scalar when the corresponding determinant is nonzero. A directed spanning forest with b_S roots expresses all remaining velocities in at most b_S parameters. If such a forest is unavailable, the test is inconclusive. For a fixed reproducible choice, propagate the lexicographically first available triple (v, u, w), then choose each remaining vertex's least fixed neighbor as anchor. Put an arc $u \to v$ when uv is a contact and the triple consisting of v, its anchor, and u has a certified nonzero determinant. Among unassigned vertices, choose a root reaching the largest number of unassigned vertices, breaking ties by label. Take its breadth-first spanning tree, remove those vertices, and repeat. The number of roots is b_S. All these operations are on the signed map and its propagated determinant signs.

Possible supports are overestimated by all nonempty unions of trivalent-edge incidence components. Reject unions having support degree one, or support degree two with certified nonzero tangent determinant. For every remaining union perform the fixed-vertex and forest calculation and require (10.8). Extra unrealizable supports cause no unsound exclusion. This proves the complete sparse-support certificate used for sparse supports.

10.6. **Certifying stress matrices by elimination and minors.** The Lean proofs certify positivity and its equality case by finite algebra on the signed matrix of an actual equilibrium. For each possible positive support, restrict M in (10.3) to its occupied labels. Its diagonal is positive, each supported off-diagonal entry has sign $-s_{ij}$, and $MX = 0$ on that support. Multiplying the matrix by $c > 0$, as in Lean, preserves these properties and the definiteness tests below.

Let F be the space of tangent flexes of the full contact set, with isolated lines fixed. If the core has n vertices and E contacts, the nonzero equilibrium relation between contact derivatives gives $E + \dim F > 2n$. For each possible positive support S, let $F_S \subset F$ consist of the flexes that vanish at its vertices. The sparse-map certificate bounds $E + 3 + \dim F_S \leq 2n$ using the pinning test of Section 10.5. The flexes that restrict to a rotation on S lie in the sum of F_S and the at most three-dimensional space of infinitesimal rotations of the core. Each such sum is proper in F. Thus one flex avoids all these subspaces at once. If the packing is locally optimal, the affine alternative gives a nonnegative stress with nonnegative second variation on this flex. Normalizing the weights and decomposing by support gives one with minimal positive support and the same nonnegative inequality. See `LinePackings/Certificates/Geometry/StressFlexDimension.lean` and `LinePackings/Certificates/Geometry/StressSupport.lean`.

The finite support checker starts with groups of contact edges forced positive together by trivalent equilibrium. It covers every nonempty admissible union of these groups. A degree-one star is impossible in the support, as is a degree-two star with independent tangents. At ten and eleven lines, a support consisting of a negative four-cycle forces the flex to restrict to a rotation by the cycle argument above. At twelve lines, any support of degree two at every occupied vertex would force $c^2 = 1/2$ by following four great-circle steps. The preliminary bound excludes that value. For each surviving support the checker identifies its exact directed-edge set and applies a positivity certificate for the corresponding principal matrix. Its

equality case forces a rotation on the support, contradicting the choice of the flex. See `LinePackings/Certificates/Geometry/SphericalStressSupports.lean`, `LinePackings/Certificates/Geometry/SphericalStressSupportChains.lean`, and `LinePackings/Certificates/Geometry/SphericalStressRouted.lean`.

For the rotation test, if the variation vanishes on a positive semidefinite support, the equality argument for (10.4) gives $v_i = Bx_i$ on that support. Write $S = (B + B^T)/2$. At a supported center i with three supported contact neighbors, the equations of tangency and of first variation make $Sx_i = 0$, since the center and its neighbors span space. Two such centers give two independent kernel vectors for S. The tangency equation at a supported point outside their span then forces $S = 0$. A single center of stress degree three suffices as well. Its positive equilibrium gives three distinct tangent lines, since any collinear pair would force the third tangent to be collinear too. The restriction of the quadratic form of S to this tangent plane vanishes along those three lines, so the binary quadratic form vanishes identically. This also gives $S = 0$. The finite test checks these alternatives against the support and the full contact graph. See `LinePackings/Certificates/Geometry/StressBranchCheck.lean` and `LinePackings/Certificates/Geometry/StressBranchSound.lean`.

Schur pivots from determinant signs. On an unmodified row the original diagonal is already positive. After eliminating some vertices, a height column

$$h_i = \det(x_a, x_b, x_i)$$

is still killed by the current Schur matrix, because X was in the original kernel. A modified pivot at i is positive if $h_i > 0$, every term $(-M_{ij})h_j$ is nonnegative for $j \neq i$, and at least one is positive. This follows from the i-th row of $Mh = 0$. The labels a, b give two exact zeros and the oriented face and star rules supply strict signs for the other heights as needed. After a positive pivot, the negated off-diagonal entry $z_{ij} = -M_{ij}$ becomes

$$z_{ij} + \frac{z_{ip} z_{pj}}{M_{pp}}.$$

Keep a sign when both terms have that sign or one term is zero. Allow an unknown sign when opposite contributions can cancel. Checking this update and every pivot proves positive definiteness on the pivot labels by square completion. For a support of order n, $n - 3$ distinct positive pivots and three independent position columns suffice for positivity and the exact kernel on the whole support. See `LinePackings/Certificates/Geometry/SphericalStressFill.lean`, `LinePackings/Certificates/Geometry/SphericalStressPivots.lean`, and `LinePackings/Certificates/Geometry/SphericalStressSchur.lean`.

A mixed minor for the last positive direction. Suppose we can prove positivity on $n-4$ independent directions. Partition the supported labels into an ordered common list V of size $n - 6$ and two ordered triples A, B, each with a certified nonzero position determinant. Put $R = (V, A)$ and $C = (V, B)$. Equilibrium gives

$$\det(M_{RR}) \det(X_A) = -\det(M_{RC}) \det(X_B).$$

Indeed multiply M_{RR} on the right by the block matrix with first column block $(I, 0)^T$ and second column block $(X_V, X_A)^T$. This gives the same result as multiplying M_{RC} by the block diagonal matrix with blocks $I, -X_B$. The sign comparison is invariant under a common reversal of the ambient orientation. A check that $-\det(M_{RC}) \det(X_A) \det(X_B) > 0$ proves $\det(M_{RR}) > 0$. Because X_B is invertible, subtract a position column combination to set all coordinates on B to zero. This

transfers the known positive directions into the space on R. On that $(n-3)$-dimensional space, positive definiteness on a codimension-one subspace together with the positive determinant gives the final positive pivot. It follows that the whole support matrix is positive semidefinite and its kernel consists of the position columns. See `LinePackings/Certificates/Geometry/SphericalStressMixed.lean`.

To check the mixed determinant, expand it as a polynomial in the positive magnitudes $|M_{ij}|$ of supported off-diagonal entries and the positive diagonals, using one variable per unordered edge. Collect like monomials. A strict coefficientwise sign certificate has all coefficients of the indicated sign and at least one nonzero coefficient. To improve the test, replace each diagonal variable by a positive slack plus a sum of selected incident magnitudes before expanding. The half-incident-total bound $2c|M_{ij}| \le M_{ii}$ permits a shift by one magnitude when $c > 1/2$. For $c^2 > 1/2$, allow up to two selected neighbors in each row, provided a row selecting two selects no other such row. Scale the corresponding heights by $\sqrt{2}$ at the rows selecting two and by one elsewhere. Then $2/(2c) < \sqrt{2}$ and $\sqrt{2}/(2c) < 1$ make each diagonal slack positive in the congruently scaled matrix. Positive row and column factors preserve the sign of the mixed determinant. These polynomial checks are in `LinePackings/Certificates/Geometry/SphericalStressMinorModel.lean`, `LinePackings/Certificates/Geometry/SphericalStressMinorPolynomial.lean`, and `LinePackings/Certificates/Geometry/SphericalStressMinorPrograms.lean`.

For the $n-4$ positive directions, one may use a partial Schur elimination or a principal block with strict weighted diagonal dominance. A matching of supported edges suffices by the same half-total estimate. When $c^2 > 1/2$, an induced union of paths of at most two edges suffices, by the $\sqrt{2}$ scaling of the middle vertices. More generally a positive integer scale r_i and upper bounds on sums of incident magnitudes can certify $M_{ii}r_i > \sum_{j\neq i} |M_{ij}|r_j$ in a chosen block. For example, at twelve lines the checked bounds on the fractions of total incident weight in one edge, in a positive triangle pair, or in a positive quadrilateral pair are $1/2$, $109/200$, and $141/200$. The pair bounds follow by projecting equilibrium on the sum of the two corresponding unit tangents. If their cosine is t, the projection in magnitude onto its unit direction is $\sqrt{(1+t)/2}$, giving the bound $1/(1+\sqrt{(1+t)/2})$ on the fraction. Use the contact or four-cycle diagonal identity for t. Cover each r_j with a sum of integer charges for such bounds. The resulting row inequality gives strict dominance by rational comparison with the preliminary lower bound on c. See `LinePackings/Certificates/Geometry/SphericalStressChargeBounds.lean` and `LinePackings/Certificates/Geometry/SphericalStressScaledMinor.lean`.

For a small example, the ten-line Petersen row 12213 uses $V = (1,2,3,4)$, $A = (0,6,7)$, $B = (5,8,9)$, with equally oriented triples and a negative mixed minor. The shifts at both ends of 1–4 make the coefficient test succeed. Its six-dimensional positive block consists of the three edges 0–3, 4–7, and 5–6. The proof and the finite data are in `LinePackings/Certificates/Geometry/PetersenStressForm.lean`. Section 13.2 explains how the case theorems combine these tests with geometric exclusions of entire maps.

11. Exact interval certificates and missing points

11.1. **A single soundness invariant.** Every parameter box carries an overestimate of all realizations represented by its parameters. The standing hypothesis remains $c \le c_N$ exactly, even when a rational box endpoint rounds c_N upwards. In particular an isolation leaf uses this exact competitive-packing hypothesis, and makes no assertion about slightly worse packings in the excess of the rounded box. An interval is a pair of integers divided by $D = 2^p$. Addition and subtraction are exact on these endpoints. For multiplication, take the minimum and maximum of the four integer endpoint products, divide by D, and round down and up respectively. For division by a positive interval, do the same with the four endpoint quotients multiplied by D. For a negative denominator interval, negate both intervals first. For squaring use zero as the lower bound if the interval contains zero. A square-root interval has endpoints $\lfloor\sqrt{D\max(0,a)}\rfloor$ and $\lceil\sqrt{Db}\rceil$, where $[a,b]/D$ is the input and $b \ge 0$. Integer square root computes both endpoints. Clipping a radicand to zero is allowed only when nonnegativity is necessary for a realization; it never certifies a strict positive determinant or a differentiable formula at zero. Any necessary equality, inequality, reconstruction, or intersection proved above preserves the following invariant:

> Every actual realization in the original box remains in the current enclosures and satisfies every imposed necessary condition.

A disjoint intersection, a wrong strict determinant sign, a negative radicand, or a violated packing inequality therefore excludes the box. A denominator interval meeting zero gives no conclusion. In particular a failed numerical solve or an undefined midpoint does not exclude a realization.

For stronger contractions use identities

$$f(x) = f(m) + \sum_i s_i(x,m)(x_i - m_i).$$

There are two separate justifications. In derivative mode m is in the box, all raw formulas are differentiable throughout it, and interval partial derivatives enclose the integrated gradient along the segment from m to x. No constraint valid only at realizations may clip a derivative or a raw expression along that segment. In algebraic difference mode, m may be outside the box and only endpoint formulas are needed. Starting from parameter differences, use the exact coefficient rules

$$\begin{aligned} S(fg) &= S(f)g(x) + f(m)S(g), \\ S(f/g) &= \{S(f) - (f(m)/g(m))S(g)\}/g(x), \\ S(f^2) &= (f(x) + f(m))S(f), \\ S(\sqrt{f}) &= S(f)/(\sqrt{f(x)} + \sqrt{f(m)}). \end{aligned}$$

They follow by subtraction and factoring. Positive reference radicands and valid denominators are required, but a feasible endpoint radicand may be zero. Feasible endpoint enclosures may be intersected with necessary bounds; raw reference enclosures may not. This distinction is needed for soundness near singular parameterizations. Any shortcut using monotonicity, such as endpoint evaluation of F_j, must also be valid on the reference interval where it is used.

For an equation $f = 0$, isolate any coordinate whose coefficient interval avoids zero:

$$x_k - m_k = \frac{-f(m) - \sum_{i \neq k} s_i(x_i - m_i)}{s_k}.$$

For inequalities use the corresponding one-sided bounds. Fixed rational multiples of necessary equations may be added to any constraint before contraction. Their values vanish at realizations, so this remains sound. Prefix constraints recorded before a later expression becomes undefined are still usable, provided endpoint and reference roles are kept distinct. Arithmetic-size limits merely make a calculation inconclusive.

A certificate is a finite binary tree. Each internal node splits a parameter into two closed intervals whose union contains the current necessary box. Contraction before splitting is allowed: it has removed only impossible points. A specified rational cut, even outside the box, is sound when both closed half-spaces are intersected and both subtrees parsed. All initial sign branches and complete parameter ranges must be covered. Every leaf must be one of:

(1) a contradiction of a necessary geometric or algebraic condition;
(2) a certified first- or second-order improvement;
(3) a contact-losing reflection (5.7) satisfying the full strict checks and the comparison-family argument;
(4) a certified isolation neighborhood of a proposed optimal core, with all other represented lines feasible;
(5) a complete placement-cover calculation as below.

The checker rejects unfinished branches, invalid axes, extra unparsed tokens, and unverified leaves. Induction on the tree, using the invariant, proves its conclusion for its entire initial box. Searching for a tree or a reconstruction plan need not be exhaustive; the validated tree and domain coverage do.

11.2. **Scalar certificates and geometric witnesses.** A rank-three certificate can work directly with a symmetric grid of Gram intervals. Start with the unit diagonal, the signed contact intervals, and the packing bound on the other pairs, using strict noncontact inequalities when the conclusion needs them. Intersect with path, fan and cyclic-sector bounds from Section 9. The necessary sector inequalities are installed only after checking the indicated neighbor order or face words against the matched rotation. With a negative four-cycle one may use $c \leq 1/\sqrt{2}$, including equality. The eleven-line certificates that use a shorter domain check that four-cycle in the same map before narrowing the domain.

For a typical scalar contraction choose two unit reference vectors p, q with $g = \langle p, q\rangle$ and $D = 1 - g^2 > 0$. For a unit x, put $t_x = \langle q, x\rangle - g\langle p, x\rangle$ and $u_x = \det(p, q, x)$. Expanding in the orthogonal directions $p, q - gp, p \times q$ gives

$$u_x^2 = D(1 - \langle p, x\rangle^2) - t_x^2, \qquad D\big(\langle x, y\rangle - \langle p, x\rangle\langle p, y\rangle\big) = t_x t_y + u_x u_y.$$

The first identity bounds the magnitudes of u_x, u_y. A pair of justified directed side signs determines the sign of their product, since a common reversal changes both signs. With unknown sign, intersect both possibilities with the old Gram interval and take the hull of the survivors. A positive lower bound on D permits division, and an empty intersection rejects the box. Other instructions implement the positive and negative four-cycle identities and the reflection relation. Each instruction is interpreted as an intersection with a necessary enclosure of the same actual Gram

entry. See `LinePackings/Geometry/Gram/RankThreeGram.lean`, `LinePackings/Geometry/Gram/RankThreeAngleReplay.lean`, and `LinePackings/Arithmetic/ScaledGramReplay.lean`.

A shared subgraph certificate needs only a signed injection of its template's required contacts into a map. Check those signs and use the weak packing inequalities for the remaining pairs. An exclusion using just these constraints then applies to every row with that template. A certificate needing the full star or the order of a face checks that data on the entire row. Such a rule can replace a stress calculation for that row, since it already precludes the selected realization. The two interfaces are in `LinePackings/Certificates/Direct/Subgraphs.lean` and `LinePackings/Certificates/Direct/FaceCases.lean`.

At a split one can check branches in separate modules using the same entering Gram intervals. At an interval partition, verify that the first interval starts low enough, each next one starts at or before the preceding upper endpoint, and the last reaches the old upper bound. For a pair-entry split, update only the two symmetric slots for that pair, retaining the other bounds. Combining the proof of coverage with the proof for every fragment gives one rule on the original whole domain. The near-candidate tree for twelve-line row 30362 uses this composition. See `LinePackings/Certificates/Map/GramNearSplit.lean` and `LinePackings/Certificates/Geometry/Near30362.lean`.

Large certificates also specify intermediate Gram grids after short blocks of contractions. Each intermediate grid is checked against the computed result from its entering state. At a split, the two new grids are checked against the corresponding updates of that state. Composing these equalities with the subtree proofs gives the check from the original Gram grid. See `LinePackings/Geometry/Gram/RankThreeCheckpoints.lean`.

A proximity leaf first applies its checked signed permutation. It encloses three independent reference vectors in the triangular frame (9.8), with positive third coordinate, and obtains the rest by their Gram products with that seed. Compare the whole framed box with the exact candidate's enclosures in the same gauge. The isolation theorem consumes the actual coherence bound and these coordinate bounds. For example, the upper-range frame test for twelve-line row 30205 uses per-coordinate differences at most $1/1900$. The squared product distance is at most $36/1900^2 < 1/100000$, which suffices for twelve-line isolation. The signed relabelling and orthogonal map of the reference frame transport that distance to the reference construction. See `LinePackings/Geometry/Gram/RankThreeFrameReplay.lean` and `LinePackings/Certificates/Geometry/TwelveFrameReplay.lean`.

A motion leaf uses the same Gram grid. For integer coefficients a_{ik}, choose $u_i = \sum_k a_{ik} x_k$ and project it tangentially to obtain $d_i = u_i - \langle u_i, x_i\rangle x_i$. Every derivative

$$s_{ij}\big(\langle d_i, x_j\rangle + \langle x_i, d_j\rangle\big)$$

is a polynomial in Gram entries. Strictly negative upper bounds at all active contacts contradict local minimality. Noncontacts have strict slack, including pairs with fixed isolated lines. This lets the certificate verify descent without constructing interval coordinates. The nine-line ring at row 1020 uses products with a reference triangle as split variables. The twelve-line motion certificates use the same principle with rank-three contractions and sector cuts. See `LinePackings/DimensionThree/`

`Nine/RingMotion/Exclusion.lean` and `LinePackings/Certificates/Direct/TwelveMotion/Sound.lean`.

11.3. **A necessary hole for an isolated line.** If the core spans $\mathbb{R}^3$, set $K = \{z : |\langle x_i, z\rangle| \le c\ \forall i\}$. It is a bounded polytope. A unit line strictly noncontacting with the core can be scaled slightly outward while staying in K, so K contains a point with squared norm greater than one. It then has such a vertex: if active normals at a point span less than $\mathbb{R}^3$, move along a line perpendicular to them to the endpoints of its maximal segment in K. Convexity of squared norm keeps at least one endpoint no smaller, and a new independent normal becomes active. At most three repetitions give three independent active normals.

Take these signed normals y_1, y_2, y_3, with Gram matrix G, determinant $\Delta > 0$, and adjugate row sums A_i. The corresponding vertex is

$$z = \frac{c}{\Delta}\sum_i A_i y_i, \qquad \|z\|^2 = \frac{c^2}{\Delta}\sum_i A_i.$$

Therefore some triple and signs must satisfy

(11.1)

$$\Delta > 0, \quad c^2\sum_i A_i - \Delta > 0, \quad |\sum_i A_i\langle y_i, x_j\rangle| \le \Delta \quad \text{for every other core vertex } j.$$

For $x = G_{12}$, $y = G_{13}$, and $z = G_{23}$, the row sums are

$$A_1 = 1 - z^2 + yz - x + xz - y, \qquad A_2 = 1 - y^2 + yz - x + xy - z,$$
$$A_3 = 1 - x^2 + xz - y + xy - z.$$

Fix the first normal sign positive and try the other four sign choices. Reject a box only if every triple/sign choice violates a necessary polynomial condition and the core's spanning is certified. This tests room for at least one isolated line, not the mutual placement of several.

11.4. **Complete covers for several missing lines.** Every projective point has a normalized representative in one of the three charts

$$(1, u, v), \quad (u, 1, v), \quad (u, v, 1), \qquad -1 \le u, v \le 1,$$

before normalization. Thus closed rational rectangles cover all possible placements. For unnormalized chart vectors z, w, the necessary conditions are polynomial:

$$(\langle x_i, z\rangle)^2 - c^2\langle z, z\rangle < 0, \qquad (\langle z, w\rangle)^2 - c^2\langle z, z\rangle\,\langle w, w\rangle \le 0.$$

The first is strict because the missing line is isolated. The checker starts with all tuples of the three chart squares, including repeated squares. It uses interchangeability of the missing lines when checking the order of cells in a tuple. Each subdivision bisects one of the chart intervals and retains both children. A leaf either contradicts a core or pair inequality or gives normalized coordinate bounds that imply isolation. All bounds are uniform over the enclosing core parameter box. The checker and its soundness proof are in `LinePackings/Certificates/Map/GramPlaceKernel.lean` and `LinePackings/Certificates/Map/GramPlaceSound.lean`.

Four nine-line branches, at indices $2, 6, 7, 9$, put seven lines in the same coordinate boxes after a signed relabelling and an orthogonal change of frame. To place the remaining two lines, choose for each a largest absolute coordinate and make it positive. Dividing by that coordinate puts its other two coordinates in $[-1, 1]^2$. Subdivide pairs of these squares and enclose the normalized inner products. A cell

is discarded when one of the two lines violates the coherence bound against the core or against the other line. A retained cell must enclose both lines in one of fourteen ordered pairs of sites. Checking the corresponding nine-line Gram boxes places each pair inside one of the proved neighborhoods of an optimal configuration. The four cases share the checked subdivision in `LinePackings/DimensionThree/Nine/HoleCover/Coverage.lean`.

12. Terminal map arguments

12.1. **Ordinary signed contact graphs for five lines.** Fejes Tóth used the contact graph in the elliptic plane to classify five lines [17]. Musin and Tarasov recovered this classification from their enumeration of irreducible spherical contact graphs [31, § 4].

Apply Proposition 5.2 using the isolation of Section 5.1. For five lines, the strict contact stars give enough constraints to classify the ordinary signed contact graph.

Write $g_{ij} = \langle x_i, x_j \rangle$ and $c = \mu(X)$, with $1/\sqrt{6} \le c \le 1/\sqrt{5} < 1$. A selected nonempty contact star has at least three neighbors: given one neighbor j, choose a unit vector u perpendicular to both x_i and x_j. Strict spanning applied to u and $-u$ gives two further, distinct neighbors. Also, for every directed contact ij, test the star at i against the nonzero tangent vector

$$v = c^2 x_i - g_{ij} x_j.$$

It is tangent since $g_{ij}^2 = c^2$, and nonzero since its inner product with x_j is $g_{ij}(c^2-1) \neq 0$. After normalization, strict spanning supplies a neighbor k with

$$0 < g_{ik}\langle v, x_k \rangle = c^4 - g_{ij} g_{ik} g_{jk}.$$

Here $k \neq j$, and $c^4 < c^3$. Consequently, either jk is a noncontact, or the contact triangle ijk has negative sign product. Call this the *undominated-star test*.

A nonempty graph on five vertices with minimum nonzero degree three either has a vertex of degree four or is a complete four-vertex core and one isolated vertex. Indeed, if there is an isolated vertex, every other nonisolated vertex must be joined to the remaining three; if there is none and no degree-four vertex, all five degrees would be three, contradicting evenness of the degree sum. For a four-vertex core, normalize the three edges at one vertex to be positive. Among the 2^3 remaining sign choices, the undominated-star test permits only three negative signs. The core therefore has Gram determinant

$$T(c) = -(c+1)^3(3c-1).$$

Its vanishing would force $c = 1/3$, below the five-line trace bound.

Otherwise label a degree-four vertex zero and switch representatives so that all its contacts are positive. Encode each of the six pairs $12, 13, 14, 23, 24, 34$ by $0, +, -$, with zero meaning a strict noncontact. Enumerate all $3^6 = 729$ words, retaining those satisfying minimum degree three and the undominated-star test at every directed edge. There are 91 retained words. First test whether some four-vertex subset has all four triangle products negative; such a subset switches to the forbidden tetrahedron. This rejects 22 words. For each remaining word, compare all entries, including noncontacts, under all permutations of five labels and all sign switches (fixing one switch, since simultaneous negation changes nothing). The resulting

classification is

case	negative tetrahedron	I	II	III	A	B
normalized words	22	12	36	12	3	6.

In cases I and II, the positive contacts are $01, 02, 03, 14, 24$ and the negative contacts are $12, 13, 34$. Case II also has the positive contact 23. In both cases $x = G_{04}$ is a strict noncontact. Let $I_r = \{0,1,2,3,4\} \setminus \{r\}$, in increasing order, and $M_{rs} = \det G_{I_r,I_s}$. Direct determinant expansion gives the respective identities

$$4c(c+1)(x-c) = -M_{43} + M_{42} + M_{31} + M_{30} + M_{21} + M_{20}, \tag{12.1}$$

$$4c(c+1)(x-c) = -2M_{43} + 2M_{42} + M_{33} - M_{22}. \tag{12.2}$$

Every 4×4 minor vanishes, forcing $x = c$ in both cases.

Case III is complete. All contacts at vertex 0 are positive, and its other positive contacts are $12, 23, 34$. Its principal 4×4 minors are $(c-1)(c+1)(5c^2-1)$, giving $c = 1/\sqrt{5}$. The signed permutation

$$G^{(\mathrm{III})}_{ij} = \epsilon_i \epsilon_j (G_5)_{\pi_i \pi_j}, \qquad \pi = (0,2,4,1,3), \quad \epsilon = (1,-1,-1,1,1) \tag{12.3}$$

identifies it with the icosahedral deletion in (3.3).

With $|x|, |y| < c$, the two additional patterns have Gram matrices

$$A = \begin{pmatrix} 1 & c & c & c & c \\ c & 1 & x & -c & -c \\ c & x & 1 & -c & -c \\ c & -c & -c & 1 & y \\ c & -c & -c & y & 1 \end{pmatrix}, \qquad B = \begin{pmatrix} 1 & c & c & c & c \\ c & 1 & x & -c & c \\ c & x & 1 & c & -c \\ c & -c & c & 1 & y \\ c & c & -c & y & 1 \end{pmatrix}.$$

The mixed minor M_{13} of A is $c(c+1)(x-1)(y-1) \neq 0$. The principal minor M_{33} of B is $(c-1)(c+1)(4c^2+x^2-1) \neq 0$, since $x^2 < c^2$ and $5c^2 \leq 1$. Both contradict rank at most three. Thus every selected configuration is the five-line reference.

The Lean check examines all 729 words and validates an explicit signed permutation for each retained word. The elementary unsigned graph assertion is checked on all 2^{10} graphs, and the four-vertex sign assertion on all eight normalized sign choices. These checks and their geometric inputs are in `LinePackings/Census/FiveGraphs.lean`, `LinePackings/Census/FiveGraphWitnesses.lean`, `LinePackings/Geometry/Contact/ContactStars.lean`, and `LinePackings/DimensionThree/Five/GraphReduction.lean`; the minor identities and the case resolution are in `LinePackings/DimensionThree/Five/GraphGram.lean`. Applying the selection principle outside the relatively open, compact reference class now excludes every competitive configuration outside that class. This proves optimality and uniqueness for five lines.

12.2. **Two reusable rigidity tests for rhombus equations.** The remaining analytic terminal maps use the same decreasing involution h_c from (6.3), but different small linear systems. We state their two elementary rigidity principles.

Lemma 12.1 (A uniform Jacobian test)**.** *Let F be continuously differentiable on a convex domain, and let J_0 be a fixed invertible square matrix with $\|J_0 v\| \geq s\|v\|$. If $\|DF - J_0\| \leq \eta < s$ everywhere, then*

$$\|F(p) - F(q)\| \geq (s-\eta)\|p-q\|.$$

In particular F is injective. If a finite coordinate symmetry preserves its domain and zero set, every zero is fixed by that symmetry.

Proof. Integrate the derivative on the segment from q to p. Its average is $J_0 + E$ with $\|E\| \le \eta$. The norm triangle inequality gives the result. □

Lemma 12.2 (A rhombus maximum principle)**.** *For a convex spherical rhombus of side* $\arccos c$*,* $0 < c < 1$*, let*

$$\beta = 2\arctan(1/\sqrt{c}), \quad m = (p+q)/2, \quad n = (p-q)/2, \quad h = \beta - m.$$

Then $h = 0$ *if* $n = 0$*, and* $0 \le h < |n|$ *otherwise. Consequently, for any finite collection of such rhombi, an identity* $n = Ch$ *implies all are squares if every row of* C *has positive coefficient sum at most one and negative coefficient sum in absolute value at most one.*

Proof. The cotangent identity is equivalent to

$$\cos m = -\frac{1-c}{1+c}\cos n.$$

Since $0 < m < \pi$, it gives $m \le \beta$. When $p \ne q$, the strictly decreasing cotangent function puts β strictly between p and q, so $h < |n|$. Set $H = \max h_j$, $M = \max|n_j|$. The coefficient assumption gives $M \le H$. If $M > 0$, every $h_j < M$, so $H < M$, a contradiction. □

12.3. **Eleven lines: the five-rhombus system.** The terminal signed map has a pole P, inner vertices Y_i, and outer vertices Z_i, with indices modulo five. Its faces have projective boundary lists

$$(P, Y_i, Z_i, Y_{i+1}), \qquad (Y_i, Z_i, Z_{i+2}, Z_{i-1}).$$

The contact signs are

$$\langle P, Y_i\rangle = c, \quad \langle Z_i, Y_i\rangle = \langle Z_i, Y_{i+1}\rangle = c, \quad \langle Z_i, Z_{i+2}\rangle = -c.$$

For the second face its consistent spherical lift is $(Y_i, Z_i, -Z_{i+2}, Z_{i-1})$. All ten faces are strictly convex rhombi. The coarse bounds give

$$69/100 < c \le c_{11} < 18/25, \qquad 7\pi/20 < \alpha < 3\pi/8.$$

The angle bounds follow by the cosine rule and rational Taylor enclosures, as in Section 8.

In the first face let β_i be its angles at P, Z_i, and p_i its other angles. Then $\beta_i = h_c(p_i)$, $\sum_i \beta_i = 2\pi$. In the second face let q_i be its angles at Y_i, Z_{i+2}, and $h_c(q_i)$ the other two. The vertex equations become

$$q_i = 2\pi - p_{i-1} - p_i, \qquad h_c(p_i) + h_c(q_i) + h_c(q_{i+1}) = p_{i+2} + p_{i+3}. \tag{12.4}$$

Every p_i, q_i lies in $(\pi/2, 2\alpha)$. For q_i, use $p_i < 2\alpha$ and $\alpha < 3\pi/8$. For p_i, first $\beta_i < 2\pi - 4\alpha < 3\pi/5$, and then

$$\cot^2(3\pi/10) = 5 - 2\sqrt{5} > 13/25 > (18/25)^2 > c^2.$$

Thus $h_c(3\pi/5) > \pi/2$, proving the assertion.

Fix c. Let $\mathcal{D}$ be the convex domain given by

$$\pi/2 < p_i < 2\alpha, \qquad \pi/2 < 2\pi - p_{i-1} - p_i < 2\alpha.$$

Let F_i be the left minus right side of the second equation in (12.4). Differentiation gives

$$-h_c'(t) = \frac{2c}{(1+c^2) + (1-c^2)\cos t}, \qquad \frac{9}{10} < \frac{2c}{1+c^2} \le -h_c'(t) \le \frac{1+c}{2c} < \frac{5}{4}$$

on $[\pi/2, 2\alpha]$. Put $a_i = -h_c'(p_i)$, $b_i = -h_c'(q_i)$. The symmetric Jacobian is

$$J_{ii} = -a_i + b_i + b_{i+1}, \quad J_{i,i-1} = b_i, \quad J_{i,i+1} = b_{i+1}, \quad J_{i,i+2} = J_{i,i+3} = -1.$$

Replace every a_i, b_i by $k = 43/40$, obtaining J_0. Every replacement error is less than $7/40$, so $\|J - J_0\|_2 \le \|J - J_0\|_\infty \le 7/8$; for symmetric matrices, the first bound follows by the eigenvector equation at a component of maximum absolute value.

If A is the five-cycle adjacency matrix and U the all-ones matrix, then $A^2 + A - I = U$ and $J_0 = (k+1)(I + A) - U$. Its eigenvalues are

$$3k - 2, \qquad (k+1)(1+\sqrt{5})/2 \text{ twice}, \qquad (k+1)(1-\sqrt{5})/2 \text{ twice}.$$

All have absolute value at least $49/40$: the first equals this value and $\sqrt{5} > 11/5$ bounds the others. Lemma 12.1 gives the injectivity constant $49/40 - 7/8 = 7/20$. Cyclic shifts preserve both $\mathcal{D}$ and the equations. All p_i are therefore equal, hence $\beta_i = 2\pi/5$.

Rotate P to the pole. The Y_i's lie at height c with equal azimuthal gaps, so form a regular pentagon. Each Z_i is the second intersection of the two contact circles about Y_i, Y_{i+1}, the first being P. Formula (9.4) fixes every Z_i and gives a staggered regular pentagon. Put $v = \cos(\pi/5)$, $w = v^2 = (3+\sqrt{5})/8$. Its height is

$$f(c) = \frac{c^2 - (1-c^2)w}{c^2 + (1-c^2)w} > 0, \qquad f'(c) = \frac{4cw}{(w + (1-w)c^2)^2} > 0.$$

Positivity follows already from $c^2 > 2/5$ and $w < 2/3$. The outer diagonal contact is

$$H(c) = c - v + (1+v)f(c)^2 = 0.$$

This is strictly increasing in the required interval, and the construction gives $H(c_{11}) = 0$. Thus $c = c_{11}$ and the entire realization is fixed. This is a global classification of the terminal map, without subdivision or a local uniqueness assumption.

The Lean proof of injectivity uses the maximum norm. It allows $0 \le p_i \le 2\alpha$ and $\pi/2 \le q_i \le 2\alpha$. On these two intervals the derivative formula gives $|h_c'(p_i) + 43/40| \le 39/100$ and $|h_c'(q_i) + 43/40| \le 3/20$, respectively. For two vectors with equal residuals let d be their difference. The corresponding q_i's differ by at most $2\|d\|_\infty$. The scalar mean value theorem in the three terms of each equation gives $\|J_0 d\|_\infty \le (39/100 + 4 \cdot 3/20)\|d\|_\infty$. The first row of the circulant inverse J_0^{-1} is $(-120, 1840, -120, -120, 1840)/4067$, whose absolute row sum is $4040/4067 < 1$. It follows that $d = 0$. The ten rhombi and all eleven vertex sums in this argument come from the signed rotation of the matched packing in `LinePackings/DimensionThree/Eleven/RingTerminal.lean`.

12.4. **Twelve lines: a maximum principle forces squares.** Label the reference projective vertices by the following unnormalized representatives, where $a = 1 + \sqrt{2}$:

i	1	2	3	4	5	6	7	8	9	10	11	12
x	1	1	1	1	1	1	1	1	a	a	a	a
y	$-a$	$-a$	-1	-1	1	1	a	a	-1	-1	1	1
z	-1	1	$-a$	a	$-a$	a	-1	1	-1	1	-1	1

These coordinates specify the signs and combinatorics, not the coordinates of a hypothetical realization. The triangular faces are $(1,3,9), (2,4,10), (5,7,11), (6,8,12)$.

Specify each quadrilateral by its opposite pairs:

j	+ pair	− pair	j	+ pair	− pair	j	+ pair	− pair
1	$(1,7)$	$(2,8)$	4	$(2,5)$	$(4,7)$	7	$(4,12)$	$(6,10)$
2	$(1,10)$	$(2,9)$	5	$(3,4)$	$(5,6)$	8	$(7,12)$	$(8,11)$
3	$(1,6)$	$(3,8)$	6	$(3,11)$	$(5,9)$	9	$(9,12)$	$(10,11)$

The marks + and − label angles only, not scalar-product signs. Every vertex lies in one triangle and three quadrilaterals.

Let B be the 12×9 matrix with entries $+1$ on a positive pair, -1 on a negative pair, and zero elsewhere; put $A = |B|$ entrywise. Use m_j, n_j, h_j from Lemma 12.2 for each face. The vertex equations give

$$Am + Bn = (2\pi - \alpha)\mathbf{1}, \qquad A\mathbf{1} = 3\mathbf{1},$$

and hence

$$Bn - Ah = (2\pi - \alpha - 3\beta)\mathbf{1}. \tag{12.5}$$

The following explicit integer matrix satisfies $RB = 4I$ and $R\mathbf{1} = 0$:

$$R = \begin{pmatrix} 1 & -1 & 1 & -1 & 1 & -1 & 1 & -1 & 1 & -1 & 1 & -1 \\ 1 & -1 & 0 & 0 & 0 & 0 & -1 & 1 & -1 & 1 & -1 & 1 \\ 1 & 1 & -1 & 1 & -1 & 1 & -1 & -1 & 0 & 0 & 0 & 0 \\ 1 & 1 & 1 & -1 & 1 & -1 & -1 & -1 & 0 & 0 & 0 & 0 \\ 1 & 1 & 1 & 1 & -1 & -1 & -1 & -1 & 1 & 1 & -1 & -1 \\ 0 & 0 & 1 & -1 & -1 & 1 & 0 & 0 & -1 & -1 & 1 & 1 \\ 0 & 0 & -1 & 1 & 1 & -1 & 0 & 0 & -1 & -1 & 1 & 1 \\ -1 & 1 & 0 & 0 & 0 & 0 & 1 & -1 & -1 & 1 & -1 & 1 \\ 1 & -1 & 1 & -1 & -1 & 1 & -1 & 1 & 1 & -1 & -1 & 1 \end{pmatrix}.$$

Multiplying (12.5) by $R/4$ gives

$$\begin{aligned} n_1 &= h_6 - h_7, & 2n_2 &= h_3 - h_4 - h_6 + h_7, \\ 2n_3 &= h_2 - h_6 + h_7 - h_8, & 2n_4 &= h_2 + h_6 - h_7 - h_8, \\ n_5 &= h_2 - h_8, & 2n_6 &= -h_2 + h_3 - h_4 + h_8, \\ 2n_7 &= -h_2 - h_3 + h_4 + h_8, & 2n_8 &= -h_3 + h_4 - h_6 + h_7, \\ n_9 &= h_3 - h_4. \end{aligned}$$

Every right side, after division by two when indicated, is a difference of two convex combinations of the h_j's. Lemma 12.2 forces $n = h = 0$, so all quadrilaterals are squares.

The vertex equation becomes $\alpha(\delta) + 3\beta(\delta) = 2\pi$. Both functions strictly increase for $0 < \delta < \pi/2$, so there is at most one solution. The explicit rhombicuboctahedral construction supplies it, giving $c = c_{12}$. Fix one face by an orthogonal transformation on the spherical cover. A regular triangle or square of the prescribed side length is determined by a shared edge and the side on which it lies: its fixed interior angle determines the next tangent direction, and its side length then determines the next vertex. Adjacent faces occupy opposite sides. Propagate across a spanning tree of the connected dual graph to fix every face and vertex. This proves congruence without invoking polyhedral rigidity.

The argument covers every convex realization of this signed map, including realizations far from the reference coordinates.

In Lean, taking the cosine of $\alpha = 2\pi - 3\beta$ and using $\cos\alpha = c/(1+c)$ and $\cos\beta = (c-1)/(c+1)$ yields $17c^2 - 14c + 1 = 0$ after clearing denominators. The bound $c > 1/2$ selects c_{12}. Each signed lifted square has equal chord midpoints on its two diagonals. Taking scalar products of these nine vector identities with all twelve representatives gives 108 linear equations in the Gram entries. Subtract the equations for the explicit construction in the same labels. The twelve diagonal and twenty-four contact differences vanish. The eighteen square diagonal differences then vanish, and the remaining twenty-four differences occur in signed chains that equate each to its own negative. Lean verifies the integer identities for all 78 entries. Equality of the Gram matrices gives the orthogonal congruence. The two computations are in `LinePackings/DimensionThree/Twelve/TerminalSquares.lean` and `LinePackings/Certificates/Terminal/TwelveRealization.lean`.

13. The finite calculations and the assembled classification

13.1. **From census coverage to case theorems.** For eight through twelve lines, the census of Section 7.4 gives a match for every eligible terminal disk. The match includes a signed relabelling of its contact core with a row of the corresponding catalogue. The catalogue sizes are

N	8	9	10	11	12
rows	86	1048	13473	37289	30861.

The matched rotation gives the ordered faces and complete vertex stars where a certificate needs them. If the core is smaller than the packing, the case theorem uses the constraints on the remaining lines. The ordinary signed-graph proof for five lines uses the finite enumeration in Section 12.1.

The certificate inputs are Lean declarations. The checkers compute with the signed maps and exact numerical bounds, and the soundness theorems interpret the resulting finite checks in the geometry of the selected packing. For example, the Gram interval rules are in `LinePackings/Certificates/Map/GramKernel.lean` and their soundness proof is in `LinePackings/Certificates/Map/GramSound.lean`. The application to an actual matched map uses `LinePackings/Certificates/Geometry/GramRealization.lean`. The size-specific certificate inputs are in `LinePackings/Certificates/Cases/` and the modules for further Gram, frame, motion, and stress checks are organized by certificate type under `LinePackings/Certificates/`.

13.2. **Case coverage by size.** For ten through twelve lines the first collection of rules reduces any hypothetical noncandidate to a row on the full-stress or stress-support list. To check the second collection of rules, encode a set of indices A by the integer with bit i set for each $i \in A$. Kernel evaluation verifies equality between the mask of the remaining rows and the mask of the rows covered by the Schur, minor, and other exclusion certificates. Reading the bit at the matched index gives a rule whose hypotheses are then supplied by the match to the selected packing.

- For eight lines, the resolution lists cover all 86 indices. Direct contact patterns, angle tests, grounded stresses, Gram contractions, and frame isolation give signed Gram equality with (4.3) for every competitive packing. See `LinePackings/DimensionThree/Eight/CatalogueExclusions.lean`.
- For nine lines, `LinePackings/DimensionThree/Nine/AllCases.lean` and `LinePackings/DimensionThree/Nine/Completeness.lean` use the checked rules for the 1048 catalogue entries. The near-candidate rules

identify a signed permutation and invoke the isolation theorem for the corresponding matrix (4.4) or (4.5).

- For ten lines, `LinePackings/DimensionThree/Ten/Completeness.lean` combines local angle, perimeter, orientation and missing-line tests, shared subgraphs, and ordered-face Gram programs with Schur certificates, direct geometric exclusions, and the Petersen mixed minor of Section 10.6. The near-core cases use isolation and the exact extension region (4.7).
- For eleven lines, the catalogue exclusions use checked negative four-cycles to obtain $c^2 \le 1/2$ for the rows with shorter Gram, angle, or placement ranges. Row 37044 forces the pole and staggered pentagons by Section 12.3. See `LinePackings/DimensionThree/Eleven/CatalogueExclusions.lean`. `LinePackings/DimensionThree/Eleven/StressRouting.lean` combines Schur certificates with determinant, isolated-face, local-angle, and ordered-face exclusions.
- For twelve lines, direct Gram and geometric rules exclude rows or force congruence by isolation. The square-face theorem of Section 12.4 resolves row 30852. See `LinePackings / DimensionThree / Twelve / CatalogueExclusions.lean`. Schur, mixed-minor, local geometry, and ordered-face certificates cover the 17691 stress and support rows, together with the specific row arguments below. See `LinePackings / DimensionThree/Twelve/StressExclusions.lean`.

At twelve lines, the Gram tree for row 30362 proves congruence via the near-candidate test. For each surviving Gram box of rows $30484, 30487, 30768$, a checked strict contact motion contradicts local minimality. After those and the other stress rules, the only possible index is 30205. The proof splits the actual coherence at

$$\frac{208841972787478}{2^{48}}.$$

Below and at the cutoff, a rank-three interval proof excludes the matched configuration. At and above it, the frame test of Section 11.2 forces congruence to the optimizer. The checked intervals start at the downward dyadic rounding of $181/250$ and end at $209563985594473/2^{48}$, an upper bound on c_{12}. The two tests are combined in `LinePackings/DimensionThree/Twelve/Row30205.lean`.

13.3. **Final assembly.**

Proof of Theorem 2.1. The cases $N = 1, 2, 3, 4, 6, 7$ were proved in Section 3. For each remaining N, let F_N be the unit configurations with $\mu(X) \le c_N$, and let $\mathcal{C}_N$ consist of all configurations congruent to the proposed optima. The constructions in Section 4 and (3.2) give $\mathcal{C}_N \subset F_N$ and coherence c_N throughout $\mathcal{C}_N$. Local isolation makes $\mathcal{C}_N$ relatively open in F_N, with five-line isolation from Section 5.1 and the remaining bounds from Section 5.2. For ten lines it suffices to isolate the nine-line core, since all competitive extensions belong to the closed family.

If $F_N \setminus \mathcal{C}_N$ were nonempty, apply Proposition 5.2. When $N = 5$, the ordinary signed-graph proof of Section 12.1 puts the selected packing in $\mathcal{C}_5$. For $N = 8, \dots, 12$, the selected packing's nonisolated vertices form an antipodal contact core with disk faces. The preliminary bounds and strict contact stars give the census parameters and pruning inequalities. Peeling one disk bounded by the doubled shortest antipodal walk yields the reachable terminal state of Section 7.4. The match gives the row, core size, and signed relabelling. The packing carried through the cut supplies the

positions of any isolated lines. The case theorem described in Section 13.2 either rules out the selected packing or identifies it as a member of $\mathcal{C}_N$. The competitive set is therefore exactly $\mathcal{C}_N$.

In particular, a packing with coherence strictly below c_N would belong to a class with coherence c_N. Attainment and congruence invariance now give the least coherence and the equality characterization. The squared Gram sums distinguish the two nine-line classes, and Section 4.4 gives the congruence quotient of the ten-line parameters. □

The three-dimensional theorem statements and proofs are collected in `LinePackings/DimensionThree.lean` and the modules it imports. For example, `LinePackings/DimensionThree/Ten.lean`, `LinePackings/DimensionThree/Eleven.lean`, and `LinePackings/DimensionThree/Twelve.lean` each combine proof of attainment with classification of the competitive set. The ten-line module also proves the parameter congruence criterion, and the eleven-line module includes uniqueness of the root in (2.3). The four-dimensional proof of Theorem 2.2 is collected in `LinePackings/DimensionFour.lean`.

13.4. **Checking the Lean proof.** Kryvonos, Liehr, and Taylor used Lean to verify their computer-assisted proof for the logarithmic and Coulomb energies of eight points on S^2 [21]. The fifteen-point Tammes preprint [27] verifies the geometric reduction in Lean, taking the plane-graph enumeration and its interval exclusions as hypotheses.

Our formalization uses Lean 4 [16] and Mathlib [24]. The Lean kernel checks the fourteen classification theorems and the finite computations used in them. The package uses Lean 4.36.0, and `lakefile.lean` pins the corresponding Mathlib release. With Elan installed, run these commands from the package root.

```
elan toolchain install leanprover/lean4:v4.36.0
printf '%s\n' 'leanprover/lean4:v4.36.0' > lean-toolchain
lake update
lake build +LinePackings:olean
```

The build checks the root module `LinePackings.lean` and its imports. It includes the attainment, census, exclusion, and terminal realization proofs used by the classifications. See `README.md` for the individual build targets.

In the `LinePackings` namespace, the three-dimensional declarations are `main3_one` through `main3_twelve`. The four-dimensional declarations are `main4_eleven` and `main4_twelve`. Their axiom dependencies are among `propext`, `Classical.choice`, and `Quot.sound`. For example, the declaration and axioms for twelve lines in $\mathbb{R}^3$ can be inspected as follows.

```
import LinePackings.DimensionThree.Twelve

#check LinePackings.main3_twelve
#print axioms LinePackings.main3_twelve
```

References

[1] K. M. Anstreicher, *Improved linear programming bounds for antipodal spherical codes*, Discrete Comput. Geom. **28** (2002), 107–114, doi:10.1007/s00454-001-0080-5.

[2] C. Bachoc and F. Vallentin, *New upper bounds for kissing numbers from semidefinite programming*, J. Amer. Math. Soc. **21** (2008), 909–924, doi:10.1090/S0894-0347-07-00589-9, arXiv:math/0608426.

[3] D. W. Barnette, *Generating the triangulations of the projective plane*, J. Combin. Theory Ser. B **33** (1982), 222–230, doi:10.1016/0095-8956(82)90041-7.

[4] E. A. Bender, E. R. Canfield, and R. W. Robinson, *The enumeration of maps on the torus and the projective plane*, Canad. Math. Bull. **31** (1988), 257–271, doi:10.4153/CMB-1988-039-4.

[5] F. G. A. van den Berg, *The optimal packing of nine lines in* $\mathbb{R}^3$, preprint, 2026, doi:10.5281/zenodo.24608928.

[6] G. Brinkmann and B. D. McKay, *Fast generation of planar graphs*, MATCH Commun. Math. Comput. Chem. **58** (2007), 323–357, `https://users.cecs.anu.edu.au/~bdm/plantri/`.

[7] A. R. Calderbank, P. J. Cameron, W. M. Kantor, and J. J. Seidel, $\mathbb{Z}_4$*-Kerdock codes, orthogonal spreads, and extremal Euclidean line-sets*, Proc. London Math. Soc. (3) **75** (1997), 436–480, doi:10.1112/S0024611597000403.

[8] H. Cohn, Y. Jiao, A. Kumar, and S. Torquato, *Rigidity of spherical codes*, Geom. Topol. **15** (2011), 2235–2273, doi:10.2140/gt.2011.15.2235, arXiv:1102.5060.

[9] H. Cohn and J. Woo, *Three-point bounds for energy minimization*, J. Amer. Math. Soc. **25** (2012), 929–958, doi:10.1090/S0894-0347-2012-00737-1, arXiv:1103.0485.

[10] R. Connelly and W. Whiteley, *Second-order rigidity and prestress stability for tensegrity frameworks*, SIAM J. Discrete Math. **9** (1996), 453–491, doi:10.1137/S0895480192229236.

[11] J. H. Conway, R. H. Hardin, and N. J. A. Sloane, *Packing lines, planes, etc.: packings in Grassmannian spaces*, Experiment. Math. **5** (1996), 139–159, `https://projecteuclid.org/euclid.em/1047565645`, arXiv:math/0208004.

[12] L. Danzer, *Finite point-sets on* S^2 *with minimum distance as large as possible*, Discrete Math. **60** (1986), 3–66, doi:10.1016/0012-365X(86)90002-6.

[13] D. de Laat, N. M. Leijenhorst, and W. H. H. de Muinck Keizer, *Optimality and uniqueness of the* D_4 *root system*, preprint, 2024, arXiv:2404.18794.

[14] P. Delsarte, J. M. Goethals, and J. J. Seidel, *Bounds for systems of lines, and Jacobi polynomials*, Philips Res. Rep. **30** (1975), 91*–105*, `https://research.tue.nl/en/publications/bounds-for-systems-of-lines-and-jacobi-polynomials/`.

[15] P. Delsarte, J. M. Goethals, and J. J. Seidel, *Spherical codes and designs*, Geom. Dedicata **6** (1977), 363–388, doi:10.1007/BF03187604.

[16] L. de Moura and S. Ullrich, *The Lean 4 theorem prover and programming language*, in *Automated Deduction—CADE 28*, Lecture Notes in Comput. Sci. **12699**, Springer, 2021, 625–635, doi:10.1007/978-3-030-79876-5_37.

[17] L. Fejes Tóth, *Distribution of points in the elliptic plane*, Acta Math. Acad. Sci. Hungar. **16** (1965), 437–440, doi:10.1007/BF01904849.

[18] M. Fickus, J. Jasper, and D. G. Mixon, *Packings in real projective spaces*, SIAM J. Appl. Algebra Geom. **2** (2018), 377–409, doi:10.1137/17M1137528, arXiv:1707.01858.

[19] I. Izmestiev, *The Colin de Verdière number and graphs of polytopes*, Israel J. Math. **178** (2010), 427–444, doi:10.1007/s11856-010-0070-5, arXiv:0704.0349.

[20] H. Knothe, *Contributions to the theory of convex bodies*, Michigan Math. J. **4** (1957), 39–52, doi:10.1307/mmj/1028990175.

[21] L. Kryvonos, L. Liehr, and M. A. Taylor, *Energy minimization for eight points on the sphere*, preprint, 2026, arXiv:2609.22077.

[22] V. I. Levenšteĭn, *Bounds on the maximal cardinality of a code with bounded modules of the inner product*, Soviet Math. Dokl. **25** (1982), 526–531.

[23] H. Maehara, *Isoperimetric theorem for spherical polygons and the problem of* 13 *spheres*, Ryukyu Math. J. **14** (2001), 41–57.

[24] The mathlib community, *The Lean mathematical library*, in *Proceedings of the 9th ACM SIGPLAN International Conference on Certified Programs and Proofs*, ACM, 2020, 367–381, doi:10.1145/3372885.3373824, arXiv:1910.09336.

[25] D. G. Mixon and H. Parshall, *Exact line packings from numerical solutions*, paper presented at SampTA, Bordeaux, 2019, arXiv:1902.00552.

[26] D. G. Mixon and H. Parshall, *The optimal packing of eight points in the real projective plane*, Exp. Math. **31** (2022), 474–485, doi:10.1080/10586458.2019.1641767, arXiv:1902.10177.

[27] mt0-svg, *The Tammes problem for fifteen points*, preprint, version 1.4.0, 2026, doi:10.5281/zenodo.23450670, `https://github.com/mt0-svg/tammes-15`.

[28] O. R. Musin, *The kissing number in four dimensions*, Ann. of Math. (2) **168** (2008), 1–32, doi:10.4007/annals.2008.168.1, arXiv:math/0309430.

[29] O. R. Musin and A. S. Tarasov, *The strong thirteen spheres problem*, Discrete Comput. Geom. **48** (2012), 128–141, doi:10.1007/s00454-011-9392-2, arXiv:1002.1439.
[30] O. R. Musin and A. S. Tarasov, *Enumeration of irreducible contact graphs on the sphere*, J. Math. Sci. (N.Y.) **203** (2014), 837–850, doi:10.1007/s10958-014-2174-7, arXiv:1312.5450.
[31] O. R. Musin and A. S. Tarasov, *Extremal problems of circle packings on a sphere and irreducible contact graphs*, Proc. Steklov Inst. Math. **288** (2015), 117–131, doi:10.1134/S0081543815010095, arXiv:1410.0744.
[32] O. R. Musin and A. S. Tarasov, *The Tammes problem for $N = 14$*, Exp. Math. **24** (2015), 460–468, doi:10.1080/10586458.2015.1022842, arXiv:1410.2536.
[33] T. Nipkow, *Verified efficient enumeration of plane graphs modulo isomorphism*, in *Interactive Theorem Proving (ITP 2011)*, Lecture Notes in Comput. Sci. **6898**, Springer, 2011, 281–296, doi:10.1007/978-3-642-22863-6_21.
[34] T. Nipkow, G. Bauer, and P. Schultz, *Flyspeck I: tame graphs*, in *Automated Reasoning (IJCAR 2006)*, Lecture Notes in Comput. Sci. **4130**, Springer, 2006, 21–35, doi:10.1007/11814771_4.
[35] R. A. Rankin, *The closest packing of spherical caps in n dimensions*, Proc. Glasgow Math. Assoc. **2** (1955), 139–144, doi:10.1017/S2040618500033219.
[36] R. M. Robinson, *Arrangement of 24 points on a sphere*, Math. Ann. **144** (1961), 17–48, doi:10.1007/BF01396539.
[37] K. Schütte and B. L. van der Waerden, *Auf welcher Kugel haben 5, 6, 7, 8 oder 9 Punkte mit Mindestabstand Eins Platz?*, Math. Ann. **123** (1951), 96–124, doi:10.1007/BF02054944.
[38] T. Sulanke, *Generating maps on surfaces*, Discrete Comput. Geom. **57** (2017), 335–356, doi:10.1007/s00454-016-9853-8, arXiv:1509.06412. The `surftri` software, version 0.989, is available at `https://tsulanke.pages.iu.edu/graphs/surftri/`.
[39] T. Sulanke and F. H. Lutz, *Isomorphism-free lexicographic enumeration of triangulated surfaces and 3-manifolds*, European J. Combin. **30** (2009), 1965–1979, doi:10.1016/j.ejc.2008.12.016, arXiv:math/0610022.
[40] P. M. L. Tammes, *On the origin of number and arrangement of the places of exit on the surface of pollen-grains*, Rec. Trav. Bot. Néerl. **27** (1930), 1–84, `https://natuurtijdschriften.nl/pub/552640/`.
[41] T. Tarnai, *Note on packings in Grassmannian space $G(3, 1)$*, J. Math. Chem. **23** (1998), 415–419, doi:10.1023/A:1019193829804.
[42] W. T. Tutte, *A census of planar maps*, Canad. J. Math. **15** (1963), 249–271, doi:10.4153/CJM-1963-029-X.
[43] L. R. Welch, *Lower bounds on the maximum cross correlation of signals*, IEEE Trans. Inform. Theory **20** (1974), 397–399, doi:10.1109/TIT.1974.1055219.

Department of Mathematics, Massachusetts Institute of Technology, Cambridge, MA 02139 USA
Email address: `cohn@mit.edu`

Department of Mathematics, Brown University, Providence, RI 02912, USA
Email address: `javier_gomez_serrano@brown.edu`

Department of Mathematics & Statistics, University of North Florida, Jacksonville, FL 32224, USA
Email address: `liudmyla.kryvonos@unf.edu`

Department of Mathematics, Bar-Ilan University, Ramat-Gan 5290002, Israel
Email address: `lukas.liehr@biu.ac.il`

Mathematical Institute, University of Oxford, Oxford, OX2 6GG, United Kingdom
Email address: `mitchtaylor@shaw.ca`